

PREVIEW ACTIVE SUSPENSION DESIGN FOR
CONVOY VEHICLES

HADI ADIBI ASL



Preview Active Suspension Design for Convoy Vehicles

© Hadi Adibi asl, B.Sc

A thesis submitted to the
School of Graduate Studies
in partial fulfillment of the
requirements for the degree of

Master of Engineering

Faculty of Engineering and Applied Science

Memorial University of Newfoundland

September, 2009

St. John's, Newfoundland, Canada

Abstract

Convoy vehicles, defined as individual vehicles traveling with close following distances on a specified path, have been recently the subject of research especially in military applications. Convoy vehicles are used to carry soldiers, weapons and army supplements. Military drivers are often young and inexperienced, and more prone to lose control of vehicles on rough terrain. In addition, Intelligent Vehicle Highway Systems with autonomous civilian vehicles travelling in platoons are an active research and experimentation topic.

The idea of communicating dynamic responses between preceding and following vehicles, to improve the followers' ride comfort and handling, has been identified as a research need for convoy vehicle systems.

This research implements a form of preview control to improve the vertical dynamics of convoy vehicles. An academic virtual convoy, composed of a lead vehicle with active suspension system, and a follower vehicle with preview-controlled active suspension, is developed in MATLAB and SIMULINK. Preview control gives a theoretical improvement over active control by further decreasing sprung mass acceleration (ride quality) and/or improving road holding. Quarter car models with two degrees of freedom (DOF) are employed for modeling and simulation. In contrast to conventional preview control with look-ahead sensors, the vertical response states of the lead vehicle are used to generate feed forward control gains in addition to feedback control gains for the preview controller of the follower vehicle.

The results show improved ride comfort and road holding of the follower vehicle with the novel preview approach compared to a lead vehicle with active suspension. Moreover, the power demand for the follower vehicle suspension is much less than for the lead vehicle.

Longitudinal dynamics of a convoy system, with five vehicles, are evaluated and an adaptive cruise control system is implemented to control the longitudinal aspects of the convoy such as relative space and velocity among vehicles. Future work will implement the state-based preview controller into such a convoy, with variations in following distance, to test the robustness of the method.

Acknowledgments

I would like to express my sincere gratitude to my supervisor Dr. Geoff Rideout, for his constant guidance, encouragement and great support, without which I could not have completed this program.

Also, I would like to thank my family with their constant support during my whole life, especially my brother, Dr. Reza Adibi asl, who has greatly encouraged me to carry out my research.

I would thank the Natural Sciences and Engineering Research Council of Canada (NSERC), AUTO21 Network of Centers of Excellence, and Memorial University of Newfoundland (MUN) for providing financial assistance for this research.

Finally, I would like to thank my dear friends who have helped me during my research, especially Farid Arvani, and all staff in the Faculty of Engineering at MUN, for fostering a very friendly atmosphere for graduate students.

Table of Contents

Abstract	ii
Acknowledgments	iv
List of Tables	viii
List of Figures	ix
Nomenclature	xiv
1. Introduction	1
1.1 Introduction	1
1.2 Problem statement	4
1.3 Contribution of the thesis	5
1.4 Thesis organization	6
2. Literature review	7
2.1 Literature review	7
2.2 Conclusion.....	18
3. Modeling of active suspension systems with the bond graph method	19
3.1 Introduction	19
3.2 Quarter car model (active vs. passive)	22

3.2.1 Improving ride comfort	26
3.2.2 Improving road holding	31
3.3 Half car model (active vs. passive)	35
3.4 Full car model (active vs. passive)	39
3.4 Conclusion.....	46
4. Longitudinal vehicle dynamics and cruise control	47
4.1 Introduction	47
4.2 Model development.....	49
4.2.1 Bond graph model	49
4.2.2 Cruise control structure	53
4.3 Results	57
4.3.1 Single bump (road profile)	57
4.3.2 Random (road profile)	61
4.4 Conclusion.....	65
5. Active suspension model with preview	66
5.1 Introduction	66
5.2 Model development.....	67
5.2.1 Conventional active-preview suspension system	67
5.2.2 State-based active with preview suspension model.....	69

5.3 Results	77
5.3.1 Single bump road profile	77
5.3.2 The effect of preview time on performance	81
5.4 Conclusion.....	82
6. Observer design.....	84
6.1 Introduction	84
6.2 Model development.....	85
6.2.1 Theory of Kalman estimator.....	85
6.2.2 Implementing estimator in SIMULINK	89
6.3 Results	92
6.4 Conclusion.....	100
7. Conclusions and future work	101
7.1 Conclusions	101
7.2 Future work	103
Bibliography	105
Appendix.....	110
Appendix A: String stability	110
Appendix B: Linear Quadratic Regulator (LQR).....	112
Appendix C: Controllability and observability	114

List of Tables

Table 3.2.1: Analogies between mechanical and electrical systems in terms of effort and flow	23
Table 3.2.2: Parameters & values of quarter car model.....	25
Table 3.3.1: Parameters and values of half car model	36
Table 3.4.1: Parameters and values of full car model.....	43
Table 4.2.1: Parameters and values of vehicles	56
Table 5.2.1: Parameters and values of the model	70
Table 5.3.1: Performance index vs. preview time	81
Table 6.3.1: Measurement and input noise parameters and values.....	92

List of Figures

Figure 1.1.1: Military convoy vehicles [AP Photo/ Ali Heidar, 2003].....	2
Figure 1.1.2: Intelligent Vehicle Highway System (IVHS) [15]	2
Figure 1.2.1: Schematic lead and follower(s) communication	5
Figure 2.1.1: Quarter car model with passive and active part [15].....	7
Figure 2.1.2: Schematic chart of suspension performances.....	8
Figure 3.2.1: Example of similar mechanical and electrical systems with bond graph modeling	23
Figure 3.2.2: Schematic quarter car model [15]	24
Figure 3.2.3: Active suspension system bond graph model (quarter car model).....	26
Figure 3.2.4: Single bump road profile.....	27
Figure 3.2.5: Sprung mass acceleration (active vs. passive).....	28
Figure 3.2.6: Suspension deflection (active vs. passive)	28
Figure 3.2.7: Tire deflection (active vs. passive).....	29
Figure 3.2.8: PSD response of sprung mass acceleration (active vs. passive).....	29
Figure 3.2.9: PSD response of suspension deflection (active vs. passive)	30
Figure 3.2.10: PSD response of tire deflection (active vs. passive)	30
Figure 3.2.11: Sprung mass acceleration (active vs. passive).....	32

Figure 3.2.12: Suspension deflection (active vs. passive)	32
Figure 3.2.13: Tire deflection (active vs. passive).....	33
Figure 3.2.14: PSD response of sprung mass acceleration (active vs. passive).....	33
Figure 3.2.15: PSD response of suspension deflection (active vs. passive)	34
Figure 3.2.16: PSD response of tire deflection (active vs. passive)	34
Figure 3.3.1: Schematic half car model [9].....	36
Figure 3.3.2: Extended model of active suspension system (half car).....	37
Figure 3.3.3: Sprung mass acceleration (active vs. passive).....	37
Figure 3.3.4: Sprung mass pitch acceleration (active vs. passive).....	38
Figure 3.3.8: PSD response of sprung mass bounce acceleration (active vs. passive)	38
Figure 3.3.9: PSD response of sprung mass pitch acceleration (active vs. passive).....	39
Figure 3.4.1: Schematic full car model [38]	40
Figure 3.4.2: Extended model of body.....	41
Figure 3.4.3: Extended model of controller	41
Figure 3.4.4: Extended model of suspension and tire	42
Figure 3.4.6: Sprung mass bounce acceleration.....	44
Figure 3.4.7: Sprung mass pitch acceleration	44
Figure 3.4.8: PSD response of sprung mass bounce acceleration.....	45
Figure 3.4.9: PSD response of sprung mass pitch acceleration	45
Figure 4.1.1: Schematic platoon system [15].....	49
Figure 4.2.1: Schematic quarter car model with longitudinal forces	50
Figure 4.2.2: Extended model of quarter-car vehicle	53

Figure 4.2.3: Relative space and velocity of vehicles [15].....	53
Figure 4.2.4: Range vs. range-rate diagram [15]	54
Figure 4.3.1: single bump	57
Figure 4.3.2: Relative distance between vehicles for single bump input.....	58
Figure 4.3.3: Relative velocity between vehicles for single bump input.....	58
Figure 4.3.4: Time delay variations for single bump input	59
Figure 4.3.5: Wheel torque (controller output) for single bump input	59
Figure 4.3.6: Spacing error ratio between vehicles in time domain for single bump input	60
Figure 4.3.7: Spacing error ratio between vehicles in frequency domain for single bump input	60
Figure 4.3.8: Random road profile.....	61
Figure 4.3.9: Relative distance between vehicles for random input.....	62
Figure 4.3.10: Relative velocity between vehicles for random input	62
Figure 4.3.11: Time delay variations for random input.....	63
Figure 4.3.12: Wheel torque (controller output) for random input.....	63
Figure 4.3.13: Spacing error ratio between vehicles in time domain for random input ...	64
Figure 4.3.14: Spacing error ratio between vehicles in frequency domain for random input	64
Figure 5.2.1: Quarter car model with look-ahead sensor [5]	67
Figure 5.2.2: Passive, active (lead), and active-preview (follower) with state communication.....	71

Figure 5.2.3: Lead-follower model and states communication.....	72
Figure 5.2.4: Extended model of active suspension of quarter car model.....	76
Figure 5.3.1: Single bump road profile.....	77
Figure 5.3.2: Body acceleration (passive, active and active preview).....	78
Figure 5.3.3: Suspension deflection (passive, active, and active preview).....	78
Figure 5.3.4: Tire deflection (passive, active, and active preview).....	79
Figure 5.3.5: Power demand (active and active preview).....	79
Figure 5.3.6: Unsprung mass motion and road tracking.....	80
Figure 5.3.7: Performance index variation vs. preview time.....	82
Figure 6.2.1: Schematic Kalman estimator diagram.....	86
Figure 6.2.2: Proposed estimator configuration.....	89
Figure 6.2.3: Schematic estimator block.....	90
Figure 6.2.4: Lead sub-model includes estimator.....	90
Figure 6.2.5: Estimator model in SIMULINK.....	91
Figure 6.3.1: Estimated road profile.....	93
Figure 6.3.2: Road roughness (input Gaussian noise).....	93
Figure 6.3.3: Body acceleration.....	94
Figure 6.3.4: Suspension deflection.....	95
Figure 6.3.5: Tire deflection.....	95
Figure 6.3.6: Power demand.....	96
Figure 6.3.7: Estimator dynamic error.....	97
Figure 6.3.8: Estimated tire deflection vs. calculated tire deflection.....	97

Figure 6.3.9: Body acceleration in frequency domain.....	98
Figure 6.3.10: Suspension deflection in frequency domain.....	99
Figure 6.3.11: Tire deflection in frequency domain	99
Figure 7.2.1: Schematic lateral motion of convoy vehicles (state communication).....	104

Nomenclature

Chapter 3:

- u : actuator force (active force)
- K : feedback gain
- A : states coefficient matrix
- B : actuator coefficient matrix
- D : input (road profile) coefficient matrix
- Q : states weight factors matrix
- R : active force weight factors matrix
- lqr : linear quadratic regulator function
- k : solution of Riccati equation
- m_s : sprung mass (body mass)
- m_u : unsprung mass
- b_s : suspension damping coefficient
- k_s : suspension stiffness
- k_t : tire stiffness
- φ_s : body pitch angle
- θ_s : body roll angle

Chapter 4:

- θ_l : road slip angle
- k : slip ratio

- r : wheel radius
- ω : wheel angular velocity
- v : wheel linear velocity along the slope
- v_x : linear forward velocity
- μ : friction coefficient
- ρ : air density
- C_d : drag coefficient
- A : vehicle frontal area
- sgn : sign function
- F_z : vertical tire force
- F_{slip} : slip resistance force
- F_{roll} : rolling resistance force
- F_{aero} : aerodynamic force
- R : relative space between target and preceding vehicle
- Δ_i : target's spacing error

Chapter 5:

- T_p : preview time
- σ : integral variable (in preview function)
- m_b : sprung mass
- m_w : unsprung mass
- C_b : suspension damping coefficient
- K_b : suspension stiffness
- K_t : tire stiffness
- P : solution of Riccati equation
- Q_1 : states weight factors matrix
- N : weight factors matrix of states and actuator

- x_s : sprung mass vertical motion
- x_u : unsprung mass vertical motion
- x_r : road profile elevation
- W : derivative of road profile function

Chapter 6:

- v : measurement noise vector
- η : input noise vector
- $E(x)$: expected function
- $Cov(x)$: covariance function
- σ : noise deviation
- G_0 : road roughness coefficient
- U_0 : vehicle speed
- L : kalman gain
- Q : input noise variance
- R : measurement noise variance
- N : measurement and input noise covariance
- \hat{x} : estimated state(s)

Chapter 1

1. Introduction

1.1 Introduction

Convoy vehicles, a series of individual vehicles traveling in close proximity on a specified path, have been recently the subject of research, especially in military applications.

Military convoys are used to carry soldiers, weapons and army supplements (Fig. 1.1.1). Many military drivers are young and inexperienced, and driver error has caused many fatal accidents in both peacetime and wartime [37]. Therefore, research about this topic is motivated, to enhance the safety of the convoy vehicles, such as military convoys and Intelligent Vehicle Highway Systems (IVHS), and avoid vibration-related driver fatigue, injury, overturning, and crashing (Fig. 1.1.2).

This thesis studies the potential benefits of replacing conventional passive suspension systems with a new generation of active systems to improve ride quality and safety. The idea of using communication between lead vehicle and followers in a convoy to improve the follower's dynamic response is the primary focus of this research. The lead vehicle thus acts as a look-ahead sensor to address practical limitations of traditional preview controlled suspensions and improve the effectiveness of active safety systems such as vehicle stability control.



Figure 1.1.1: Military convoy vehicles [AP Photo/ Ali Heidar, 2003]



Figure 1.1.2: Intelligent Vehicle Highway System (IVHS) [15]

The main issues in controlling convoy vehicle systems are:

Vertical dynamics and active suspension systems: reducing the body oscillation of each vehicle when it hits a bump to improve ride comfort of passengers. Furthermore, controlling the variation in the tire force of the vehicle enhances the stability and road holding ability.

Longitudinal dynamics and cruise control systems: the relative distance and velocity among vehicles in a platoon must be controlled to avoid crashes and enhance both individual and string stability of the convoy system. The main concern is that when a vehicle hits a bump, the forward velocity drops, and then the relative space between vehicles will be disturbed. Adaptive Cruise Control (ACC) systems will be implemented to control the relative space and velocity of vehicles in a simulated platoon.

Lateral dynamics and active steering control systems: the yaw motion of each vehicle in a convoy must be controlled to guarantee the individual and string stability of the vehicles laterally. In other words, by applying an active steering control system to generate correction torques about the yaw axis of a vehicle, each vehicle can better track the specified path, especially during cornering and spinning, and therefore the whole system stability will be improved. Sudden road obstacles can provide such disturbances in both military convoys and IVHS applications.

This research will be focused on the vertical dynamic aspects of the convoy vehicles, as well as some treatment of longitudinal dynamics.

Lateral dynamics and active steering control will be the subject of future work.

1.2 Problem statement

Using preview information of road irregularities to generate feed forward control gains, in addition to feedback gains in active suspension system, has been evaluated [2]. As will be mentioned in Chapter 5, implementing an active suspension system with some preview time significantly improves ride comfort by reducing body acceleration, and improves road holding by reducing tire deflection. Furthermore, the required power, which is called power demand, for the actuators is significantly reduced when preview is added to active suspension systems.

Conventionally, preview information is provided by placing sensors in front of the front bumper of the vehicle, which are called look-ahead sensors [5]. Therefore, the road irregularities are detected just before the vehicle hits them.

Using look-ahead sensors for each vehicle in a convoy is expensive, sensors are vulnerable, and can be confused by water or snow such as when potholes are filled with water.

This research proposes a lead-follower model to solve the problem of using look-ahead sensors. In fact, the lead vehicle plays the role of the look-ahead sensor.

The most significant advantage of this method is that the lead vehicle is subjected to the road irregularities in advance and communicates its response to the follower vehicles.

The lead vehicle model outputs, which are a combination of car body, unsprung mass and suspension/tire states, will be used to estimate the road profile for followers.

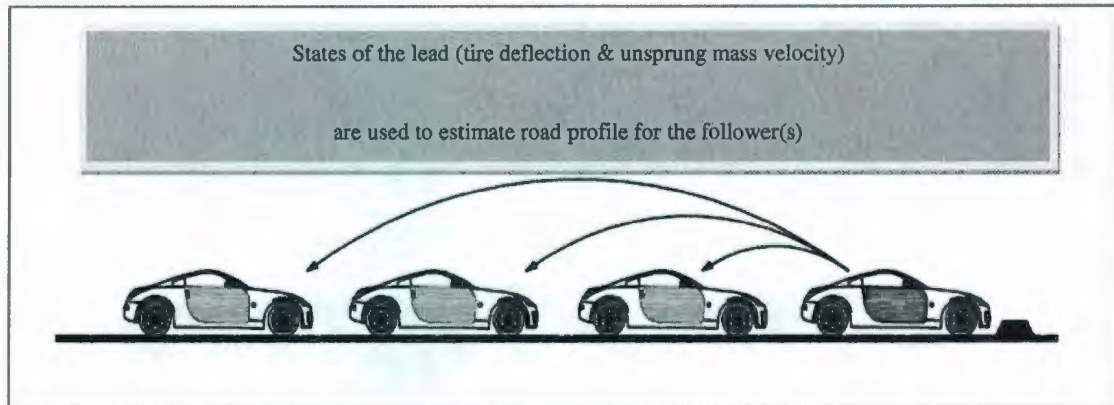


Figure 1.2.1: Schematic lead and follower(s) communication

1.3 Contribution of the thesis

As mentioned previously, the main contribution of this research is designing a lead-follower vehicle model to improve ride quality and safety of convoy vehicles. The proposed model is to emulate active suspension systems with look-ahead sensors, but should be more reliable and cheaper. Modeling and simulation is carried out with MATLAB and SIMULINK [33].

Also, as part of the research, the longitudinal dynamics of convoy vehicles with adaptive cruise control system is evaluated. The effect of road irregularities on forward velocity is investigated. The modeling and simulation of this part is carried out using the bond graph method in 20SIM [20]. Future work will implement the state-based preview controller into convoy vehicles with longitudinal control, to study the robustness of the

control method to uncertainties in following distance and time. In this thesis, constant known following distance and time are assumed.

1.4 Thesis organization

Chapter 2 provides the literature review of active and preview-active suspension modeling and design, and state observer design.

Chapter 3 designs active suspension systems for quarter car, half car, and full car models. Active suspension systems are compared with their passive counterparts.

Chapter 4 presents the longitudinal dynamics of convoy vehicles and evaluates the effect of road irregularities on longitudinal velocity. An adaptive cruise control system is implemented in which individual and string stability of the convoy is investigated.

Chapter 5 presents the convoy (lead-follower) model, with state communication from lead vehicle to follower(s). The suspension performance of passive, active and active with preview is evaluated.

Chapter 6 describes the methods to estimate some states, e.g. tire deflection, which are not measurable or difficult to measure. A Kalman observer (estimator) is used for this purpose. Also, the effect of an input noise and a measurement noise on the proposed state-based preview-controlled active suspension system is investigated.

Chapter 7 provides concluding discussion about this research and presents future work.

Chapter 2

2. Literature review

2.1 Literature review

Suspension systems of vehicles have been significantly developed during the last several decades. The main purposes of a suspension system are improving ride comfort of passengers and enhancing road holding.

A quarter car representation of a vehicle is shown in Fig. 2.1.1.

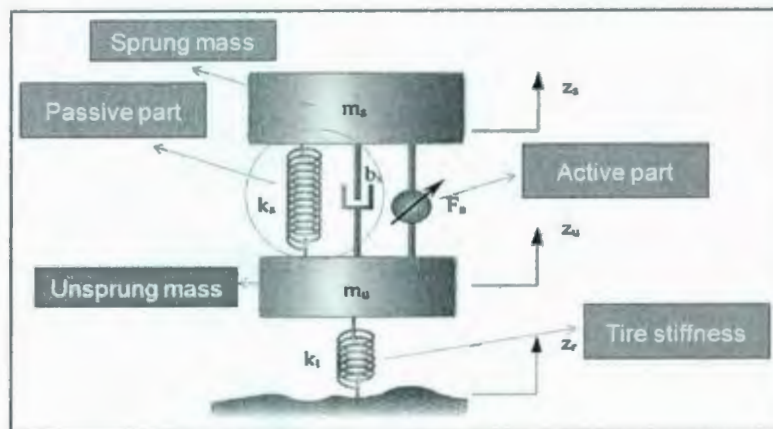


Figure 2.1.1: Quarter car model with passive and active part [15]

Suspension systems can be categorized as passive, semi-active, and active [15]:

Passive suspension system: the simplest suspension, which contains passive elements such as springs and shock absorbers. Early Egyptians used a simple leaf spring as a suspension system.

Semi active suspension system: in semi active suspensions, the viscous damping coefficient of the shock absorber can be controllable. The performance advantages of semi-active suspension systems are lower than for active suspension systems, but semi active suspension systems are generally less expensive and consume less energy than active suspension systems.

Active suspension system: active suspension systems use a separate actuator to exert independent force, typically in parallel with suspension passive elements, to reduce the vibration of the car body and improve road holding.

The schematic chart below, Fig. 2.1.2, shows the typical comparison among passive, semi-active, and active suspension systems based on the cost and performance of the system.

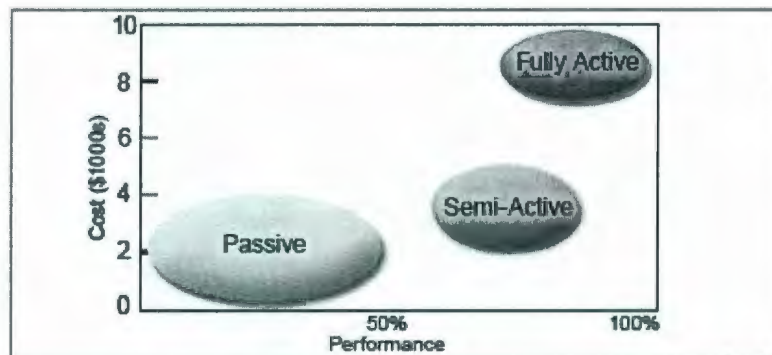


Figure 2.1.2: Schematic chart of suspension performances

In addition to the above types of suspension systems, this thesis uses and develops the concept of active-preview suspension system, or active suspension systems which preview the road ahead of the vehicle and feed the road profile to the active suspension controller. The proposed research will show the benefits of preview information to

improve ride comfort and road holding of a vehicle, and will propose a new method of generating the preview information.

The main focus of this chapter is on previous researches on active suspension, and active suspension with preview.

Rajamani [15] gives a thorough review and comparison of passive, semi-active and active suspension systems. Actuator forces in active suspensions are calculated using optimal control theory.

The author mentions two types of control strategies, which could be implemented in active suspension system: feed forward, and feedback.

In a feed forward model, the controller generates the output signal (actuator force) based on the preview road signals, which could be detected by sensors, in such a way to reduce the effect of disturbances on the system. On the other hand, the feedback model uses the signals from the system output and the road disturbance (input) to generate the actuator force to attenuate the vehicle body response.

Theoretically, the performance of the feed forward model is much better than feedback control method, but due to some limitations in case of measuring inputs and disturbances (preview inputs), the feed forward model is often impractical [19]. Therefore, the feedback control method has been mostly applied to tune active suspension systems.

The primary outputs of a suspension system are sprung mass velocity, suspension deflection, and tire deflection. Transfer functions of those outputs with respect to road

profile are chosen to show the effect of a feedback controller on suspension system. Moreover, the results of active and passive suspension systems are compared, especially at some critical points such as sprung and unsprung mass natural frequency.

The main variables in a suspension system, which are taken into account to improve the suspension performance, are body acceleration, suspension rattle space (working space), and tire deflection. A designer can weigh the system to significantly improve one of those variables, but there is a trade off among the suspension variables. In other words, improving one of those variables (body acceleration, suspension rattle space, and tire deflection) will disturb the other one(s) [see Chapter 3].

Hrovat [4] surveys applications of optimal control theory to generate active force in active suspension systems of quarter, half, and full car models. A comprehensive review of active suspension systems implemented in different types of vehicle models is given [see Chapter 3].

Moreover, Hrovat's paper develops the concept of performance index for the above mentioned models. Also, the effect of sprung mass jerk (the derivative of acceleration) is evaluated for a quarter car model.

In the case of half car model, a technique to decouple the half car into two quarter car models is mentioned, and the effect of preview information of front suspension for rear suspension is evaluated. The small amount of preview is enough to reduce the tire deflection, and a preview time up to 1 sec can significantly reduce body acceleration.

The results for the proposed models indicate that implementing Linear Quadratic Regulator (LQR) control for a suspension system (quarter, half, or full car model) can significantly improve the desired suspension state variables upon choosing suitable weight factors for the performance index.

A typical performance index equation is shown below (Equation 2.1.1). The inputs of a performance index function are the states of a system and actuator force, and the outputs are weight factors matrices (Q and R). The desired weight factors (regulators) are chosen to minimize performance index (J). More details are provided in Chapter 3.

$$J = \int_0^{\infty} (X \cdot Q \cdot X^T + u \cdot R \cdot u^T) dt \rightarrow \text{Performance Index} \quad (2.1.1)$$

Bender [1] is among the first authors to consider road preview information to generate active suspension forces. This paper evaluates the active suspension system with preview for single degree of freedom (DOF) quarter car models. The author considers two methods for optimizing the trade-off between vehicle responses.

In the first method, which is based on Wiener filter theory, the main approach is synthesizing the optimum characteristics (transfer function) of a free configuration system. The second approach, which is practically easier than the first one, employs a parameter search technique to optimize fixed desired suspension variable(s).

The results for the proposed model in [1] illustrate that applying the preview method reduces both body oscillation and clearance space (also called “rattle space”, related to suspension travel) compared to active suspension systems without preview.

Hac [2] used a preview function for both active suspension system and semi-active suspension systems. A quarter car with two DOF was used, optimal control theory was used to generate feedback gains, and a preview function was implemented to generate feed forward gains. The preview information was provided by placing sensors in front of the vehicle to detect the road profile. The strategy of implementing a semi-active system with some preview time is almost the same as for the active system with preview [10], except that the actuator force in the active suspension model is replaced by the product of the variable damping coefficient and suspension vertical velocity.

The results, which are evaluated for a single bump and random road profile, in both the time domain and frequency domain show improvement of body acceleration, tire deflection, and suspension deflection of the semi-active with preview model compared to traditional semi-active and passive suspensions.

The semi-active suspension with preview does not perform as well as the active suspension, because an active system supplies as well as dissipates energy. The semi-active system merely dissipates energy.

The effect of preview time for semi-active suspension systems is studied by Soliman and Crolla [11]. This paper shows the effect of a look-ahead sensor to feed preview information to improve ride comfort (body acceleration), and tire dynamic forces (tire deflection). A Pade approximation technique is employed to simulate the preview information inputs to the control box, and estimate the outputs.

The results of an active suspension system with and without preview, semi-active suspension system with and without preview and passive suspension system, show that the performance of the semi-active suspension system with preview is almost the same as for active system without preview. The main effect of the preview method in a semi-active model is the significant reduction of the body acceleration peak value at the resonance frequency. Moreover, the body acceleration and dynamic tire forces are significantly reduced in a semi-active model with preview in comparison with semi-active without preview and passive systems. This conclusion can be potentially used in convoy vehicles, which will be studied in this research. The proposed convoy vehicle model in this thesis is based on a fully active suspension system; however, replacing fully active suspensions by semi-active suspensions will significantly reduce the cost of a system.

Results in [11] illustrate that more preview time will give better results, but a preview time greater than 0.15 (sec) did not significantly improve the system performance. Short optimal preview times are also mentioned in Hac [2].

The effect of preview time on suspension performance has also been studied by Thompson and Pearce [5]. Their model is a quarter car with two DOF which is subjected to a step input. The look-ahead sensors are placed some distance ahead of the vehicle to detect the road variations and send them to the preview function generator.

The results of the paper show the variation of performance index, which is assumed to be a quadratic integral type, versus preview time to define the maximum effective preview time. The optimal preview time for their proposed model and parameters was 0.25 sec.

In another paper by Thompson and Pearce [9], the above scenario is evaluated for a half car model with four DOF, which is subjected to a random road profile. In addition to the effect of preview time and preview sensor distance on performance index, which is calculated based on direct computation, the effect of time delay for rear suspension in the half car model is studied.

Langlois et al. [8] modeled an active-preview suspension system using a quarter car (two DOF) and full car model with ten DOF. The results are evaluated for both a single bump, and random road profile. The strategy to design optimal feedback, and feed forward control gains was the same as in the paper by Thompson and Pearce [5].

The results show better performance of preview active suspension systems compared to active suspensions, and both are significantly better than a passive suspension (for both types of road profile). Also, the effect of vehicle forward velocity (longitudinal) on RMS value of suspension deflection and pitch angle was evaluated, and it was shown that in both cases the active system with preview is much better than both active (zero preview) and passive for improving ride comfort.

Marzbanrad et al. [3] studied active suspension with preview for a full car model with seven DOF subjected to haversine (sinusoidal single bump) and stochastic filtered white

noise. Preview information (sensors) significantly improved performance index, power demand, and system sensitivity to the velocity and mass of the vehicle.

Models of active, active with delay (for rear suspension), and active with preview suspensions were illustrated and compared with a passive suspension. The results show improvement in performance index, and mean-square acceleration under rough road excitation. Moreover, optimal preview control shows significant improvement of the performance index and mean square acceleration for all types of road profiles. The power demand for active preview is less than for an active suspension. A short preview time is enough to obtain the desired results, and the results are not significantly affected by increasing the preview time. Finally, they show that the performance index is not sensitive to the sprung mass, which could vary with the number of passengers and carried load, for all types of road profile.

Marzbanrad et al. [12] studied the stochastic optimal preview control of a vehicle suspension system. This paper presented the effect of preview time on active suspension performance using a half car model with four DOF. The active force is generated based on stochastic optimal control theory, and the states of the model are estimated by using Kalman filter theory. Suspension performance and power demand for passive, active, active preview and active with delay time suspensions were compared.

The results show better performance of active suspension systems with preview compared to active and passive. Also, the required power for active with preview is significantly reduced compared to active systems without any preview time. The

literature discusses which states are considered measurable, and which are typically estimated. Yu and Crolla [13] and Marzbanrad et.al [12] focus on the required measurements for estimating tire deflection. As will be seen in Chapter 6, the research presented in this thesis will require estimation of the tire deflection.

Designing an observer to estimate some state(s), which are difficult to measure or even immeasurable, is discussed by Yu and Crolla [13]. This paper presents a state estimator, based on Kalman filter theory, for an active suspension system of a quarter car model with two DOF. The main contribution of this paper is choosing the best configuration of measured state(s) to estimate immeasurable state variables. For this purpose, five sets of measured state variables are considered such as: Set 1 (suspension deflection, body velocity), Set 2 (suspension deflection, wheel velocity), Set 3 (body velocity, wheel velocity), Set 4 (suspension deflection, wheel velocity, body velocity), and Set 5 (suspension deflection).

It is shown that the most accurate estimation is obtained based on Set 4. Furthermore, this paper compares an adaptive estimator with a constant estimator. The variation in road input condition and the variations in system parameters (e.g. body mass) affect variations in estimator gains; therefore, the necessity of an adaptive estimator is investigated.

Designing an adaptive estimator requires more calculation. However, for a range of road inputs and system parameters, there was no significant advantage of using adaptive

estimator gains instead of constant estimator gains. For typical passenger cars, estimator performance was insensitive to normal variations in vehicle parameters.

Vahidi and Eskandarian [6] evaluate the effect of preview uncertainties on active suspension systems with preview time, and show the benefits of using preview information to reduce the effect of the uncertainties. Two types of uncertainties were evaluated: preview sensor noise, and possible presence of false soft objects on the surface of the road. The results show that longer preview time can be more affected by measurement noise. Also, it was shown that in both cases the tire deflection is the state most sensitive to preview noise, while suspension deflection is less affected. Furthermore, preview sensors significantly improve body acceleration, suspension deflection, and tire deflection.

Karnopp [7] proposed a long train (convoy) model of quarter cars with two DOF. The main goal of the paper was generating active actuator forces based on the preview information (the states) of the preceding vehicles. Unlike the previous papers which used a preview function to generate feed forward gains; the preview model in Karnopp is based on the dynamic equations of vehicles.

The dynamic equations of the platoon were considered, along with a criterion function, which contained sprung mass acceleration and suspension deflection. A continuous form of the convoy model was used, analogous to a fluid mechanic system, to which Lagrangian and Eulerian analysis was applied. The dynamic equations of the continuum

model generated the active force value based on preceding vehicles. The evaluation was based solely on the dynamics of the system, and there was no control method applied.

2.2 Conclusion

This chapter presented relevant research about active suspension and active suspension with preview systems. Implementing an active suspension system significantly improves one of the suspension variables (body acceleration, suspension rattle space, and tire deflection); however, the trade off among the variables causes the other variable(s) to be worsened as the primary variable of interest improves.

All researches show that after a certain point, longer preview time does not significantly improve suspension performance, and results in the system consuming more power. Preview information is typically provided by placing look-ahead sensors on or ahead of the front bumper, which has some limitations [see Chapter 5].

The proposed method in this thesis is replacing the look-ahead sensors by states of a lead vehicle [Chapter 5, Chapter 6].

Chapter 3

3. Modeling of active suspension systems with the bond graph method

3.1 Introduction

The main goal of this chapter is evaluating active vs. passive suspension systems with the aid of the bond graph method.

The bond graph method has attracted considerable attention in modeling and simulation of dynamic systems [18]. Arguably the biggest advantage of this method is its ability to model systems with elements from different energy domains. Also, sub models of varying complexity can be built for different automotive subsystems or components, and then easily combined. Visual inspection of a bond graph can reveal the presence of algebraic loops and dependent states which create implicit or differential-algebraic equations. Moreover, combining bond graphs with block diagrams, iconic diagrams, and interfacing with MATLAB makes the bond graph method a powerful tool for modeling, simulation and control of dynamic systems.

Three models of a vehicle's suspension system have been proposed:

- Quarter car model, with two degrees of freedom (DOF)
- Half car model, with four DOF
- Full car model, with seven DOF

The results are evaluated in both the time domain and frequency domain (power spectral density). The results in the frequency domain can be particularly interesting when the system frequency approaches the natural, or resonance, frequency. In the following results, the body acceleration, especially bounce acceleration, has been considered as the main parameter of passenger ride comfort. Therefore, the reduction of body acceleration at natural frequency has been strongly weighted.

The main parameters, or states, in the suspension system are body acceleration, suspension deflection, and tire deflection. An optimal control theory or Linear Quadratic Regulator (LQR) design is employed to generate the active force. In other words, the LQR method is used to optimize the performance index (J) of proposed models.

$$\dot{X} = AX + Bu + Dw \rightarrow \text{State equation} \quad (3.1.1)$$

$$J = \int_0^{\infty} (X \cdot Q \cdot X^T + u \cdot R \cdot u^T) dt \rightarrow \text{Performance Index} \quad (3.1.2)$$

$$K = \text{lqr}(A, B, Q, R) \rightarrow \text{Feedback gain} \quad (3.1.3)$$

$$u = -KX \rightarrow \text{Active force} \quad (3.1.4)$$

In performance index equation (Equation 3.1.2), the state vectors (X) and actuator force (u) are calculated to minimize performance index (J).

As can be seen in the equation sets, the MATLAB command “lqr” is used to generate feedback gain. The feedback gain (K) is the symmetric positive-definite matrix of the Riccati equation:

$$A^T k + kA - \frac{kBB^T}{R} + Q = 0 \rightarrow \text{Riccati Eq.} \quad (3.1.5)$$

$k \rightarrow$ solution of Riccati Eq.

$$K = -\frac{kB}{R} \rightarrow \text{Feedback gain} \quad (3.1.6)$$

The matrix (A) is related to system parameters, and the matrix (B) is related to actuator forces. The matrices (Q) and (R) are the weighting matrices, chosen based on the desired improvement in the system parameters. Different weighting factors can be used to emphasize ride quality, suspension deflection or road holding. More details about system parameters and performance index are provided in the following sections.

Minimizing sprung mass acceleration, suspension travel, and tire force variations are competing objectives, and the designer must choose to weight one more heavily at the expense of the others.

Also, all models are evaluated for both a single bump, and a random road profile.

The details of each model and the results are shown in following sections.

3.2 Quarter car model (active vs. passive)

Bond graph modeling is employed to model quarter, half, and full car models. A brief tutorial of using bond graph modeling is presented in this part:

Bond graph is a graphical description of dynamic systems, and used to model different types of dynamic systems from different types of energy domains.

Two types of junctions are used to connect elements in a model:

- Zero junction (0): the property of zero junction is that elements with common effort (e) connect to this junction, and the algebraic summation of flow (f) is zero.

$$e_1 = e_2 = e_3 = \dots \quad \sum_i f_i = 0$$

- One junction (1): the property of one junction is that elements with common flow (f) connect to this junction, and the algebraic summation of effort (e) is zero.

$$f_1 = f_2 = f_3 = \dots \quad \sum_i e_i = 0$$

In Table 3.2.1, the analogies between mechanical and electrical domains in terms of effort and flow are listed. A simple example in Fig. 3.2.1, illustrates the analogy between mechanical (mass, spring, and damper) and electrical (inductance, capacitance, and resistance) systems with bond graph modeling [18].

Table 3.2.1: Analogies between mechanical and electrical systems in terms of effort and flow

Variable	General	Mechanical	Electrical
Effort	$e(t)$	Force (torque)	Voltage
Flow	$f(t)$	Velocity (angular velocity)	Current
Momentum or Impulse	$p = \int edt$	Momentum (angular momentum)	Flux linkage
Displacement	$q = \int fdt$	Distance (angle)	Charge
Power	$p(t) = e(t)f(t)$	$F(t)V(t)[\tau(t)\omega(t)]$	$e(t)i(t)$
Energy (kinetic)	$E(p) = \int fdp$	$\int VdP[\int \omega dH]$	$\int id\lambda$; Magnetic
Energy (potential)	$E(q) = \int edq$	$\int FdX[\int \tau d\theta]$	$\int edq$; Electric

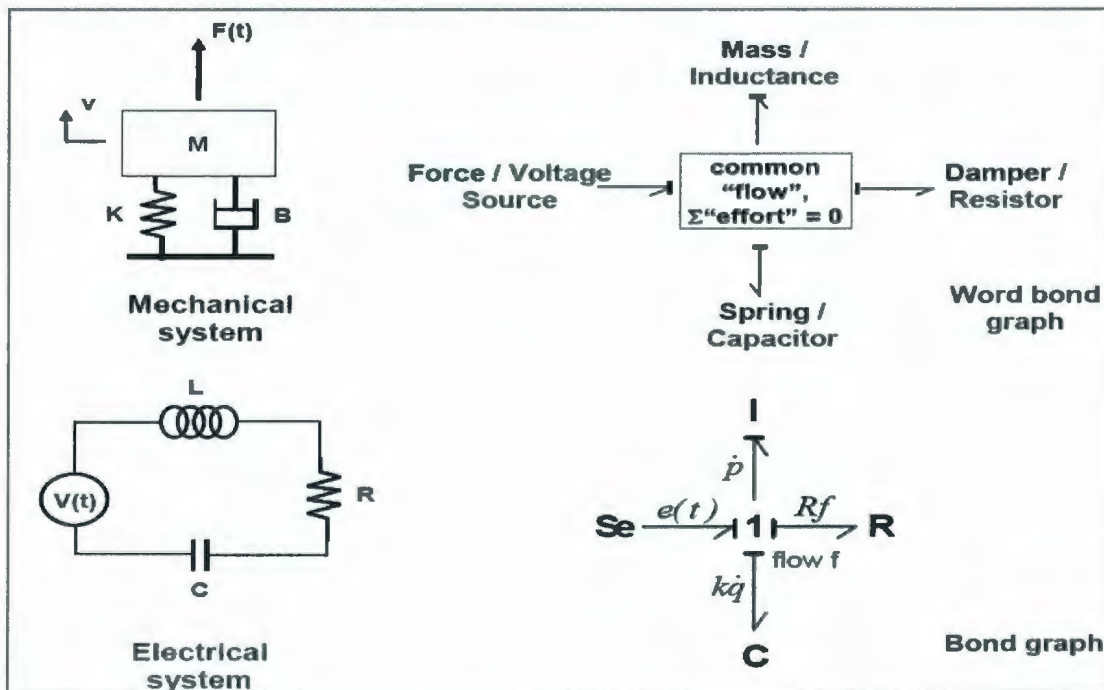


Figure 3.2.1: Example of similar mechanical and electrical systems with bond graph modeling

The schematic model of the active suspension system based on the quarter car model is shown in Fig. 3.2.2. The system has two degrees of freedom (vertical motion of a sprung and unsprung mass). The parameter values are given in Table 3.2.2.

Four states are used to describe the quarter car model, and these states are fed to an optimal controller to generate actuator force, which is placed in parallel with suspension stiffness and damper (see the actuator in Fig. 3.2.2). All models are built with the bond graph method and are simulated in the 20SIM environment [20]. Also, the calculation of control gains is carried out in MATLAB.

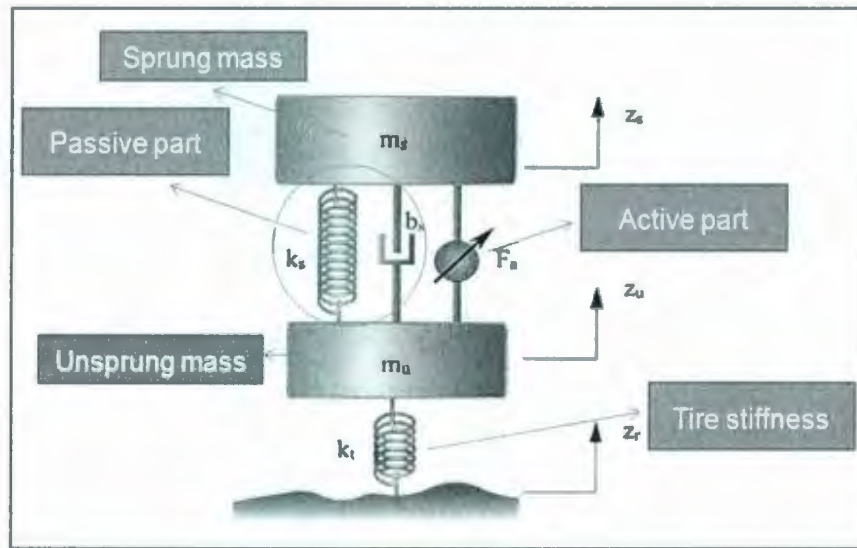


Figure 3.2.2: Schematic quarter car model [15]

The equations of motion for the proposed quarter car model are:

$$m_s \ddot{z}_s + b_s (\dot{z}_s - \dot{z}_u) + k_s (z_s - z_u) = F_a \quad (3.2.1)$$

$$m_u \ddot{z}_u + k_t (z_u - z_r) - b_s (\dot{z}_s - \dot{z}_u) - k_s (z_s - z_u) = -F_a \quad (3.2.2)$$

Table 3.2.2: Parameters & values of quarter car model

Parameter	Value
Sprung mass (M_s)	1136 kg
Unsprung mass (M_u)	60 kg
Suspension damping (b_s)	3924 N/(m/s)
Suspension stiffness (k_s)	36294 N/m
Tire stiffness (k_t)	1824700 N/m

The proposed bond graph model is shown in Fig. 3.2.3. The model is composed of five main parts:

Sprung mass (body): this part is shown with (I) and (MSe) elements at the most upper part of the model. The (I) element is used to simulate mass of the body and the (MSe), modulated source of effort, is used to simulate the weight of the body.

Unsprung mass: the elements of this part, which are similar to the sprung mass, indicates the mass and weight of the suspension, wheel, axel, and lower body of the vehicle.

Passive suspension: the passive suspension system, which is shown with C (stiffness) and R (damping coefficient), is placed between sprung and unsprung masses. As can be seen, a 1 junction is used to connect passive suspension elements together which have a common velocity.

Tire (wheel): the tire model is simulated with C element which indicates the stiffness of the tire (wheel). The tire damping is assumed negligible. The tire model is placed between road profile, which is shown with MSf (modulated source of flow), and unsprung mass in the lowest part of the model.

Active force (actuator): this part, which is simulated with modulated source of effort (MSe) along with saturation block, takes the states of the system, multiplied by the feedback gain (K) and then generates active force.

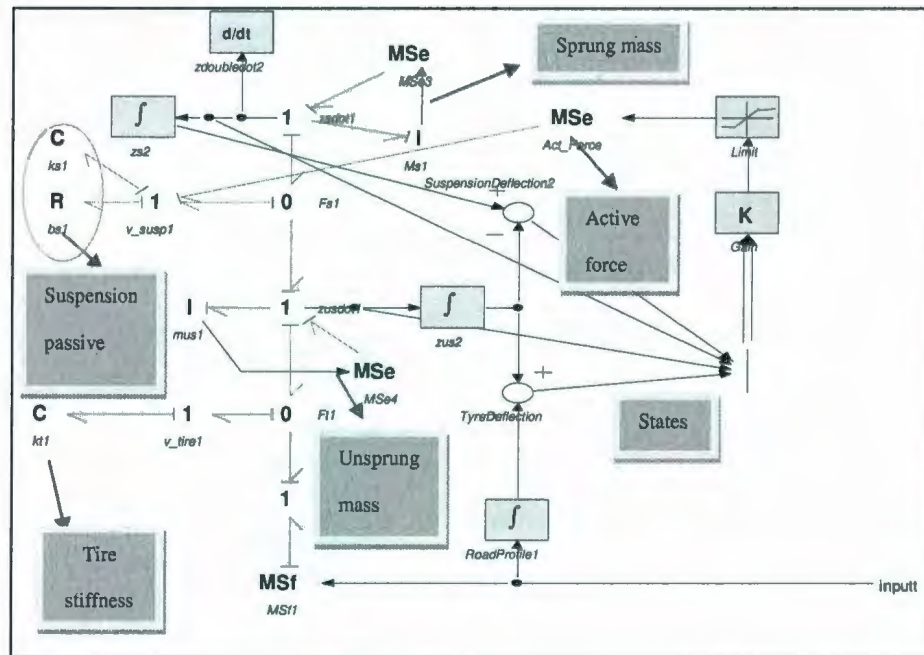


Figure 3.2.3: Active suspension system bond graph model (quarter car model)

3.2.1 Improving ride comfort

The proposed road profile is a single bump with height of 0.2 m, and the duration is from 1 sec to 2 sec (Fig. 3.2.4).



Figure 3.2.4: Single bump road profile

The main purpose of this section is implementing an optimal controller to improve ride comfort of the vehicle, by reducing body acceleration.

The weighting factors and matrices used to tune the active suspension system for the quarter car model are:

$$Z = \begin{pmatrix} z_1 \\ z_2 \\ z_3 \\ z_4 \end{pmatrix} = \begin{pmatrix} z_s - z_u \\ \dot{z}_s \\ z_u - z_r \\ \dot{z}_u \end{pmatrix} \rightarrow \begin{pmatrix} \text{suspension deflection} \\ \text{sprung mass velocity} \\ \text{tire deflection} \\ \text{unsprung mass velocity} \end{pmatrix} \quad (3.2.3)$$

$$Q = \text{diag}([44,12,100,0]), \quad R = 1e - 6 \quad (3.2.4)$$

The diagonal weight matrix of states, Q, is considered to improve the body acceleration, by increasing the second states' weight factor (body velocity). In other words, increasing a weight factor penalizes large variations of that state by increasing their contribution to the cost function.

As shown in Fig. 3.2.5, Fig. 3.2.8, Fig. 3.2.6 and Fig. 3.2.9, the sprung mass acceleration and suspension deflection of the active system is significantly reduced compared to the passive suspension. However, the tire deflection and road holding are worsened in order to improve the ride quality (Fig. 3.2.7 and Fig. 3.2.10).

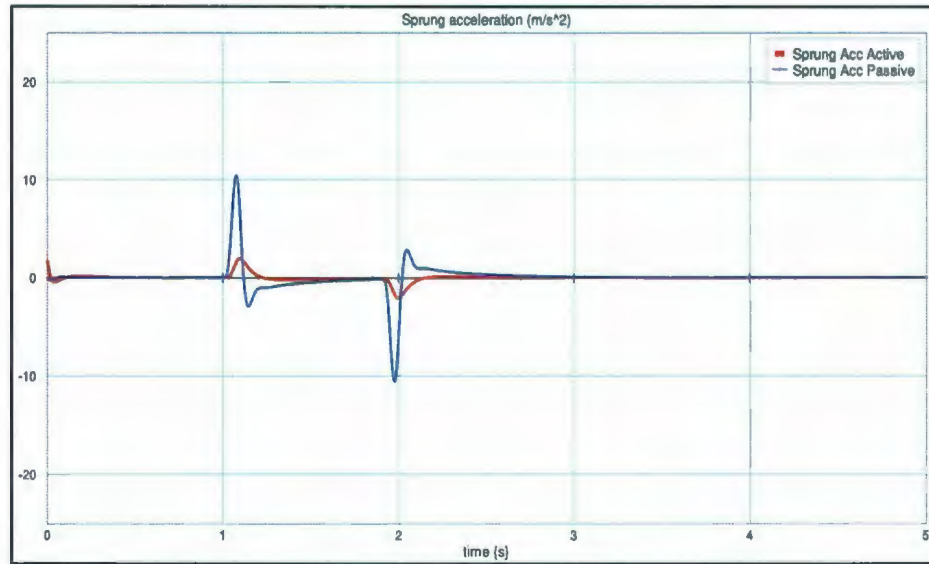


Figure 3.2.5: Sprung mass acceleration (active vs. passive)

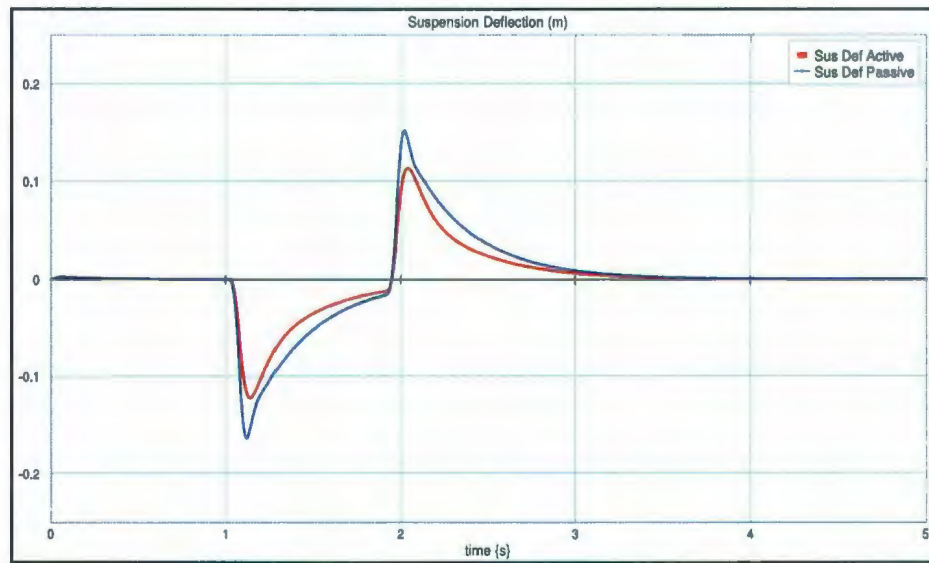


Figure 3.2.6: Suspension deflection (active vs. passive)

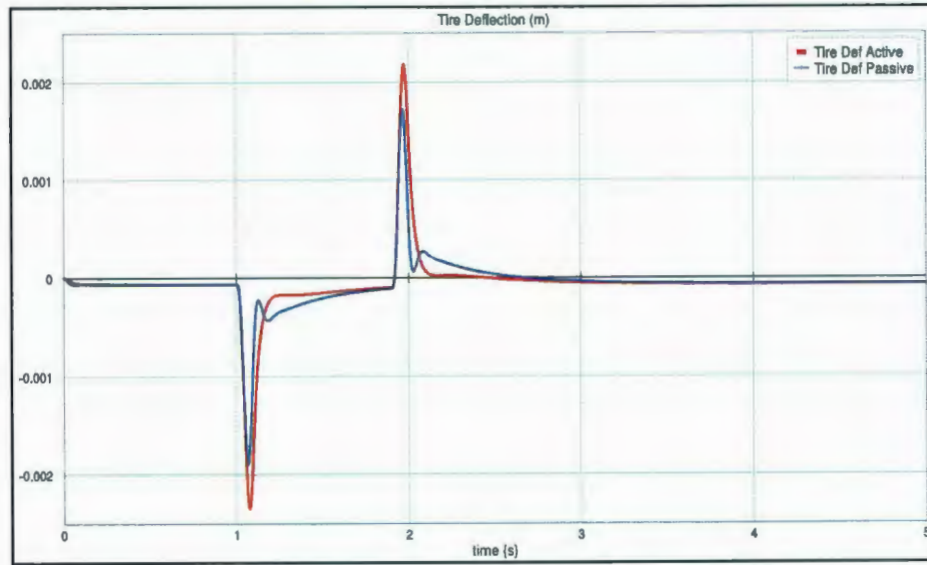


Figure 3.2.7: Tire deflection (active vs. passive)

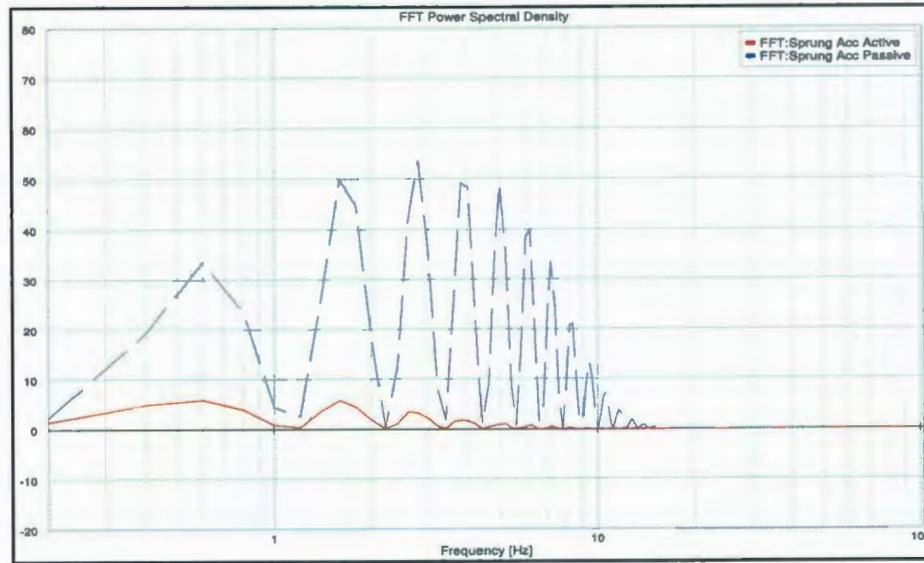


Figure 3.2.8: PSD response of sprung mass acceleration (active vs. passive)

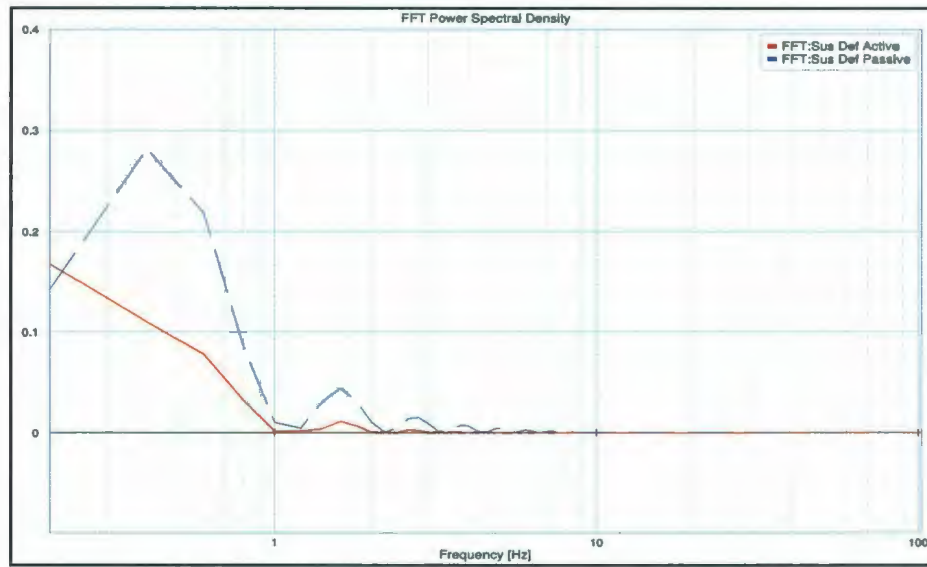


Figure 3.2.9: PSD response of suspension deflection (active vs. passive)

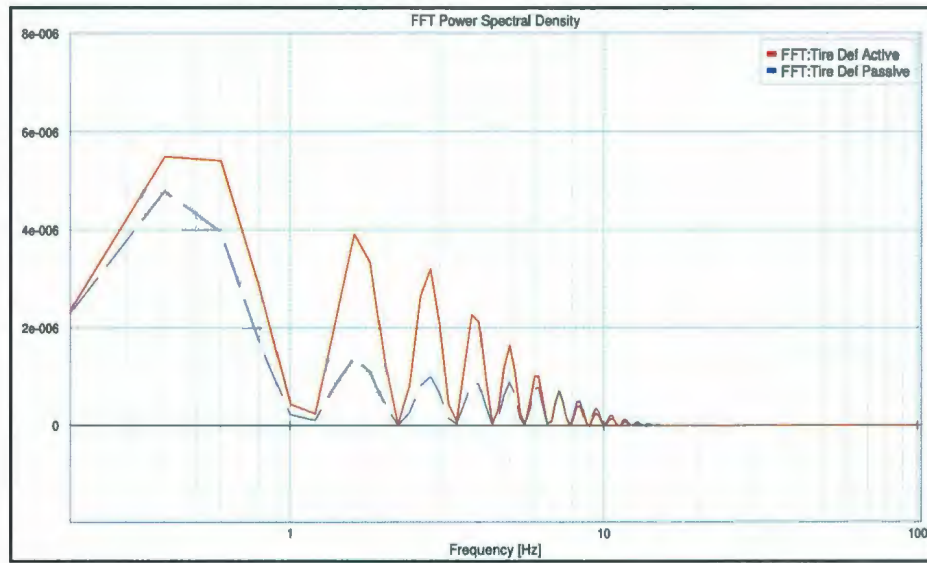


Figure 3.2.10: PSD response of tire deflection (active vs. passive)

3.2.2 Improving road holding

The tradeoff issue in an active suspension system implies that improving ride comfort disturbs a road holding and vice versa. In Section 3.2.1, the weight factors of the optimal controller are chosen to obtain better ride comfort.

This section proposes the weight factors to reduce tire deflection and improve road holding.

$$Z = \begin{pmatrix} z_1 \\ z_2 \\ z_3 \\ z_4 \end{pmatrix} = \begin{pmatrix} z_s - z_u \\ \dot{z}_s \\ z_u - z_r \\ \dot{z}_u \end{pmatrix} \rightarrow \begin{pmatrix} \text{suspension deflection} \\ \text{sprung mass velocity} \\ \text{tire deflection} \\ \text{unsprung mass velocity} \end{pmatrix} \quad (3.2.5)$$

$$Q = \text{diag}([10, 1, 1e5, 0]), \quad R = 1e-6 \quad (3.2.6)$$

As can be seen in the Q matrix, the third element, which is related to the tire deflection state, is significantly weighted.

The body acceleration is slightly improved (Fig. 3.2.11, Fig. 3.2.14).

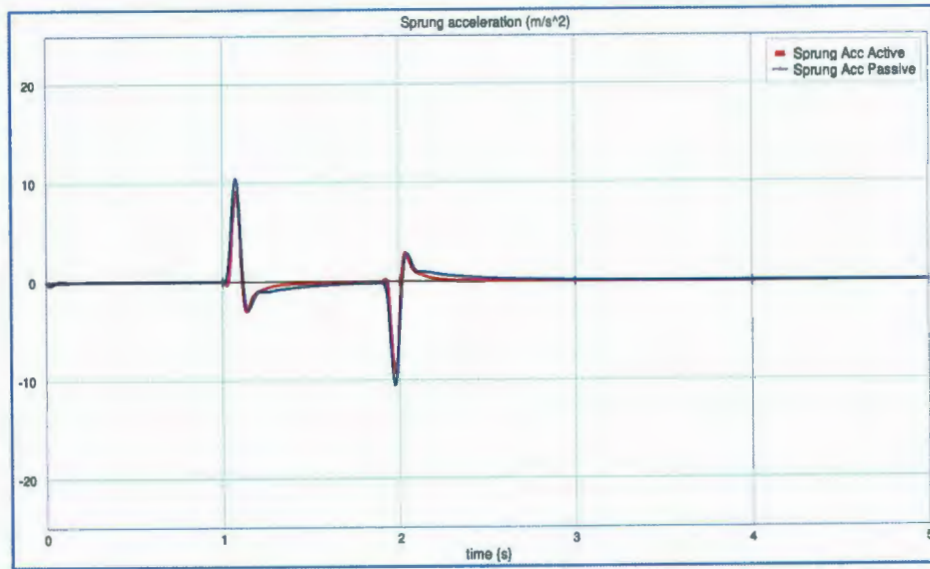


Figure 3.2.11: Sprung mass acceleration (active vs. passive)

The suspension deflection is worsened (Fig. 3.2.12, Fig. 3.2.15).

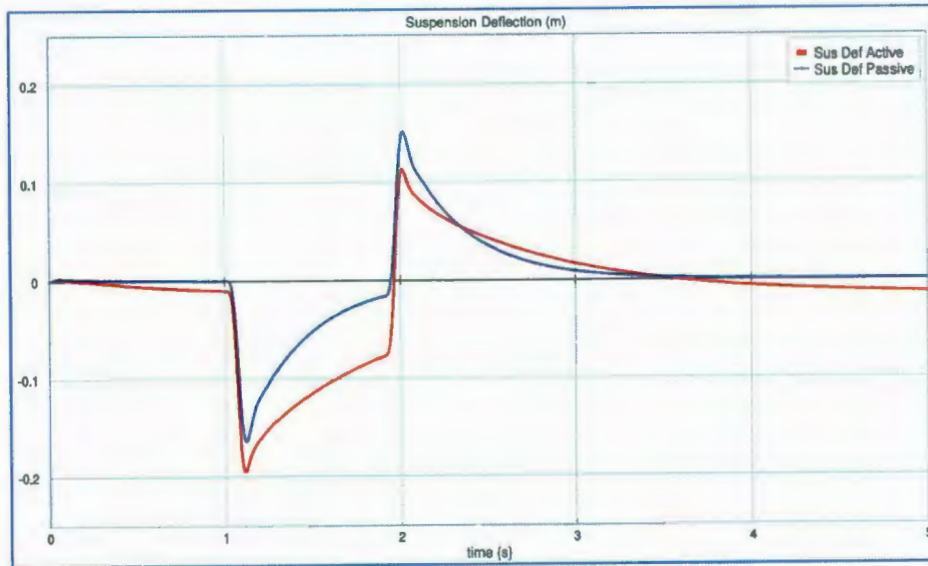


Figure 3.2.12: Suspension deflection (active vs. passive)

The tire deflection is significantly reduced, and therefore, the road holding is improved (Fig. 3.2.13, Fig 3.2.16).

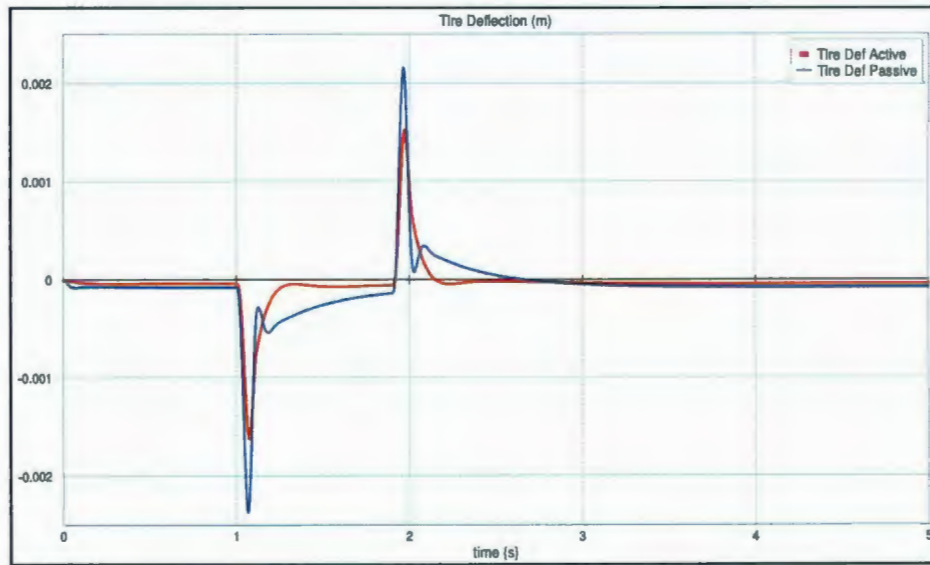


Figure 3.2.13: Tire deflection (active vs. passive)

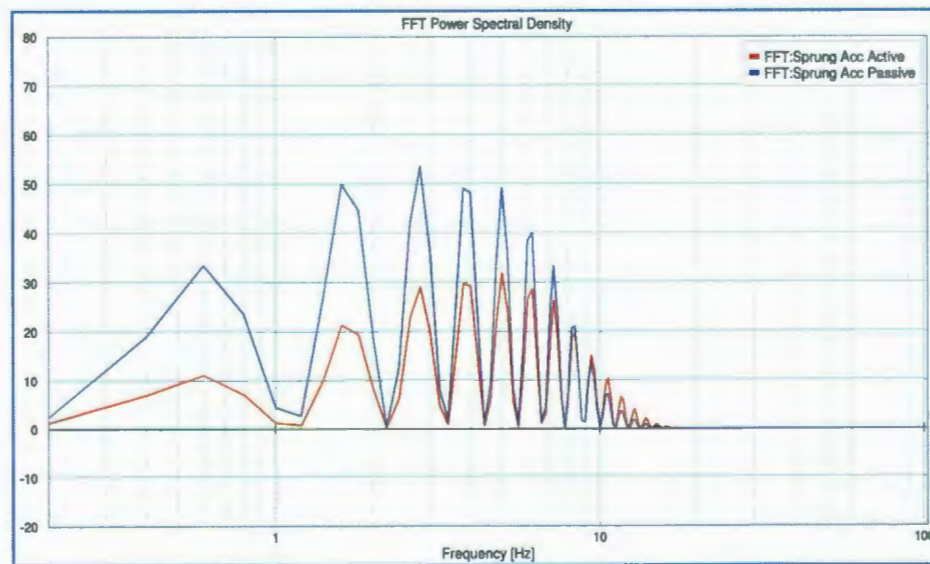


Figure 3.2.14: PSD response of sprung mass acceleration (active vs. passive)

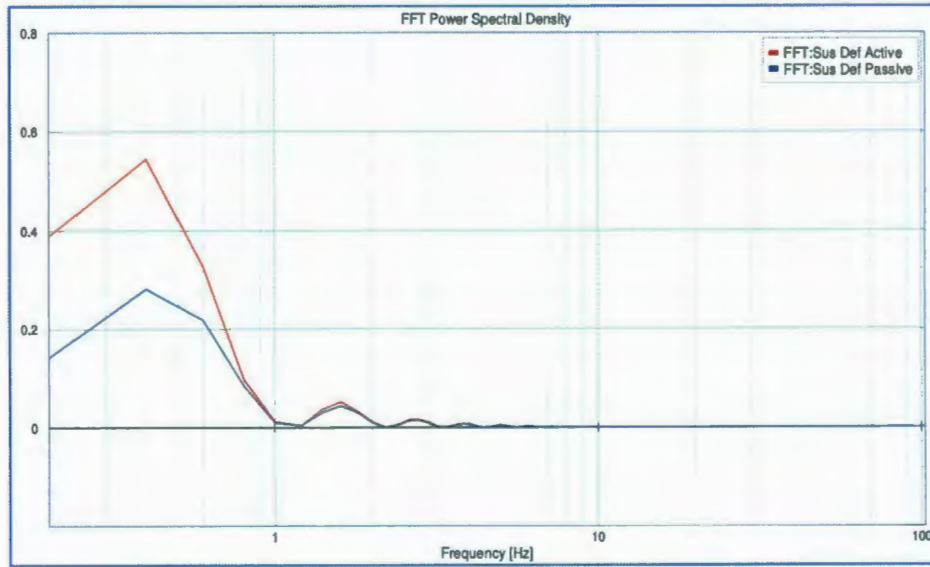


Figure 3.2.15: PSD response of suspension deflection (active vs. passive)

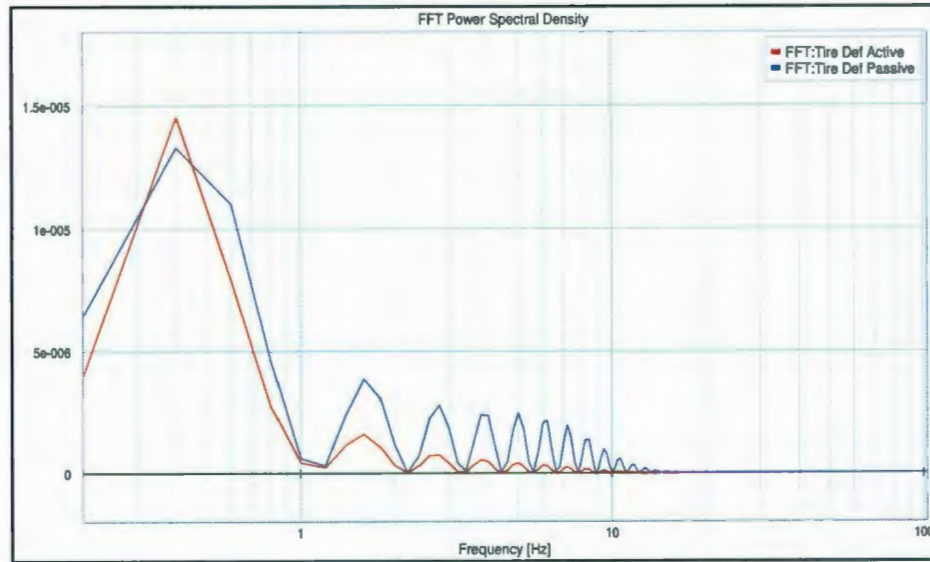


Figure 3.2.16: PSD response of tire deflection (active vs. passive)

3.3 Half car model (active vs. passive)

The proposed quarter car model, which was evaluated in Section 3.2, is the simplest model of a vehicle. Nonetheless, the quarter car model is fairly applicable to evaluate active vs. passive suspension systems and to obtain useful information from suspension systems even though it just contains the vertical (bounce) motion of the suspension system. The next step in realizing more realistic vehicle and suspension systems (if desired) is the half car model which contains pitch angle of the body in addition to the bounce motion.

The schematic half car model with four DOF is shown in Fig. 3.3.1, and the parameters are listed in Table 3.3.1.

The proposed half car model is the longitudinal view of a car, where the front wheels hit the bump, and the rear ones are subjected to the bump after some delay which is calculated based on the vehicle's wheelbase and velocity. The delay time for this case study is 0.1 sec (wheelbase is 2.8 m, and the forward velocity is assumed 28 m/s).

The states and weight matrices, to improve ride comfort, for proposed half car model is:

$$\text{States: } X = [x_s, \dot{x}_s, \varphi_s, \dot{\varphi}_s, x_{u1}, \dot{x}_{u1}, x_{u2}, \dot{x}_{u2}] \quad (3.3.1)$$

$$Q = \text{diag}([6.25, 1, 0.06, 6.25, 0, 0, 0, 0]), R = \text{diag}([1e-7, 1e-7]) \quad (3.3.2)$$

Table 3.3.1: Parameters and values of half car model

Parameters	Values
Sprung mass (M_s)	1136 kg
Pitch moment of inertia (I_p)	2400 kg m ²
Unsprung mass (M_u)	60 kg
Suspension damping (C_s)	3924 N/m/s
Suspension stiffness (k_s)	36294 N/m
Tire stiffness (k_u)	182470 N/m
Distance from c.g to front wheel (l_1)	1.15 m
Distance from c.g to rear wheel (l_2)	1.65 m

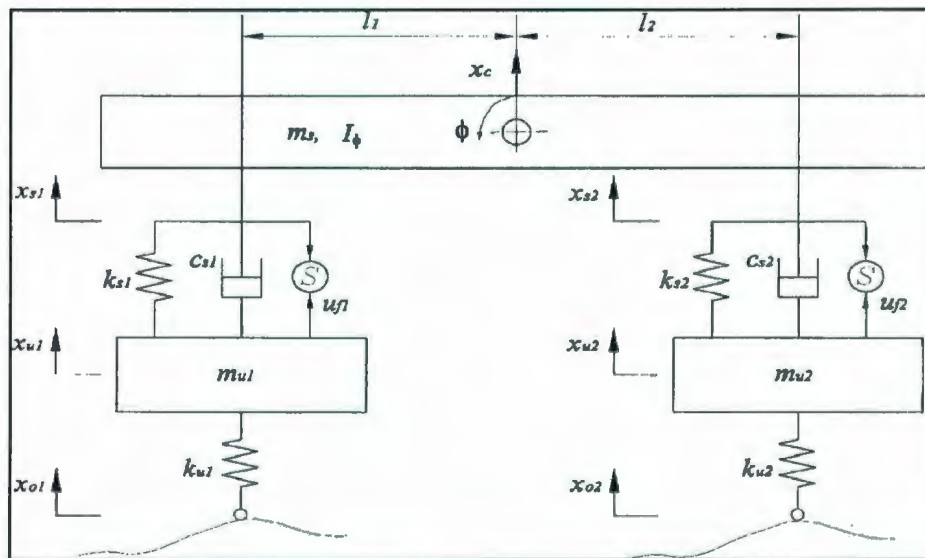


Figure 3.3.1: Schematic half car model [9]

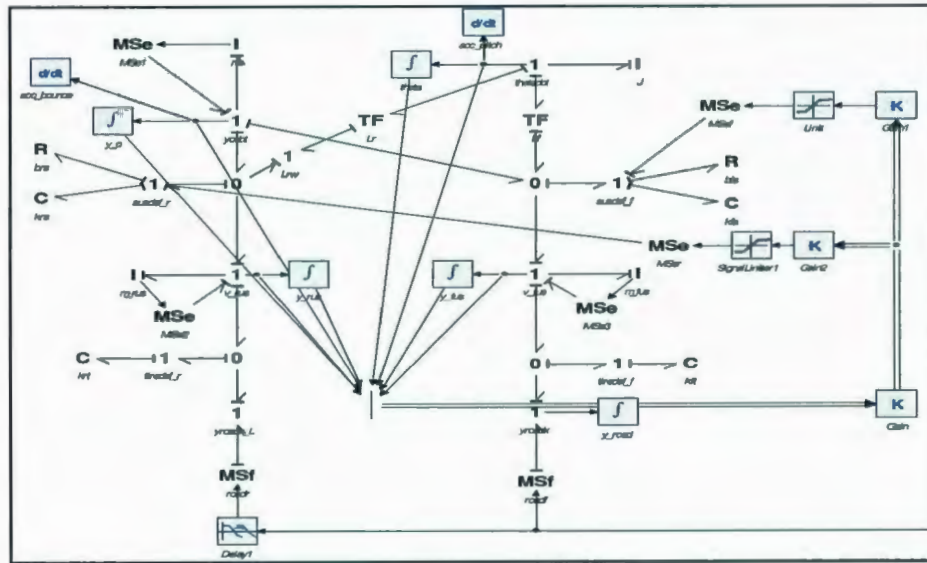


Figure 3.3.2: Extended model of active suspension system (half car)

As shown in Fig. 3.3.3 and Fig. 3.3.5, the body bounce acceleration is significantly improved. However, the pitch angular acceleration of the sprung mass is slightly improved as well (Fig. 3.3.4, Fig. 3.3.6).

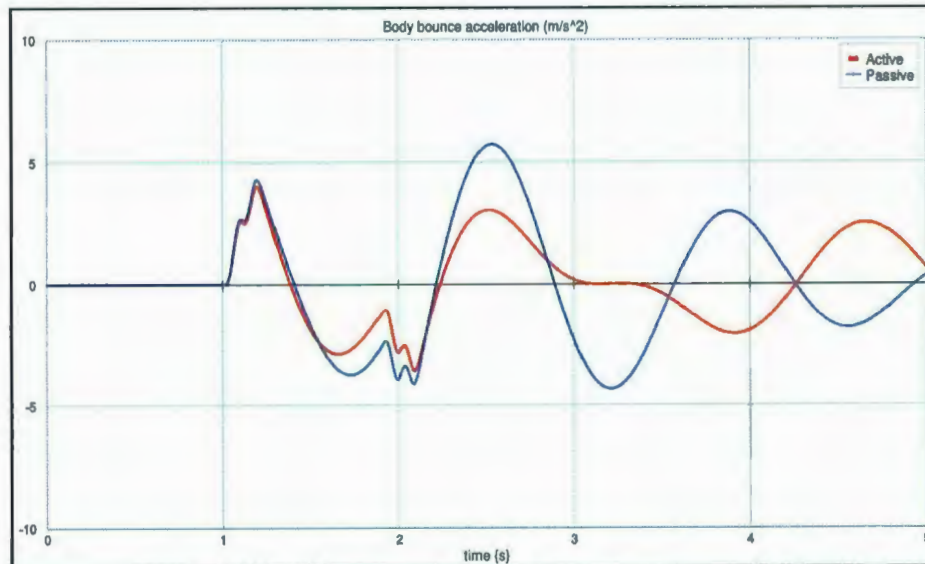


Figure 3.3.3: Sprung mass acceleration (active vs. passive)

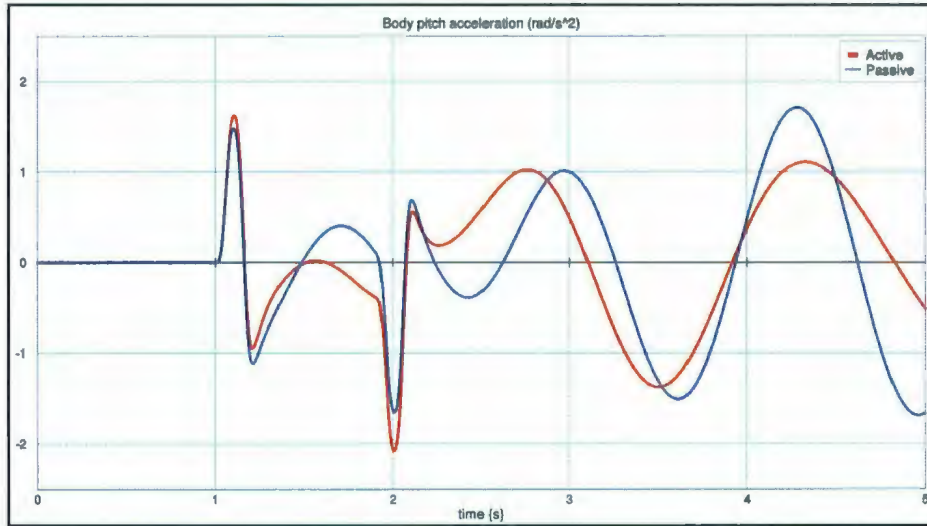


Figure 3.3.4: Sprung mass pitch acceleration (active vs. passive)

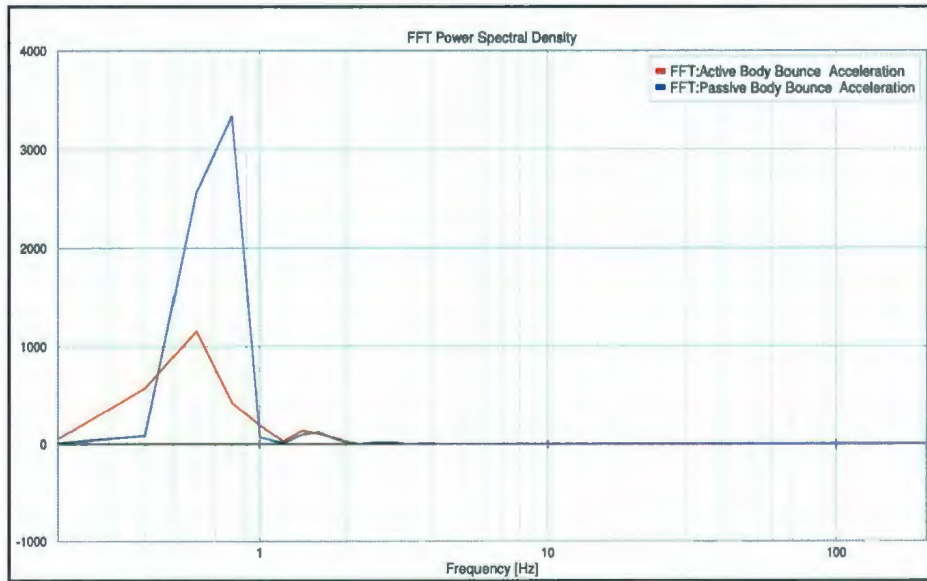


Figure 3.3.8: PSD response of sprung mass bounce acceleration (active vs. passive)

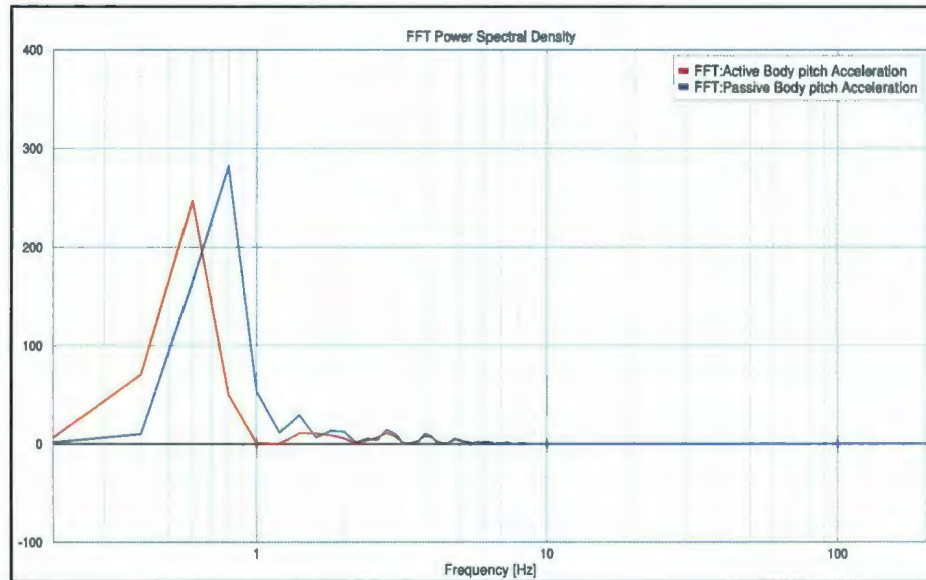


Figure 3.3.9: PSD response of sprung mass pitch acceleration (active vs. passive)

3.4 Full car model (active vs. passive)

The half car model, which was evaluated in Section 3.3, can show the effect of body pitch motion, but still is not capable of depicting other degrees of freedom of a real vehicle. In addition to bounce and pitch motion of the half car model, roll and yaw motion also exists [36].

The proposed model, in this section, is a linear full car model with seven degrees-of-freedom (DOF). The schematic model is shown in Fig. 3.4.1. The main body (sprung mass) has three DOF (bounce, pitch, and roll), and each suspension system has one DOF (vertical motion of the unsprung mass m_u).

Also, the model is asymmetric in its response due to the road profile as well as the location of the center of mass.

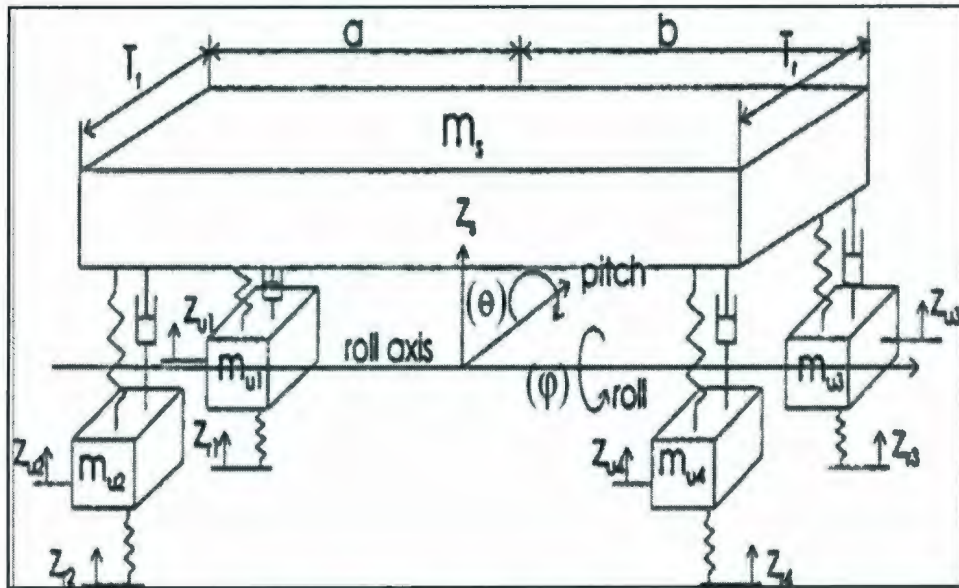


Figure 3.4.1: Schematic full car model [38]

The sub-models of the full car model are shown in Fig. 3.4.2, Fig. 3.4.3, and Fig. 3.4.4. The full car model is divided into three sub-models, the main body sub-model (Fig. 3.4.2), the control system sub-model (3.4.3), and the unsprung mass sub-model (Fig. 3.2.4). The road profile, single bump (Fig. 3.2.3) is delayed for rear wheels by 0.1 seconds, and to show the significant effect of a roll motion, the road irregularities of the right hand side are two times higher than the left hand side.

The states and weight matrices to improve ride comfort for the proposed full car model are:

$$\text{states: } X = [z_s, \dot{z}_s, \theta, \dot{\theta}, \varphi, \dot{\varphi}, z_{u1}, \dot{z}_{u1}, z_{u2}, \dot{z}_{u2}, z_{u3}, \dot{z}_{u3}, z_{u4}, \dot{z}_{u4}]^T \quad (3.4.1)$$

$$Q = \text{diag}([10, 1, 20, 1, 1, 1, 0, 0, 0, 0, 0, 0, 0, 0]) \quad (3.4.2)$$

$$R = \text{diag}([1e - 8, 1e - 8, 1e - 8, 1e - 8])$$

The sprung mass sub-model, Fig. 3.4.2, depicts the relation between sprung mass bounce, pitch, and roll motion with unsprung mass vertical motion at each corner. As can be seen, the transformer elements “TF” are employed for this purpose.

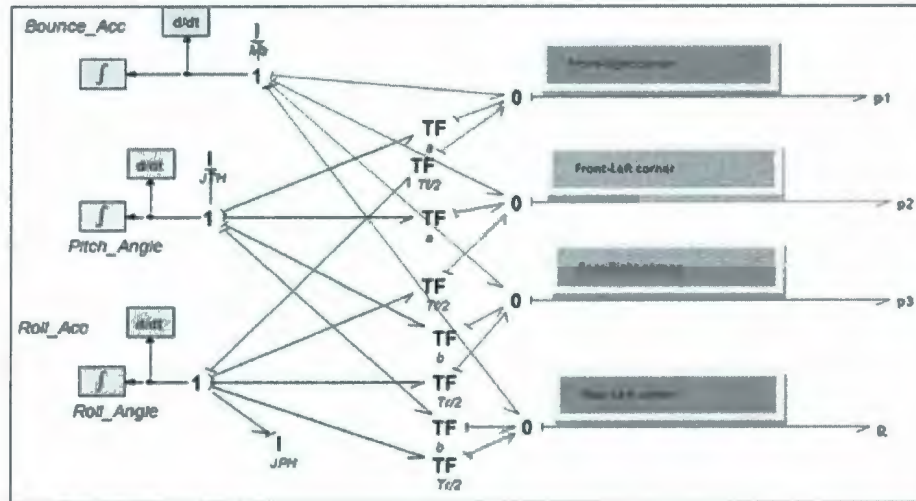


Figure 3.4.2: Extended model of body

The optimal controller, Fig. 3.4.3, takes the 14 states of the system as inputs, and then, generates actuator force at each corner.

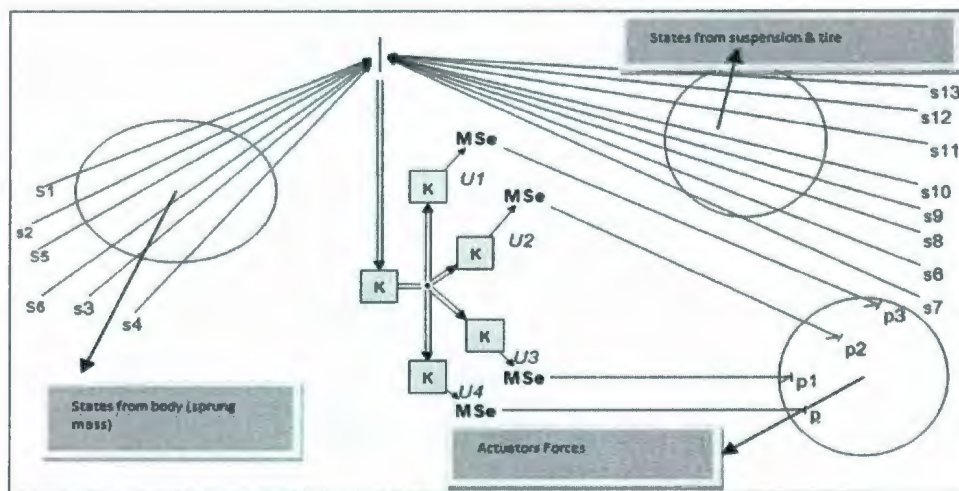


Figure 3.4.3: Extended model of controller

An unsprung mass sub-model is placed at each corner of the main body. As can be seen in Fig. 3.4.4, which represents the front-right and the front-left unsprung mass sub-model, the sub-model input is road profile and the each corner contains the tire stiffness model, passive suspension model, and actuator force, which is exerted in parallel with passive elements.

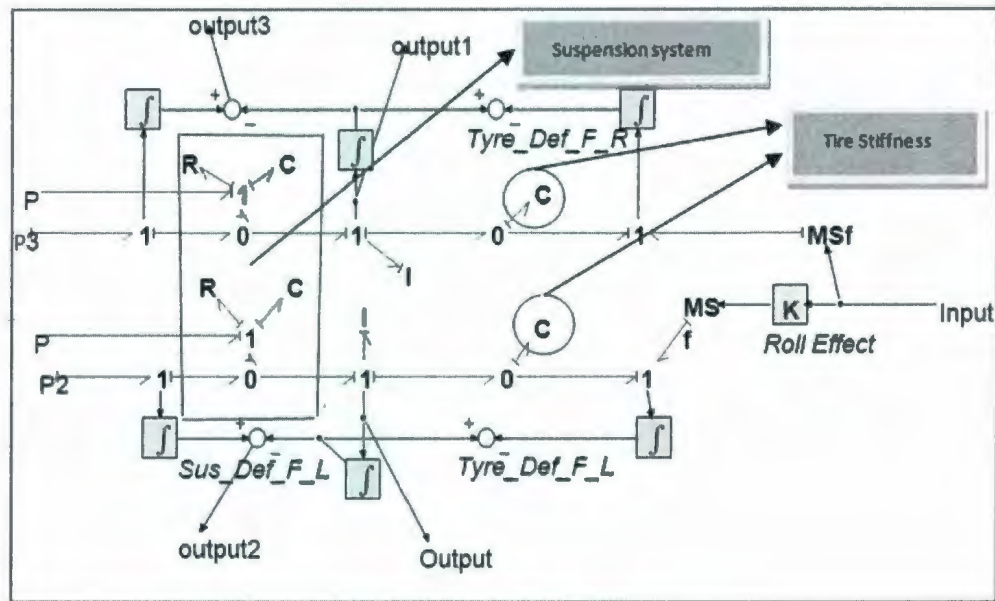


Figure 3.4.4: Extended model of suspension and tire

Table 3.4.1: Parameters and values of full car model

Parameters	Values
Sprung mass (M_s)	1136 kg
Pitch moment of inertia (I_p)	2400 kg m ²
Roll moment of inertia (I_r)	400 kg m ²
Unsprung mass (M_u)	60 kg
Suspension damping (b)	3924 N/m/s
Suspension stiffness (k_s)	36294 N/m
Tire stiffness (k_t)	182470 N/m
Distance from c.g to front wheel (a)	1.15 m
Distance from c.g to rear wheel (b)	1.65 m
Front track width (T_f)	0.505 m
Rear track width (T_r)	0.557 m

The following plots, Fig. 3.4.6 and Fig. 3.2.7, show the sprung mass bounce and pitch acceleration respectively. The bounce acceleration is improved, but the pitch acceleration is not significantly changed. The frequency domain results illustrate the significant reduction of bounce acceleration (Fig. 3.2.8).

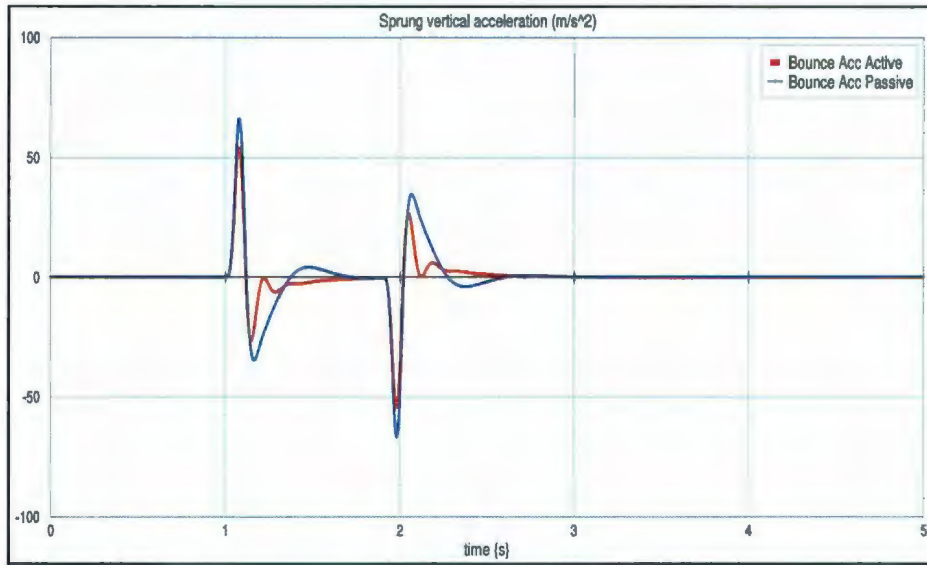


Figure 3.4.6: Sprung mass bounce acceleration

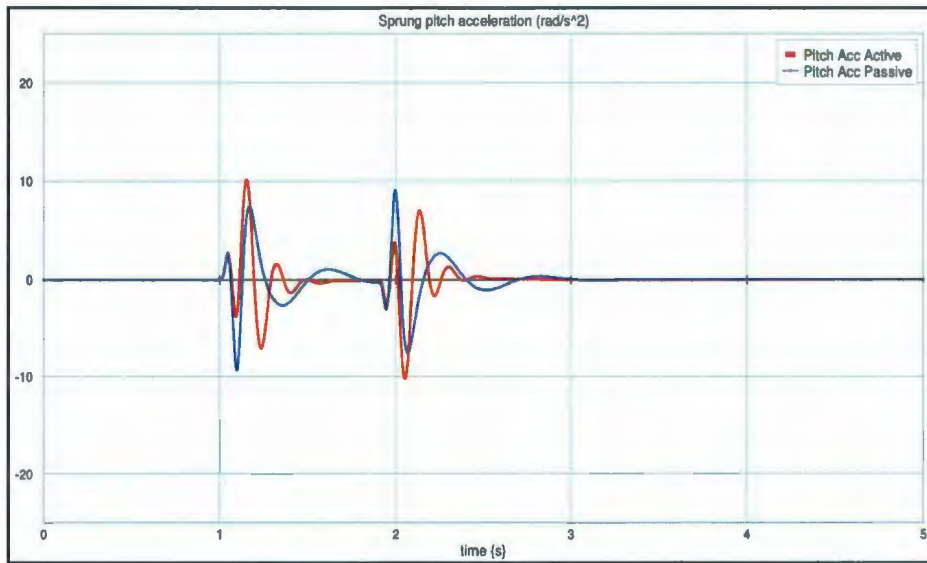


Figure 3.4.7: Sprung mass pitch acceleration

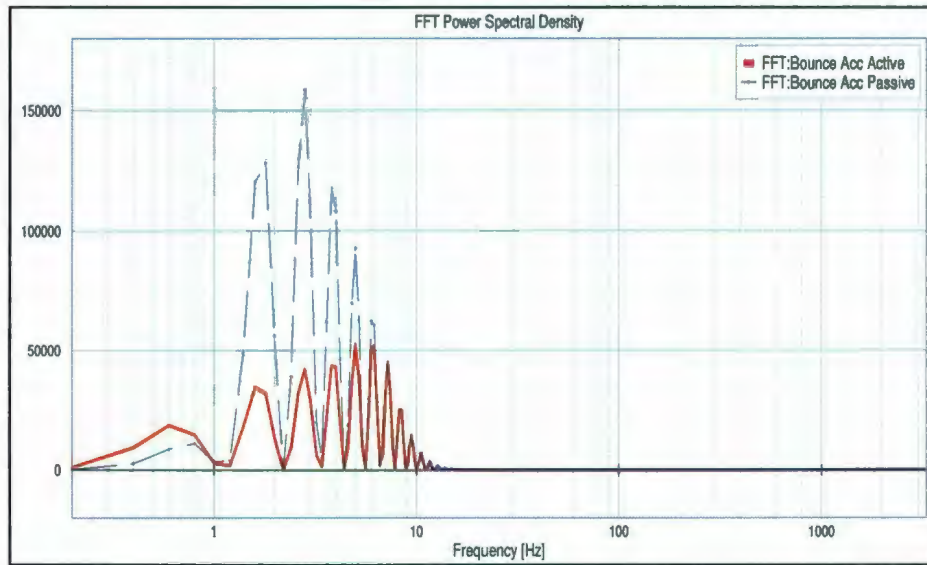


Figure 3.4.8: PSD response of sprung mass bounce acceleration

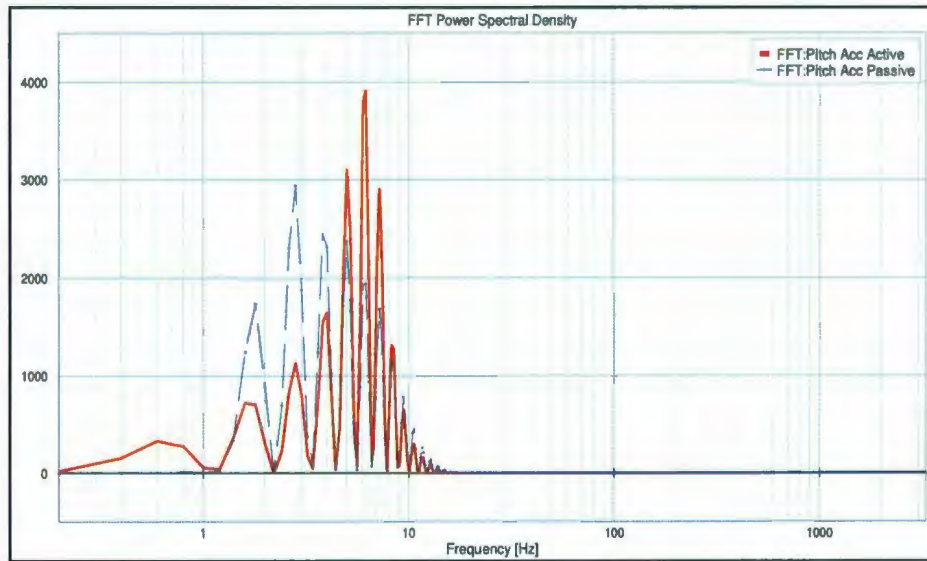


Figure 3.4.9: PSD response of sprung mass pitch acceleration

3.4 Conclusion

This chapter describes modeling and simulation of an active suspension system with the bond graph method. The models have ranged in complexity from the simplest two DOF quarter car model, four DOF half car model, and then to a more realistic seven DOF full car model. Optimal control theory was employed to generate the actuator force, and the performance of the active suspension vs. the passive counterparts were evaluated in both the time and frequency domains.

In Chapters 5 and 6, the proposed quarter car model is employed in SIMULINK to simulate convoy vehicles.

Chapter 4

4. Longitudinal vehicle dynamics and cruise control

4.1 Introduction

This chapter models the longitudinal dynamics of convoy vehicles, and how to control the longitudinal distance among vehicles to avoid crashes and increase the platoon stability in the longitudinal direction.

The main concepts in this chapter are: platoon, longitudinal dynamic, and cruise control. The main contribution of evaluating longitudinal dynamics of a convoy vehicle in this research is showing the effect of variable following distance and delay time, which in future research will be counted as system uncertainties, in a convoy.

Platoon: a platoon, or convoy, is a series of individual vehicles traveling with small following distances on the same path (Fig. 4.1.1). The main issues in a platoon system are enhancing individual and string stability of the platoon. Individual stability means that each vehicle must adjust its velocity and acceleration to maintain a safe spacing with respect to immediate front and rear vehicles. String stability means that the spacing error among the adjacent vehicles must be controlled to prevent propagation and amplification in the platoon longitudinal direction [15, 23].

Longitudinal dynamics: generally, the main dynamical features of a platoon are divided into longitudinal, vertical, and lateral dynamics. Chapter 3 evaluated the vertical

dynamics of vehicles and suspension systems. In Chapter 5, the vertical dynamics of lead-follower vehicle models will be evaluated. Lateral dynamics deals with yaw motion of vehicles during spinning, and while changing lanes to avoid obstacles. The longitudinal dynamics are related to dynamics of platoons in the platoon motion direction. The main issues which affect the longitudinal dynamics are external, or environmental, disturbances such as bad weather conditions and road irregularities (bumps, and potholes). Moreover, driver's inattention could affect the longitudinal velocity and space among vehicles in a platoon.

Cruise control: a cruise control system is used to reduce the effect of disturbances, and enhance the stability of a platoon system. As mentioned previously, some external disturbances such as bad weather conditions and road irregularities, as well as driver's error, affect a platoon system, and in the worst case scenario the vehicles will crash inside the platoon system. A cruise controller is implemented to reduce the effect of disturbances to guarantee both individual and string stability of a platoon system (see Section 4.2.2).



Figure 4.1.1: Schematic platoon system [15]

4.2 Model development

This section presents a model of a convoy, which contains five quarter-car models, and a cruise controller. The platoon system is modeled with the bond graph method using 20SIM software [20]. The results for both single bump and random road profile are evaluated.

4.2.1 Bond graph model

The model contains five sub models. The road profile is used as a system input, and applied to the vehicles based on a delay time, which varies during the journey as vehicle velocity varies.

The details of each sub model are shown in Fig. 4.2.2. Quarter car models with nonlinear elements are used for this purpose. As can be seen each sub model contains three main parts: longitudinal elements, controller, and conventional vertical quarter car model.

Nonlinear elements: the longitudinal dynamics of a vehicle are significantly affected by system nonlinearities such as wheel-road interaction (the effect of slip and rolling), and the aerodynamic resistance, which is related to the vehicle's shape and velocity. A schematic quarter car model, shown in Fig. 4.2.1, depicts the longitudinal and vertical dynamic elements [28].

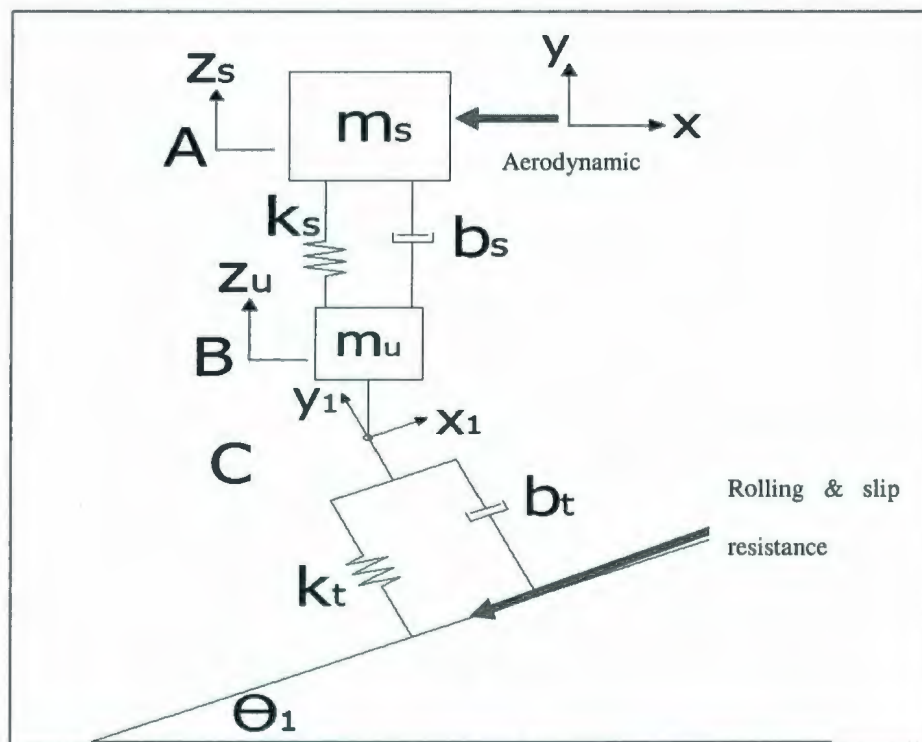


Figure 4.2.1: Schematic quarter car model with longitudinal forces

This model assumes a road slope input as a function of distance travelled.

$$\begin{pmatrix} V_{cx} \\ V_{cy} \end{pmatrix}_1 = \begin{pmatrix} \cos\theta_1 & \sin\theta_1 \\ -\sin\theta_1 & \cos\theta_1 \end{pmatrix} \begin{pmatrix} V_{cx} \\ V_{cy} \end{pmatrix} \rightarrow \text{velocity relations in two coordinates} \quad (4.2.1)$$

$$k = \frac{rw - v}{v} \rightarrow \text{slip ratio} \quad (4.2.2)$$

$$F_{slip} = \frac{\text{sgn}(k)|F_z| |\mu| |k|}{k_{max}} \rightarrow \text{slip resistance force} \quad (4.2.3)$$

$$F_{rolling} = \text{sgn}(v) \left[c_1 + c_2 F_z + c_3 \frac{F_z}{p} + c_4 \frac{F_z^2}{p} \right] \rightarrow \text{rolling resistance force} \quad (4.2.4)$$

$$F_{aero} = 0.5\rho A c_d |v_x| v_x \rightarrow \text{aerodynamic force} \quad (4.2.5)$$

Where:

w → Wheel angular velocity

v → Linear velocity along the slope

r → Wheel radius

v_x → Linear forward velocity

F_z → Vertical tire force

μ → Friction coefficient

ρ → Air density

c_d → Drag coefficient

A → Vehicle frontal area

c_1, c_2, c_3, c_4 → Constant

Equation 4.2.1 describes a coordinate transformation between road-oriented coordinates and the inertial frame. Sprung mass and suspension motion is assumed to occur in the inertial frame (vertical). Equation 4.2.1 is represented by the MTF element in the bond graph of Fig. 4.2.2. Equation 4.2.2 and 4.2.3 describe nonlinear tire slip resistance, which is due to the tensional compliance of the tire, and the fact that during acceleration and braking, the hub velocity v may be different from the tangential velocity rw of a wheel that rolls without slip. Equation 4.2.4 and 4.2.5 are expressions for rolling resistance and aerodynamic drag.

Controller: the combination of PID, saturation ($-1000 \text{ N.m} \dots 1000 \text{ N.m}$), and gains is proposed to model the adaptive cruise control system. The input signal to the PID controller is determined based on the range-range rate diagram which is explained in Section 4.2.2. The output signal of the PID box is used as the wheel torque to either accelerate or decelerate to adjust the target vehicle in desired distance with preceding vehicles.

Conventional quarter car model: the conventional quarter car model, which has two degrees of freedom in vertical direction, is comprised of sprung mass, unsprung mass, suspension stiffness, suspension damping, tire stiffness, and damping.

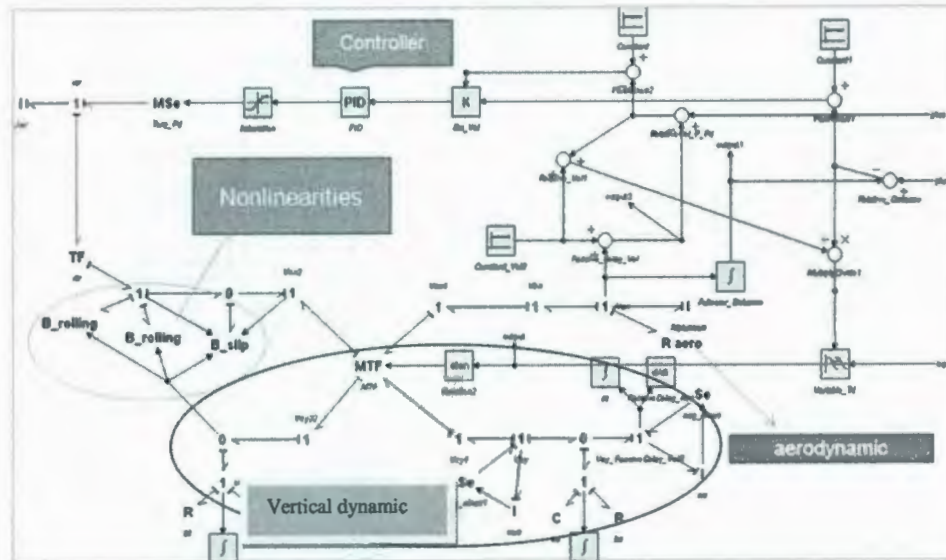


Figure 4.2.2: Extended model of quarter-car vehicle

4.2.2 Cruise control structure

The input signal to the PID controller is determined based on the range-range rate diagram, developed by Fancher and Bareket (1994), shown in Fig. 4.2.3, and Fig. 4.2.4. The diagram indicates the structure of an adaptive cruise control system, and based on the vehicle's velocity and spacing error the applied signal is switched. The relative velocity and relative space between target and preceding vehicles are fed to the controller, and then based on the range- range rate diagram the controlled signal is chosen.

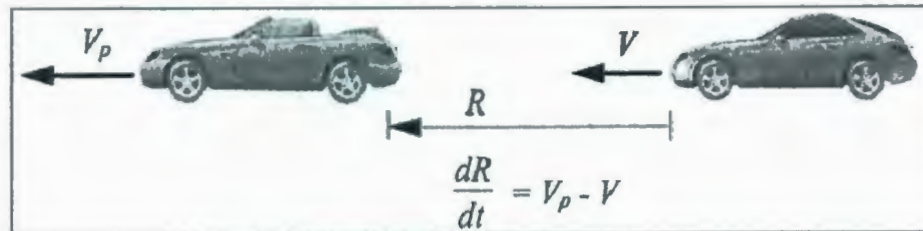


Figure 4.2.3: Relative space and velocity of vehicles [15]

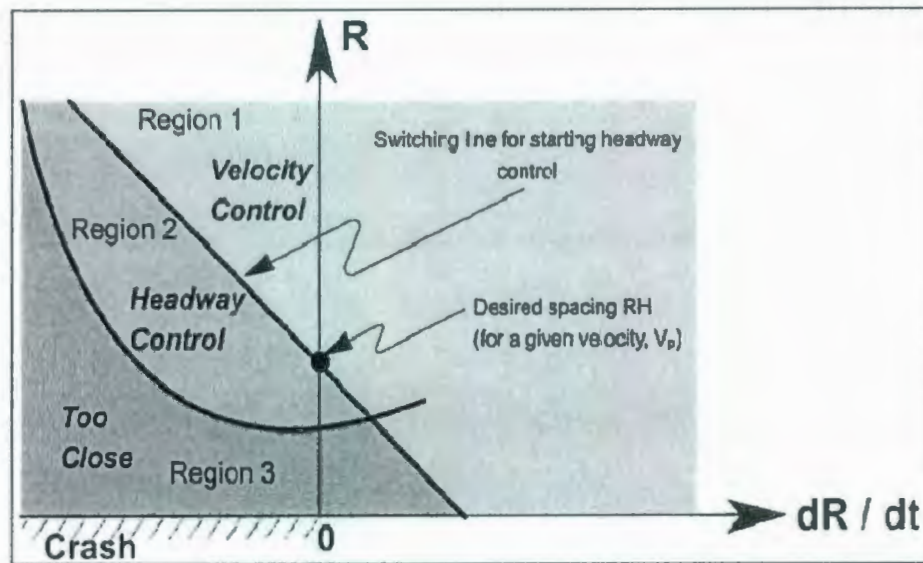


Figure 4.2.4: Range vs. range-rate diagram [15]

As can be seen in Fig. 4.2.4, there are two main regions (1 and 2) in the diagram, called Velocity Control and Headway Control (or space control). These regions are separated with a switching line, which is determined based on the desired spacing and maximum measurable range. Also, at region 3, when the space between vehicles is too tight, then the target vehicle must decelerate at the maximum allowable deceleration to avoid a crash. In other words, it indicates that if the relative space is large enough and relative velocity is positive big enough then the velocity control system (conventional cruise control) can be applied, otherwise, both space and velocity control (adaptive control) system must be taken in account.

The idea of switching between velocity and space control, region 1 and 2, along with PID controller is used to design an adaptive cruise control system for the proposed convoy model in this research.

The desired space between vehicles is 10 m, the initial velocity of each vehicle is 10 m/s, and the slope of the switching line is chosen as 10 sec.

$$R - R_d = -TR \quad (4.2.6)$$

Where, R_d and T are desired space between vehicles and the slope of the switching line respectively.

As mentioned previously, an adaptive cruise control system (ACC) is implemented to ensure individual stability of each vehicle as well as string stability of the whole system.

Individual stability means that the spacing error between target and preceding vehicles converges to zero due to road disturbances, but considering just individual stability of vehicles does not guarantee the overall stability of a platoon. For example in long convoys if there is some spacing error between the first and second vehicles in the platoon, then the spacing error can be amplified along the platoon. Therefore, the “string stability” needs to be taken into account. The concept of string stability was developed by Swaroop and Hedrick (1996) (Appendix A). The following equations show how to calculate string stability of the platoon [15, 23].

$$H_s = \frac{\Delta_i}{\Delta_{i-1}} \rightarrow \text{The spacing error ratio in frequency domain} \quad (4.2.7)$$

$\Delta_i \rightarrow$ target (vehicle) spacing error

$\Delta_{i-1} \rightarrow$ preceding (vehicle) spacing error

$$\|H_s\| \leq 1 \rightarrow \text{Spacing error ratio in a frequency domain} \quad (4.2.8)$$

$$h_t > 0, (\forall t \geq 0) \rightarrow \text{spacing error ratio in a time domain} \quad (4.2.9)$$

The criteria of string stability are mentioned in Equation 4.2.8 and Equation 4.2.9.

The model parameters and values are mentioned in Table 4.2.1. The proposed quarter car parameter's values are for a heavy truck. The PID gains are determined by trial and error.

Table 4.2.1: Parameters and values of vehicles

Parameters	Values
Sprung mass	7257 kg
Unsprung mass	700 kg
Suspension damping	31800 N/(m/s)
Suspension stiffness	2.5E6 N/m
Tire stiffness	5E6 N/m
Tire damping	0 N/(m/s)
Wheel inertia	18.76 kg.m ²
Proportional gain (K _p)	100
Derivative time constant (T _d)	2 sec
Integral time constant (T _i)	10 sec

4.3 Results

The simulation results are carried out for both a single bump and random road profile inputs.

4.3.1 Single bump (road profile)

The height of the single bump is 0.2 m, and the duration is 0.2 sec, as shown in Fig. 4.3.1.

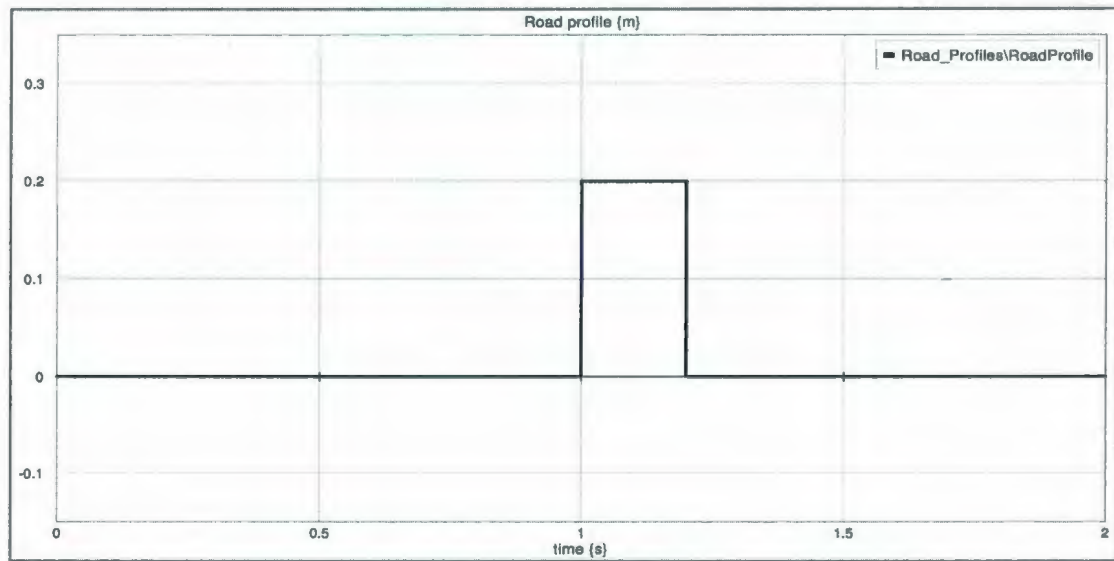


Figure 4.3.1: single bump

As can be seen in following plots, when the vehicle hits the bump, the longitudinal velocity is decreased, and consequently the relative distance and time delay are disturbed. The target vehicle adjusts its velocity, by accelerating or decelerating, based on the relative distance and velocity signals of preceding vehicles. The required torque, with saturated value of 1000 N.m, for accelerating or decelerating of target vehicles is shown in Fig. 4.3.5.

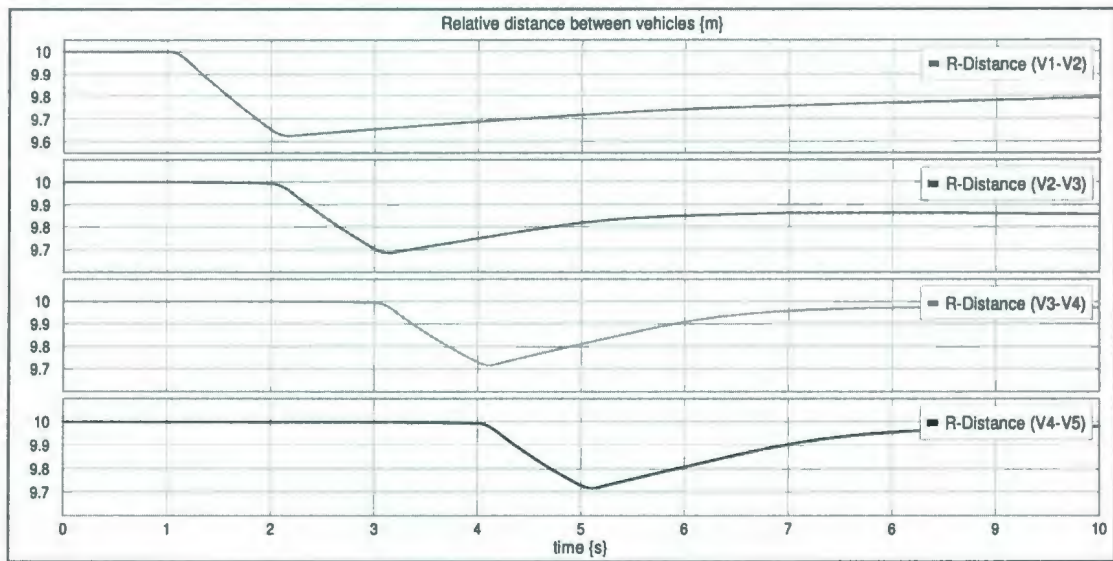


Figure 4.3.2: Relative distance between vehicles for single bump input

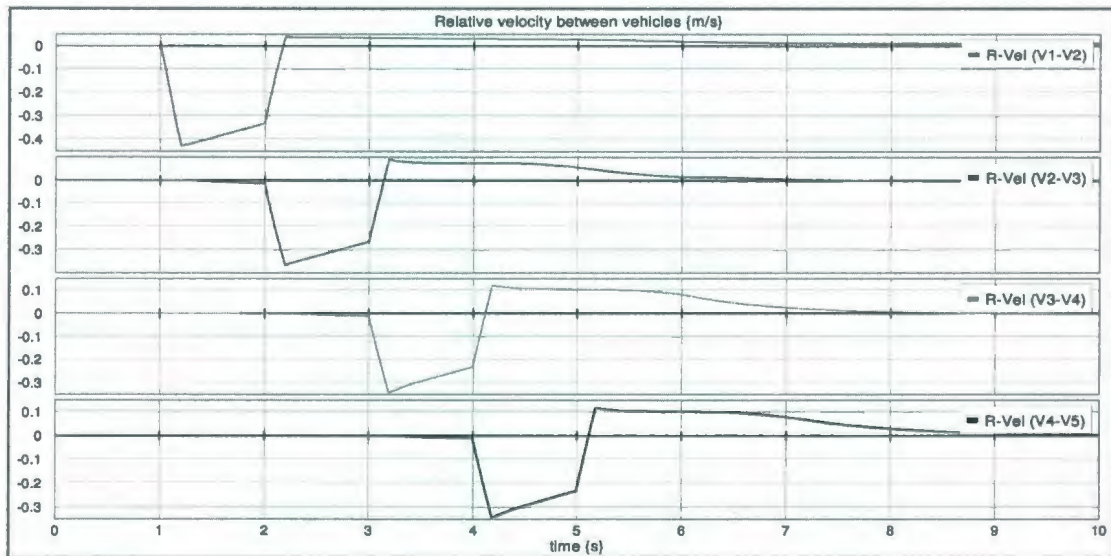


Figure 4.3.3: Relative velocity between vehicles for single bump input

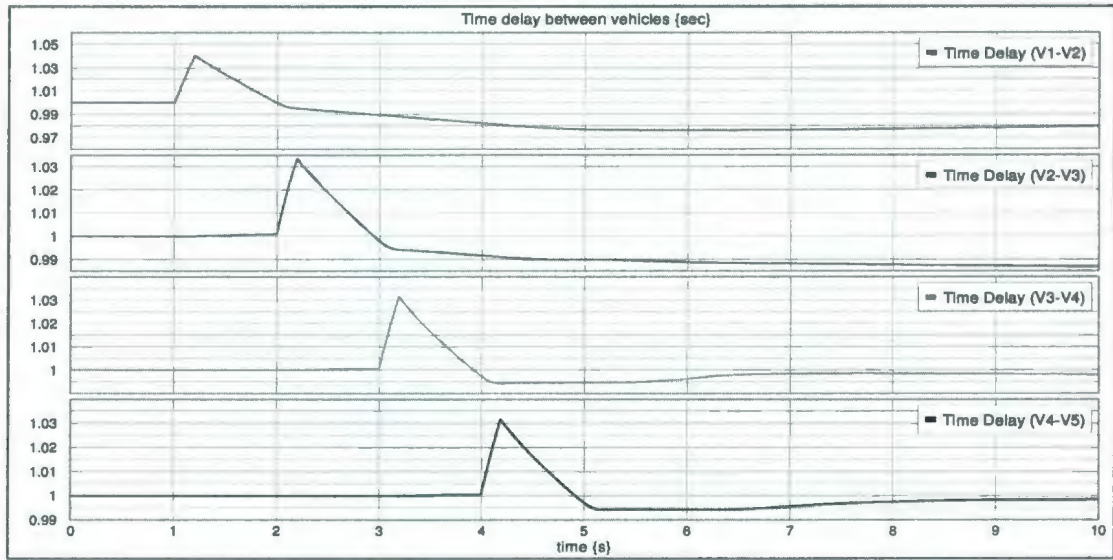


Figure 4.3.4: Time delay variations for single bump input

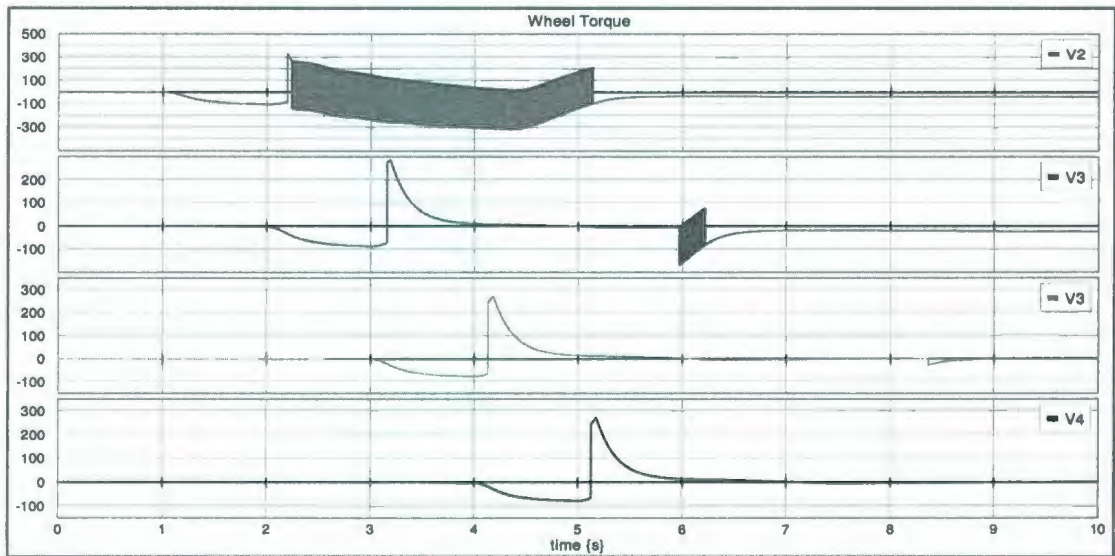


Figure 4.3.5: Wheel torque (controller output) for single bump input

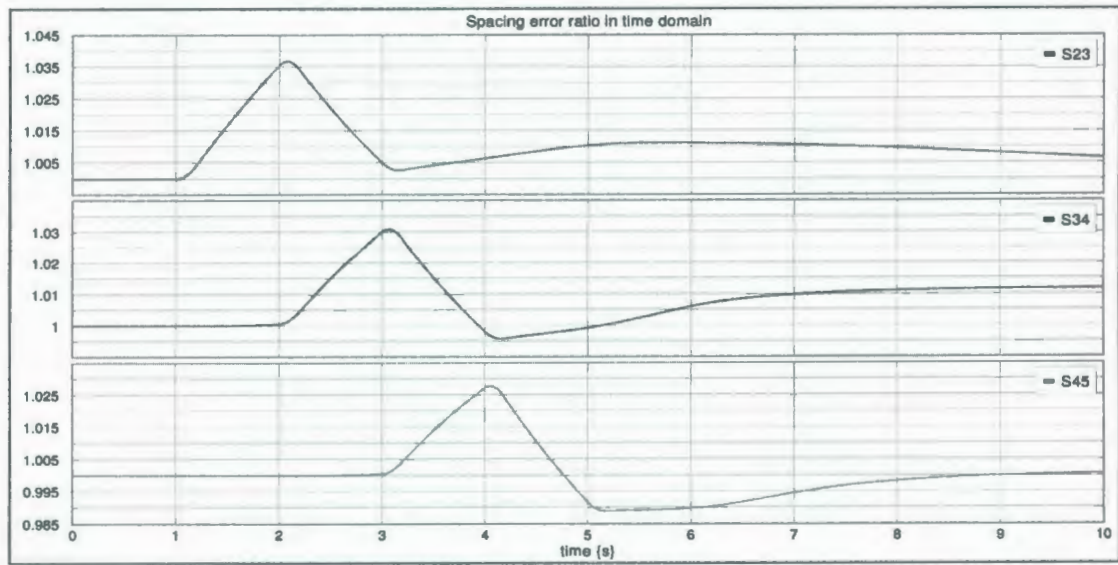


Figure 4.3.6: Spacing error ratio between vehicles in time domain for single bump input

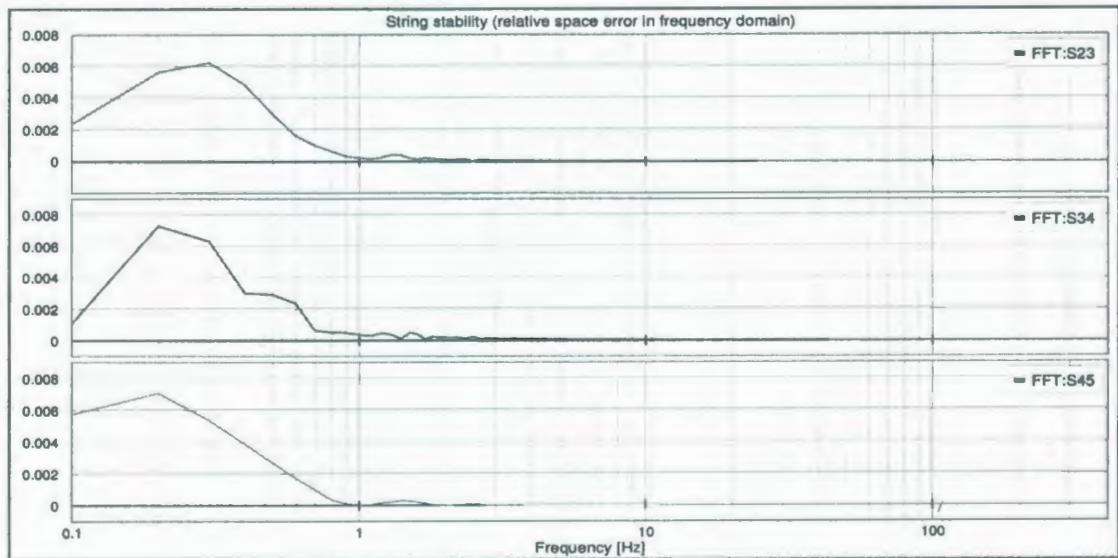


Figure 4.3.7: Spacing error ratio between vehicles in frequency domain for single bump input

In Fig. 4.3.6 and Fig. 4.3.7, the string stability of the proposed convoy is demonstrated. The transfer functions are much less than unity (Fig. 4.3.7), suggesting that the convoy will remain string stable.

4.3.2 Random (road profile)

A random road profile is illustrated as a model of continuous road roughness, rather than a model of a single discrete bump. Both types of road inputs are important in predicting vehicle response.

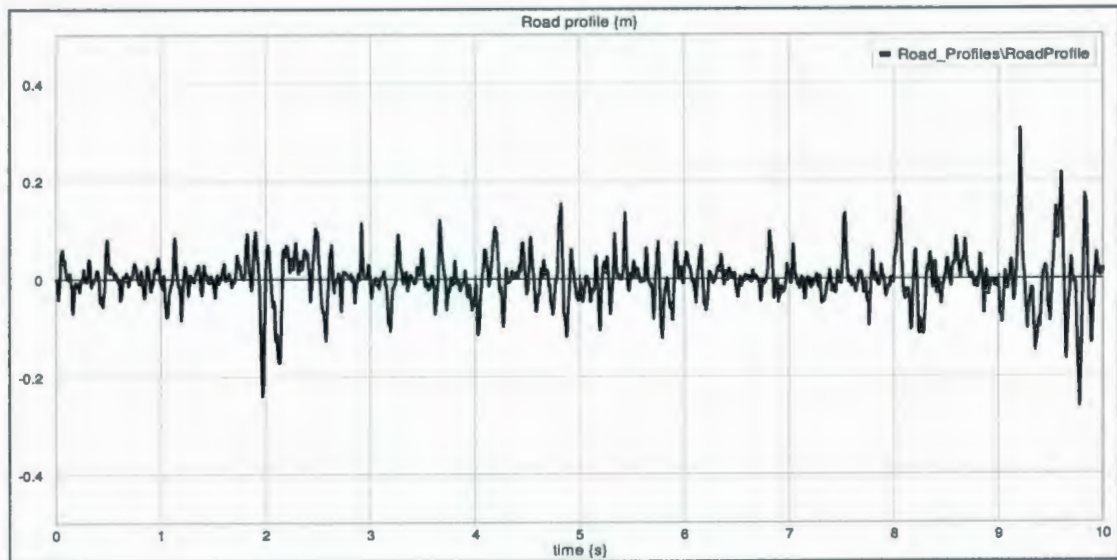


Figure 4.3.8: Random road profile

The results for the random road profile show the ability of the cruise controller to maintain both individual (Fig. 4.3.9 and Fig. 4.3.10) and string stability (Fig. 4.3.13 and Fig. 4.3.14).

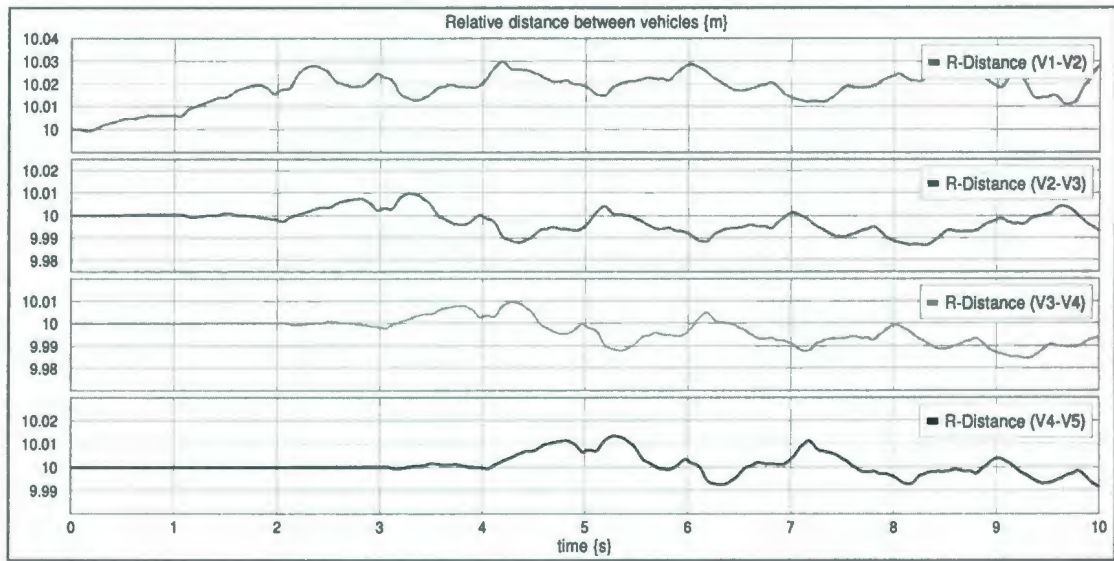


Figure 4.3.9: Relative distance between vehicles for random input

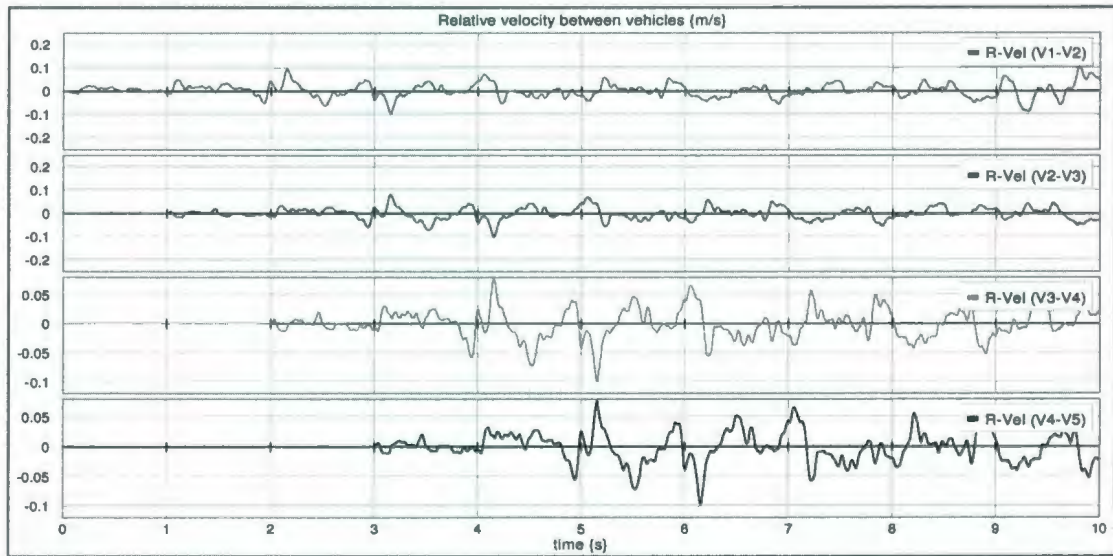


Figure 4.3.10: Relative velocity between vehicles for random input

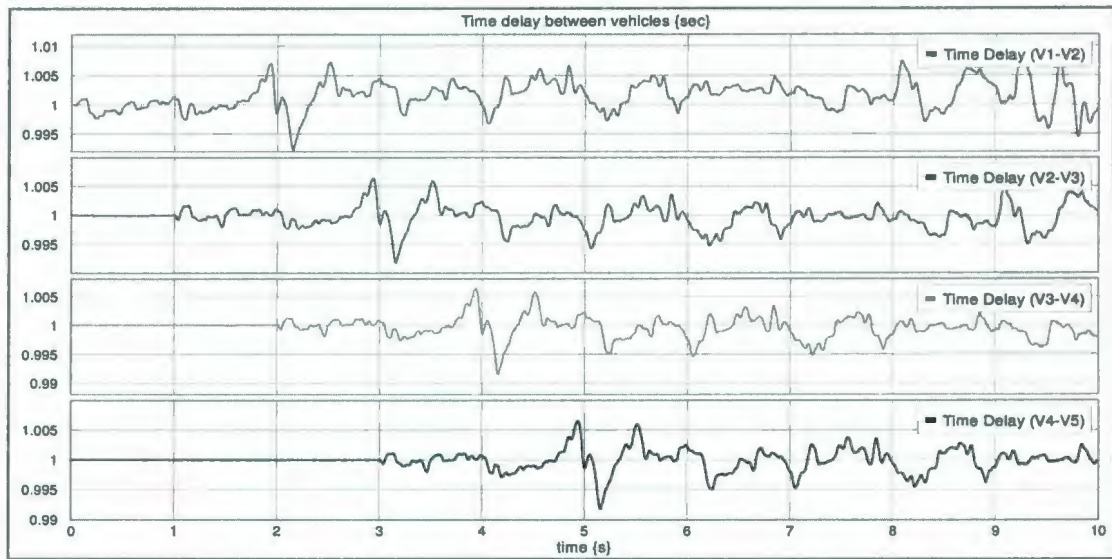


Figure 4.3.11: Time delay variations for random input

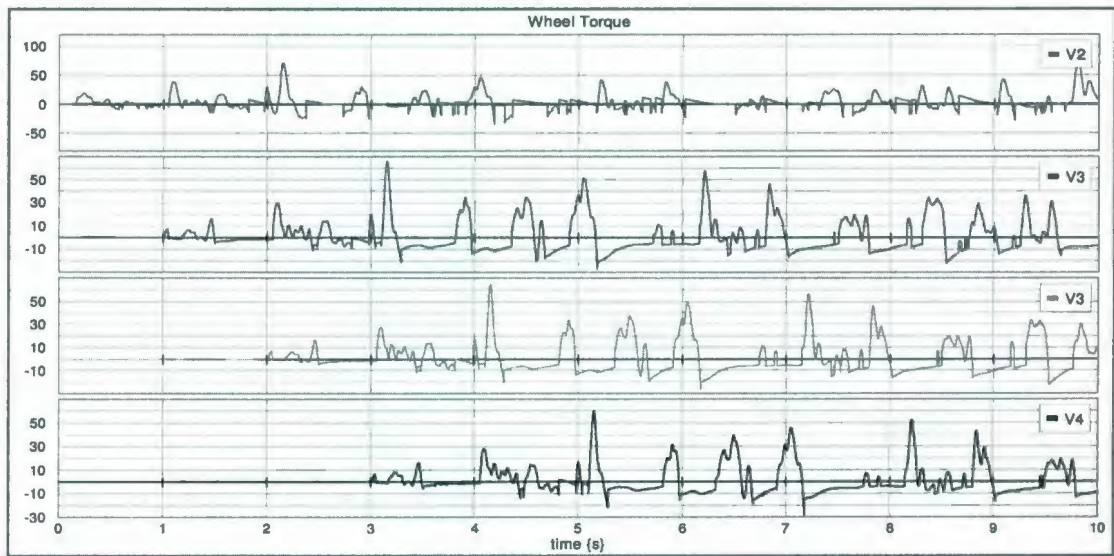


Figure 4.3.12: Wheel torque (controller output) for random input

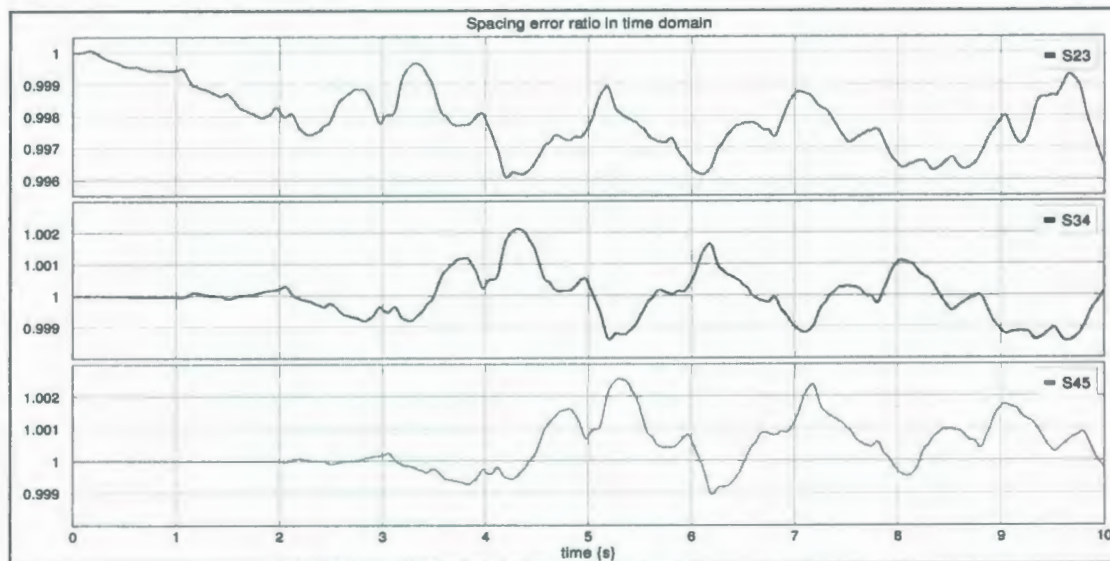


Figure 4.3.13: Spacing error ratio between vehicles in time domain for random input

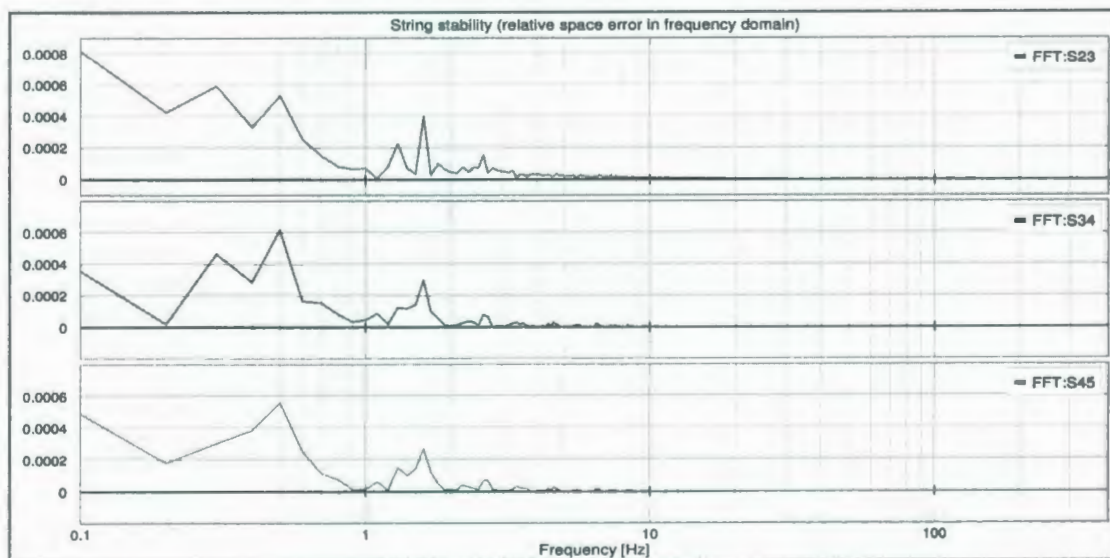


Figure 4.3.14: Spacing error ratio between vehicles in frequency domain for random input

4.4 Conclusion

This chapter has studied longitudinal dynamics of a convoy. The proposed model, which has been subjected to single bump and random road profiles, illustrates the significant benefits of the implemented cruise control system (ACC) to maintain both individual and string stability of vehicles.

The variation in a relative space, or time delay, between vehicles is important and must be taken in account while communicating preview information from a lead vehicle to followers [see Chapter 6]. As will be mentioned in Chapter 7, the following distance uncertainties and delay time are significant issues in using preview information in a convoy, therefore applying the longitudinal uncertainties in a convoy vehicle would be significant potential future research.

Chapter 5

5. Active suspension model with preview

5.1 Introduction

This chapter presents an active suspension model with preview, and evaluates the effect of preview time on the tuning of an active suspension system.

The main strategy in active-preview suspension is detecting the road irregularities some time before hitting them.

The conventional active-preview model uses sensors, which are placed some distance ahead of the front bumper, to detect road irregularities. The disadvantages of using sensors in the front bumper are:

- Sensors are expensive and vulnerable
- Sensors can be confused by water or snow

The proposed model in this research uses the lead vehicle as a preview sensor. The states of the lead vehicle are communicated to follower(s). The lead vehicle thus plays the same role as a sensor in detecting road profile.

Section 5.2 will show how to replace look-ahead sensors by lead vehicle's states, and then the results of the proposed lead-follower model will be shown in Section 5.3.

5.2 Model development

This section presents a model of conventional active preview suspensions, and the newly developed model of lead-follower with state communication.

All modeling and simulation has been executed in MATLAB and SIMULINK.

5.2.1 Conventional active-preview suspension system

A schematic quarter car model with active suspension system and look-ahead sensor is shown in Fig. 5.2.1. As can be seen in this figure, the sensor is placed a distance P_s ahead of the front bumper. The preview time is measured based on the forward velocity of the vehicle V , and the distance of the sensor from the front bumper P_s .

Therefore, the preview time is: $T_p = P_s / V$

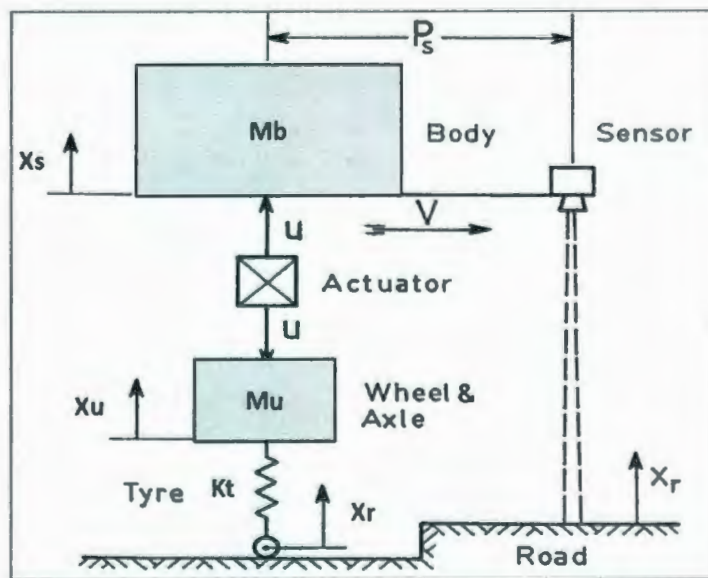


Figure 5.2.1: Quarter car model with look-ahead sensor [5]

The preview function is calculated and implemented as a feed forward gain, which contributes to the actuator force. Given a vehicle model with state space equations:

$$\dot{x} = Ax + Bu + DW \quad (5.2.1)$$

$$u(t) = -\frac{B^T [Kx(t) + g(t)]}{R} \rightarrow \text{Actuator force (feedback \& feedforward)} \quad (5.2.2)$$

$$A^T K + KA - \frac{KBB^T K}{R} + Q = 0 \rightarrow \text{Riccati equation (calculate } K \text{ matrix)} \quad (5.2.3)$$

$$J = \frac{1}{2} \int_0^{\infty} (x^T Qx + u^T Ru) dt \rightarrow \text{Performance index} \quad (5.2.4)$$

$$g(t) = \int_0^{T_p} \exp(A_c^T \sigma) K.D.W(t + \sigma) d\sigma \rightarrow \text{Preview function} \quad (5.2.5)$$

Where:

$$A_c = A - \frac{BB^T K}{R}$$

$W(t)$ → Derivative of road profile

T_p → Preview time

Q, R → Weighting factors

A, B, D → System parameters

The process of calculating actuator force, feedback plus feed forward gain is almost the same as calculating actuator force for an active suspension system (Chapter 3). However, we need to solve for the preview function at each time step to calculate feed forward gain.

The parameters and values such as the system parameters and weight factors, for the proposed model, are given in the form of MATLAB m-file in the next part (Section 5.2.2).

5.2.2 State-based active with preview suspension model

The proposed convoy model has the three sub-models: vehicles with passive, active (lead), and active-preview (follower) suspensions. The passive model is used to compare the results with active (lead), and active preview (follower) models (Fig. 5.2.2).

The road profile must be implemented inside the preview function. The road profile function is generated based on the states of the lead vehicle, a combination of tire deflection and unsprung mass velocity ($w_{est} = x_4 - \dot{x}_3$). This method helps to eliminate sensors, which would normally be used to detect road profile in a preview suspension, on each vehicle.

The proposed model is based on the quarter car suspension system. The quarter car equations of motion and state variables are same as quarter car model in Section 3.2.

$$States = \begin{pmatrix} x_s - x_u \\ \dot{x}_s \\ x_u - x_r \\ \dot{x}_u \end{pmatrix} \rightarrow \begin{pmatrix} suspension\ deflection \\ \dots \\ sprung\ velocity \\ \dots \\ tire\ deflection \\ \dots \\ unsprung\ velocity \end{pmatrix} \quad (5.2.6)$$

If unsprung mass acceleration can be measured with an accelerometer and integrated to get x_u , and if tire deflection can be measured, then road profile x_r can be calculated and sent to following vehicles. Tire deflection is practically impossible to measure. Therefore, this variable will have to be estimated. This Chapter proceeds with preview controller development assuming that tire deflection can be measured, in order to show benefits of road profile preview information to following vehicles. Chapter 6 develops an estimator for x_r . The following equations show how road profile factors into the preview function $g(t)$ which contributes to active suspension controller gain.

$$W(t) = \dot{x}_r(t) = \dot{x}_u(t) - d(x_u(t) - x_r(t))/dt \rightarrow \text{Derivative of road profile} \quad (5.2.7)$$

$$g(t) = \int_0^{T_p} \exp(Ac^T\sigma) K.D.W(t + \sigma)d\sigma \rightarrow \text{Preview function} \quad (5.2.8)$$

The system parameters and values are given in Table 5.2.1.

Table 5.2.1: Parameters and values of the model

Parameter	Value
Sprung mass (M_b)	100 kg
Unsprung mass (M_w)	10 kg
Suspension damping (C_b)	100 N/(m/s)
Suspension stiffness (K_b)	10000 N/m
Tire stiffness (K_t)	100000 N/m
Preview time (T_p)	0.5 sec

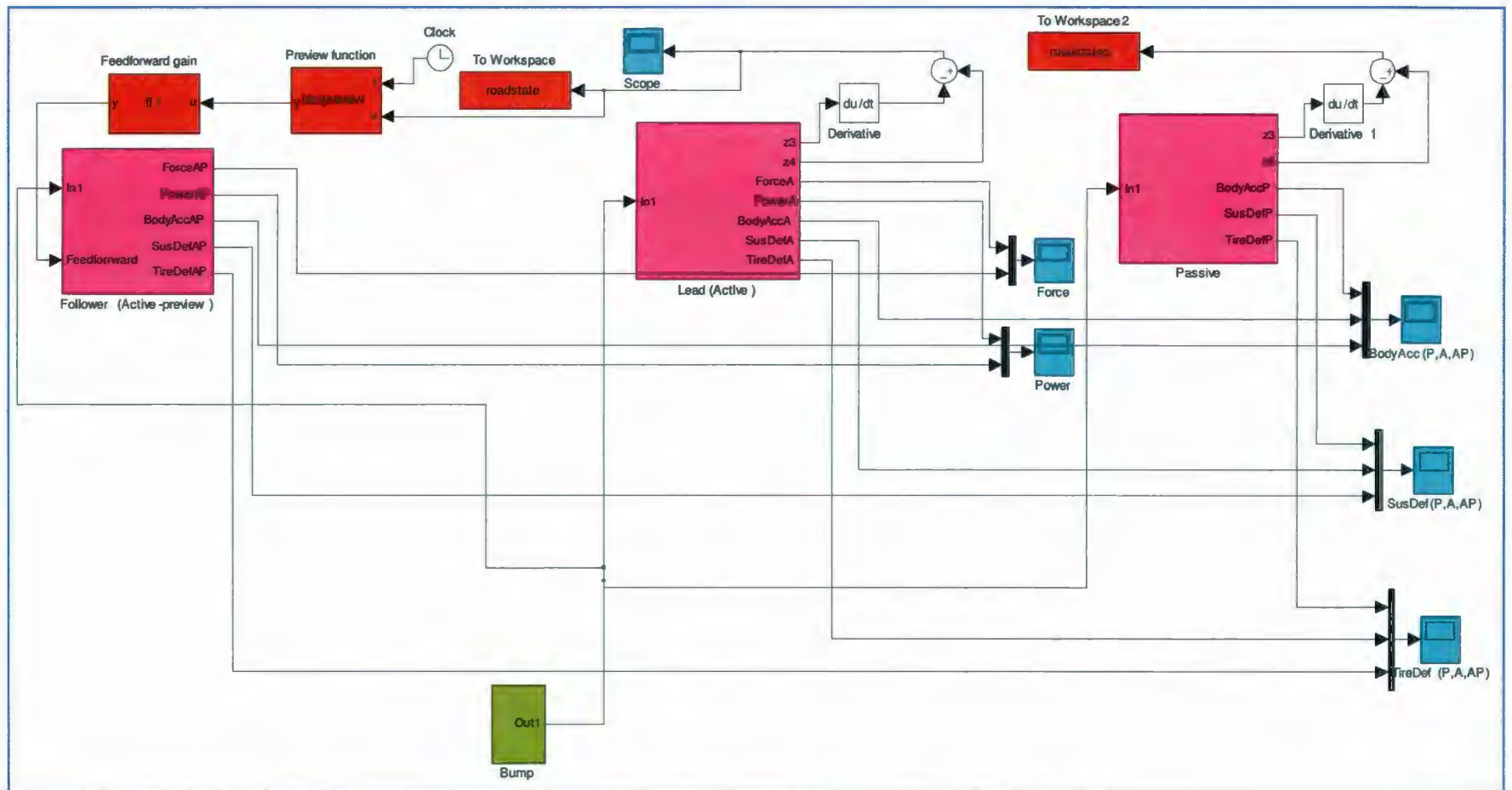


Figure 5.2.2: Passive, active (lead), and active-preview (follower) with state communication

An embedded function is used in SIMULINK to evaluate the road profile function inside the preview function and generate feed forward gain.

<pre>function y = ff1(u) R=(1/(mb^2)); y = (-R^(-1))*B'*u;</pre>	<pre>function y=testpreview(t,w) eml.extrinsic('F'); y=ones(4,1); y=feval('F',t);</pre>
--	--

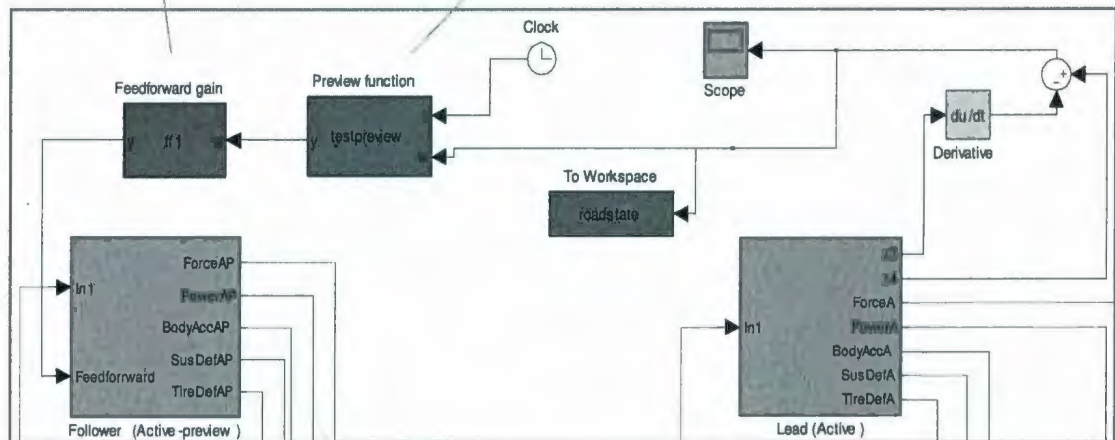


Figure 5.2.3: Lead-follower model and states communication

The proposed performance index and the Riccati equation are mentioned in Equations 5.2.9 and 5.2.10, (more details are shown in m-file box).

$$J = \frac{1}{2} \int_0^{\infty} (x^T Q_1 x + x^T N u + u^T R u) dt \quad (5.2.9)$$

$$A^T P + PA - PBR^{-1}B^T P + Q_1 = 0 \quad (5.2.10)$$

As shown above, the preview function block evaluates the function (F) at each time step.

The function (F) is called from an m-file:

```
function y=F(t)

global x1 x2 % global variable assigned the simulink state base road
profile to workspace

x1=roadstate.time;

x2=roadstate.signals.values;

%Parameters

mb=100; % Sprung (body) mass

mw=10; % Unsprung mass

cb=100; % Suspension damping

kb=10000; % Suspension stiffness

kt=100000; % Tire stiffness

%Matrix

A=[0 1 0 -1;
```

```

-kb/mb -cb/mb 0 cb/mb;

0 0 0 1;

kb/mw cb/mw -kt/mw -cb/mw]; % System parameters matrix

B=[0;

1/mb;

0;

-1/mw]; % Actuator coefficient matrix

D=[0;

0;

-1;

0]; % Road profile matrix

%Optimal control matrix and elements

r1=1e4;

r2=1e2;

Q1=(1/(mb^2))*[kb^2+r1*mb^2 2*cb*kb 0 -2*cb*kb;

```

```

2*cb*kb cb^2+r2*mb^2 0 -2*cb^2;

0 0 0 0;

-2*cb*kb -2*cb^2 0 cb^2]; % State's weight factor matrix

N=(1/mb^2)*[-kb; -cb; 0; cb]; % State and actuator weight factor matrix

R=(1/(mb^2)) % Actuator weight factor

S=N;

% [P, Lm, G] =are(A,B,Q1,R,S); % Riccati equation (P is a solution of
Riccati equation)

P=[ 1.5850e3    0.0920e3    1.5869e3    -0.0008e3
    0.0920e3    0.0171e3    0.0772e3    0.0000
    1.5869e3    0.0772e3    2.5118e3    -0.0003e3
   -0.0008e3    0.0000   -0.0003e3    0.0001e3]; %r1 1e4, r2 1e2

An=A-B*R^(-1)*N';

Ac=An-B*(1/R)*B'*P;

Acp=Ac';

PD=P*D;

```

```

h=@(sig) (expm(sig*Acp))* (PD)*interp1(x1,x2,t+sig); % Preview function

y=quadv(h,0,0.5); % Using numerical integral (quadratic vector) to
solve preview function

```

The road profile function is replaced by “*interp1(x1, x2, t+sig)*”, which indicates the interpolation among data from lead states.

The extended model of the active suspension vehicle is drawn in Fig. 5.2.4. The results for passive, active, and state preview are shown at the next part.

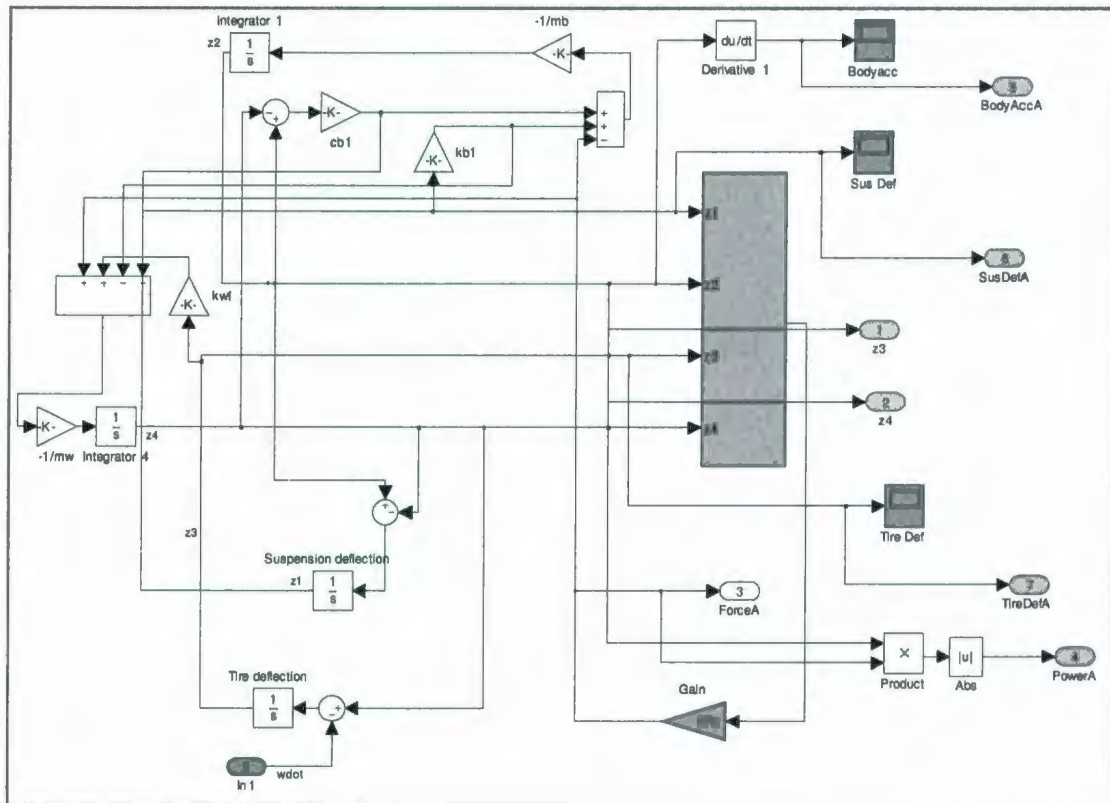


Figure 5.2.4: Extended model of active suspension of quarter car model

5.3 Results

The simulation is carried out for a single bump road profile as the system input.

The main outputs used to compare the performance of active-preview with active and passive suspensions are body acceleration, tire deflection, suspension deflection, and power demand.

5.3.1 Single bump road profile

The road profile in this part is a single bump with a height of 0.2 (m), and is a half cosine wave. (Fig. 5.3.1)

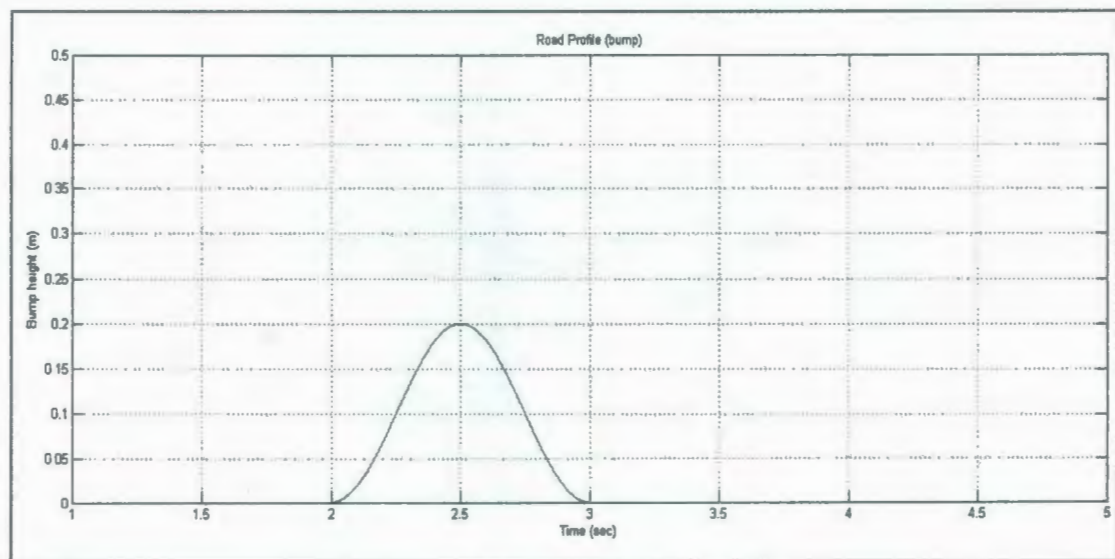


Figure 5.3.1: Single bump road profile

The sprung mass acceleration (body acceleration) illustrates that using active suspension with preview (follower vehicle) significantly enhances the system's ride quality (Fig. 5.3.2).

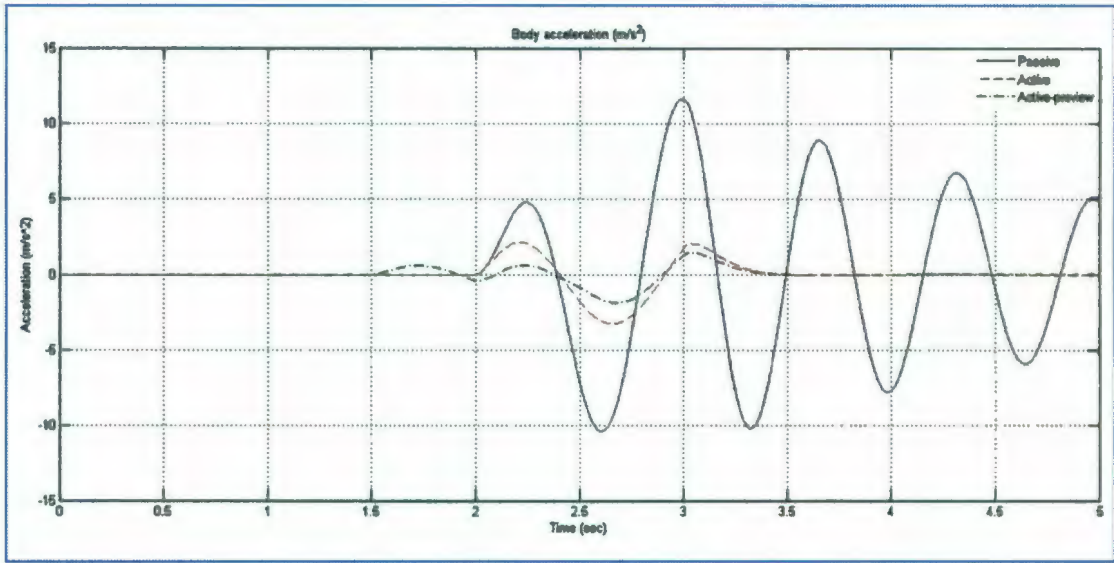


Figure 5.3.2: Body acceleration (passive, active and active preview)

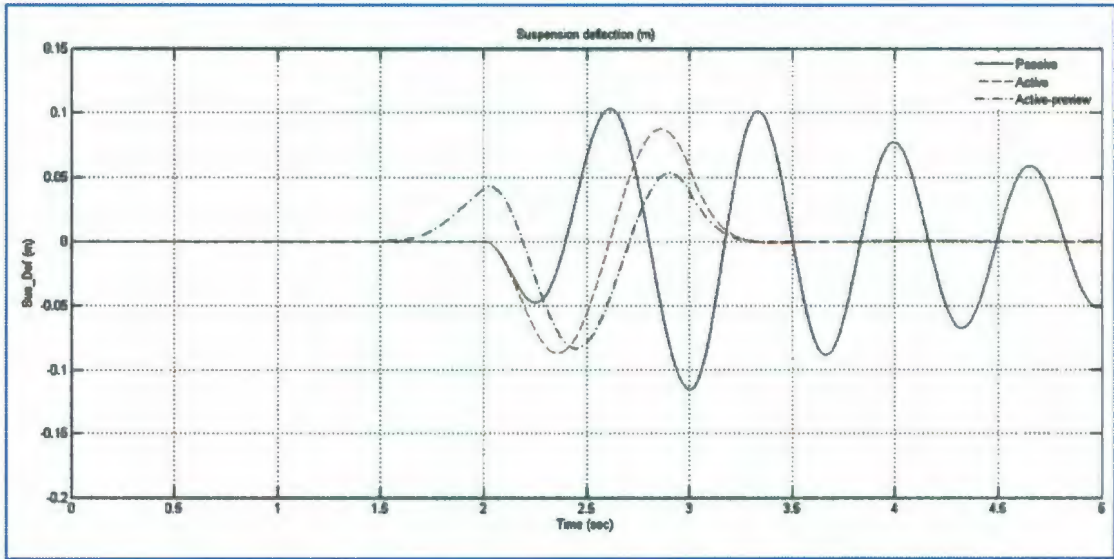


Figure 5.3.3: Suspension deflection (passive, active, and active preview)

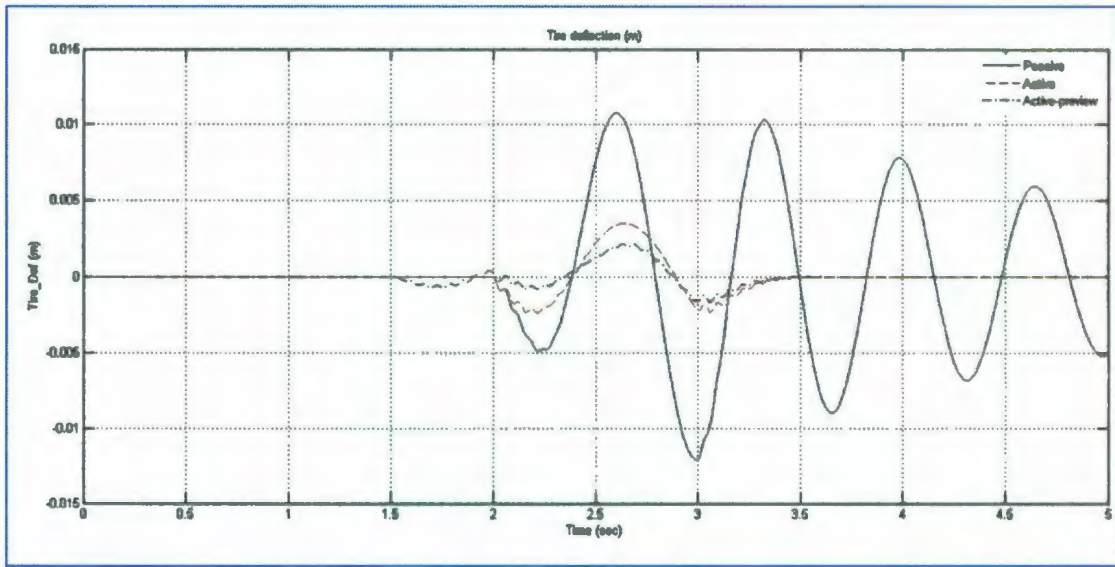


Figure 5.3.4: Tire deflection (passive, active, and active preview)

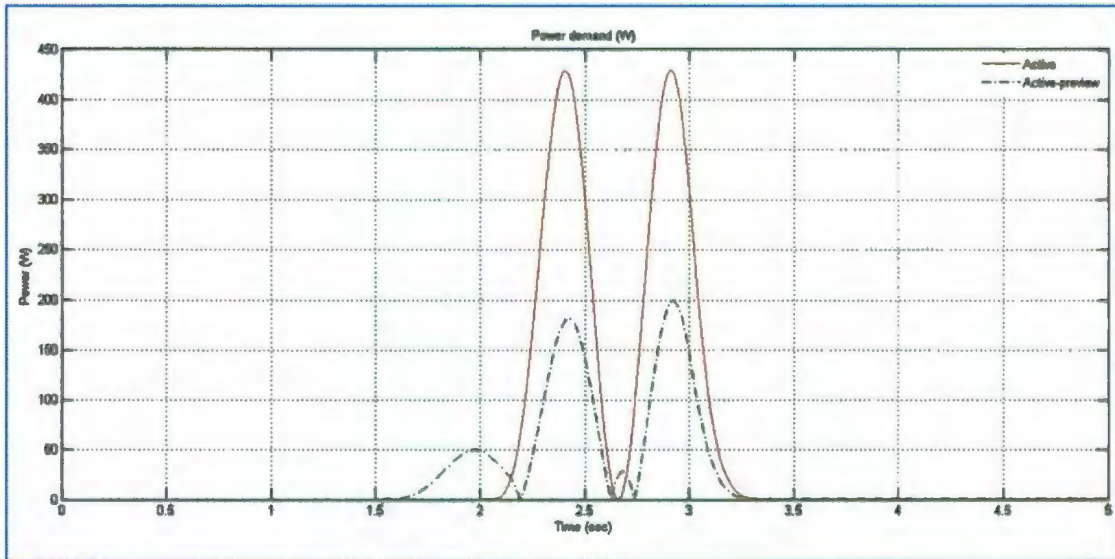


Figure 5.3.5: Power demand (active and active preview)

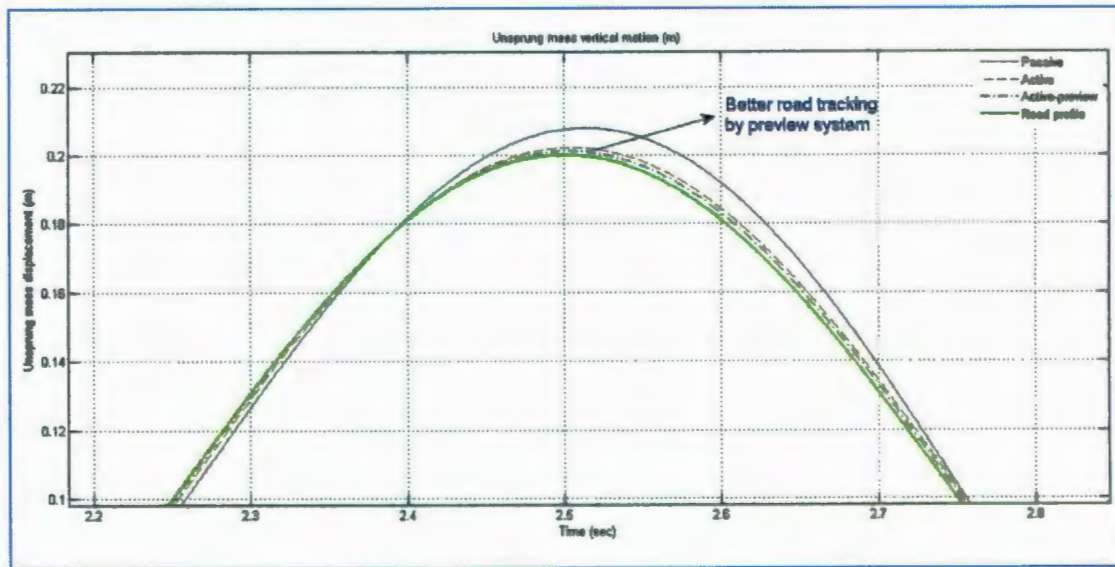


Figure 5.3.6: Unsprung mass motion and road tracking

The results of the active-preview suspension show better performance in all cases compared to the active and passive suspension. The body acceleration and tire deflection are reduced compared to the active suspension and significantly improved compared to passive model. Moreover, the road profile is tracked by the active-preview suspension much better than the active and passive suspensions.

The suspension deflection and power demand are significantly reduced in the active-preview suspension compared to the active suspension.

The preview time in these simulations was chosen as 0.5 sec, which is the optimal preview time in the case of the proposed model [3]. The effect of preview time on performance index is evaluated in Section 5.3.2.

5.3.2 The effect of preview time on performance

The effect of preview time on performance index (J) has been evaluated for the active-preview (follower) vehicle.

The result shows the optimal range of preview time for the proposed system is in the range of [0.4...0.6].

Table 5.3.1: Performance index vs. preview time

Preview time (sec)	Performance index
0.01	1446
0.05	1421
0.1	1371
0.3	878
0.4	707
0.5	571
0.7	603
1	749

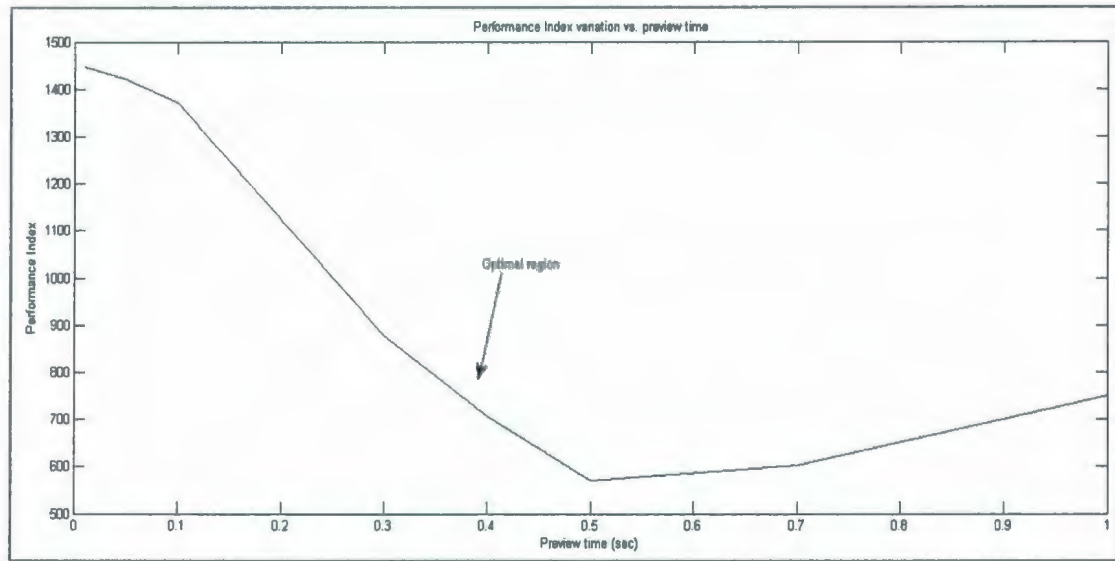


Figure 5.3.7: Performance index variation vs. preview time

The desired preview time is the lowest preview time that minimizes the performance index, e.g. in this case study, the preview time is chosen 0.5(sec).

5.4 Conclusion

This chapter has studied an active suspension system with preview. The preceding results illustrate the better performance of the active-preview model, in terms of body acceleration, suspension deflection, tire deflection, and power demand, compared to the active and passive counterparts.

The main contribution of this chapter has been generating the road profile, which is used in the preview function of follower vehicle, based on the states of the lead vehicle instead of with a look-ahead sensor. It has been assumed that all the lead's states are measurable.

However, measuring the tire deflection is practically impossible, and therefore must be estimated [see Chapter 6].

Moreover, the effect of preview time on performance index has been evaluated, and then the optimal range of preview time has been found (Fig. 5.3.7). The optimal preview time is comparable to times reported in the literature [2, 3, and 5]. Chapter 6 will build on the results of this chapter by designing a compensator, a preview controller with 0.5 second preview time, along with an optimal estimator for tire deflection that can take into account road input and measurement noise.

Chapter 6

6. Observer design

6.1 Introduction

This chapter presents the observer design to estimate some states which are not easily measurable, such as tire deflection.

As mentioned in the previous chapter, the road profile, which is required for the preview function that generates feed forward control gains in active-preview suspension systems, is calculated based on the states of the lead vehicle.

The required states, which are tire deflection and unsprung mass vertical velocity, must be measured or estimated to generate the road profile for follower(s).

The unsprung mass velocity, vertical velocity of the wheel, axle, and suspension system, can be measured by implementing sensors, but the tire deflection cannot be easily measured. In other words, in reality, the tire deflection is not measurable and must be estimated.

The objective of this chapter is to design an estimator (observer) system to estimate tire deflection of the lead vehicle, and apply it in the feed forward control gain of follower(s).

A Kalman filter, or Kalman estimator, is proposed for this purpose. The extended SIMULINK model and the details of estimator are shown in Section 6.2.

6.2 Model development

This section presents the background and mathematical formulation of Kalman estimation theory. Furthermore, a SIMULINK model of the Kalman estimator is implemented (Fig. 6.2.3).

6.2.1 Theory of Kalman estimator

As mentioned previously, one of the main issues in designing an active suspension system is how to measure the states of a system. In some cases, to reduce the need for sensors, which would be expensive and sometimes unreliable, it is worthwhile to design and implement an observer.

Some state variables cannot be practically measured, in which case the estimation method is used to estimate those variables based on the known parameters and states. The estimation of immeasurable state variables is also called observation.

If the state observer observes all the state variables of the system, it is called a full order state observer. An observer that estimates fewer than n state variables, where n is the dimension of the state vector is called a reduced order observer. For instance, the observer (estimator) in this research estimates tire deflection based on the other measured states. The controllability and observability conditions are mentioned in Appendix C.

The schematic diagram, Fig 6.2.1, shows the structure of the Kalman estimator used in this research.

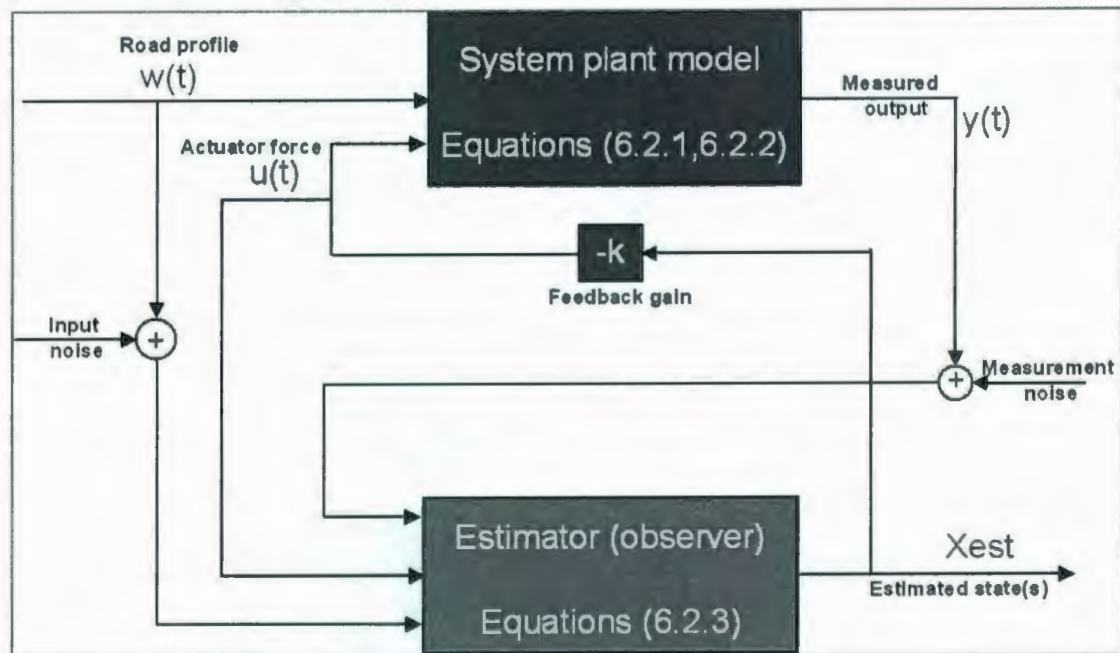


Figure 6.2.1: Schematic Kalman estimator diagram

As can be seen in the diagram, the upper block represents the system (plant) (Equation 6.2.1, 6.2.2).

$$\dot{x}(t) = Ax(t) + Bu(t) + Dw(t) \quad (6.2.1)$$

$$y(t) = Cx(t) + v(t) \quad (6.2.2)$$

The inputs to the block are road profile $w(t)$ and actuator force $u(t)$, which is calculated based on the LQ method [4]. The output of the system block is $y(t)$, which is called the measured equation. For instance, in the proposed model, the measured equation equals the product of system states and matrix $C = [1 \ 0 \ 0 \ 0; 0 \ 1 \ 0 \ 0; 0 \ 0 \ 0 \ 1]$, which indicates that the first (suspension deflection), second (sprung mass velocity), and fourth (unsprung

mass velocity are measurable states. The measurement error is simulated by White Gaussian Noise $v(t)$.

The estimator block, Equation 6.2.3, represents the Kalman estimator formulation [12] which takes the measured equation $y(t)$, road profile $w(t)$, input or process noise $\eta(t)$, and actuator force $u(t)$ as the inputs, and then, calculates the estimated state(s) ($\hat{x}(t)$).

$$\dot{\hat{x}}(t) = A\hat{x}(t) + Bu(t) + L(t)[y(t) - C\hat{x}(t)] + D[w(t) + \eta(t)] \quad (6.2.3)$$

Where:

$\hat{x}(t) \rightarrow$ Estimated state

$L(t) = (P(t)C^T + N)R \rightarrow$ Observer gain

(P is the solution to the following algebraic Riccati equation)

$AP(t) + P(t)A^T - P(t)C^TRCP(t) + DQD^T = 0 \rightarrow$ Riccati equation

$Q = E(\eta(t)\eta(t)^T) \rightarrow$ Input noise variance

$R = E(v(t)v(t)^T) \rightarrow$ Measurement noise variance

$N = E(\eta(t)v(t)^T) \rightarrow$ Measurement & input noise covariance

$$E(\eta(t)) = E(v(t)) = 0$$

The function $E(X)$ represents the expected value, which can be calculated in MATLAB, and can be expressed based on the vector's covariance $Cov(X)$ function.

In statistics, covariance indicates that how much two variables change together [34].

The covariance function property can be briefly summarized as:

$$\text{Cov}(A, B) = \begin{bmatrix} C_{11} & C_{12} \\ C_{21} & C_{22} \end{bmatrix} \quad (6.2.4)$$

Where:

$$C_{11} : \text{Variance of } A \text{ or } \text{Cov}(A, A^T)$$

$$C_{22} : \text{Variance of } B \text{ or } \text{Cov}(B, B^T)$$

$$C_{21} = C_{12} : \text{Covariance of } B \text{ or } \text{Cov}(A, B^T)$$

The relation between the expected value function $E(X)$ and the covariance function $\text{Cov}(X)$ can be shown as:

$$\text{Cov}(A, B) = E(A \cdot B) - E(A)E(B) \quad (6.2.5)$$

In the case of a Kalman estimator, as mentioned before, the expected function of each noise vector is considered zero. In other words, the expected function of two white noise vectors is equal to the covariance of two vectors.

$$\text{Cov}(\eta(t), \eta(t)^T) = E(\eta(t) \cdot \eta(t)^T) - E(\eta(t))E(\eta(t)^T) \quad (6.2.6)$$

$$\text{Cov}(v(t), v(t)^T) = E(v(t) \cdot v(t)^T) - E(v(t))E(v(t)^T)$$

$$\text{Cov}(\eta(t), v(t)^T) = E(\eta(t) \cdot v(t)^T) - E(\eta(t))E(v(t)^T)$$

Where:

$$E(\eta(t)) = E(v(t)) = 0$$

Therefore:

$$Cov(\eta(t), \eta(t)^T) = E(\eta(t) \cdot \eta(t)^T) \quad (6.2.7)$$

$$Cov(v(t), v(t)^T) = E(v(t) \cdot v(t)^T)$$

$$Cov(\eta(t), v(t)^T) = E(\eta(t) \cdot v(t)^T)$$

6.2.2 Implementing estimator in SIMULINK

The proposed estimator model is implemented in the lead vehicle, which has an active suspension system, to estimate the lead vehicle's tire deflection. Then, the tire deflection along with the unsprung mass velocity is used to generate the road profile which is implemented in the preview function in the follower vehicle.

$$w_{est} = x_4 - \dot{x}_3 \rightarrow \text{Estimated derivative road profile} \quad (6.2.8)$$

The SIMULINK sub-model, which contains the estimator, is shown in Fig. 6.2.2, 6.2.3, 6.2.4, 6.2.5.

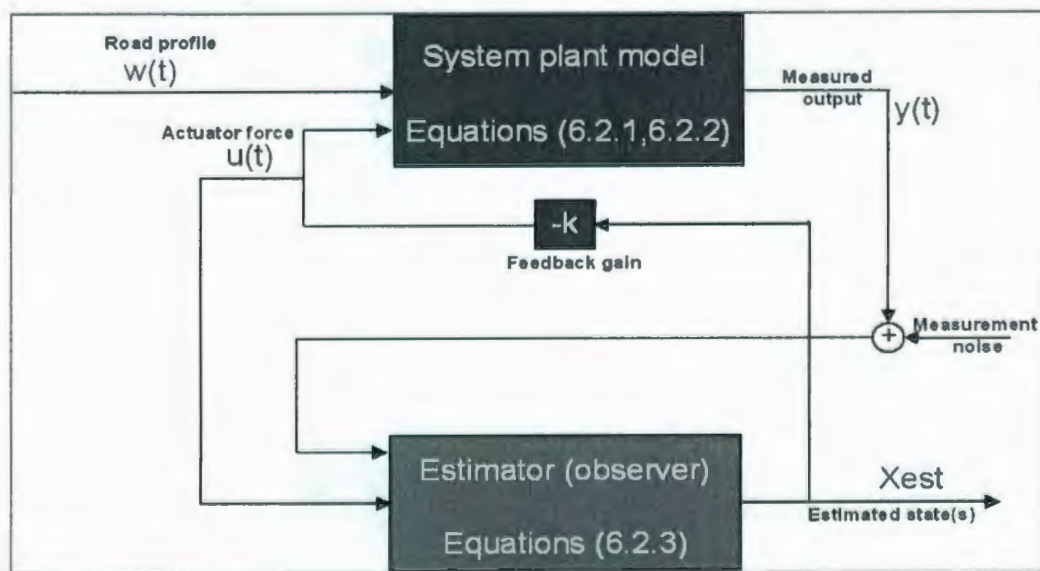


Figure 6.2.2: Proposed estimator configuration

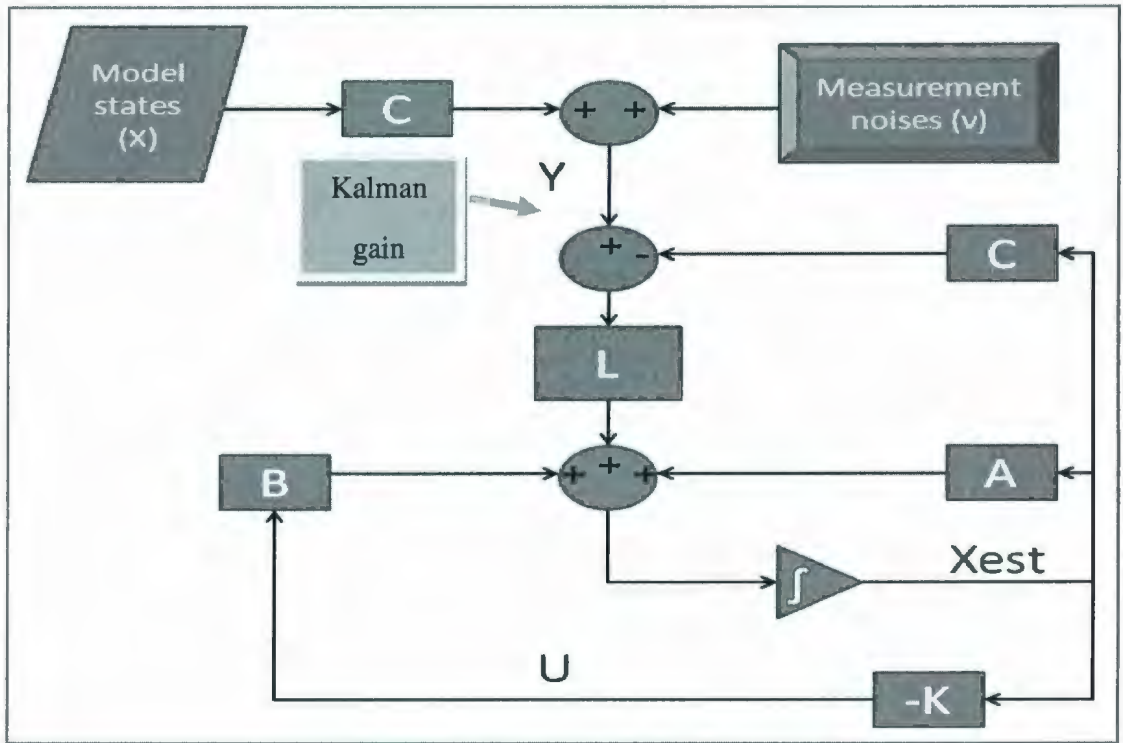


Figure 6.2.3: Schematic estimator block

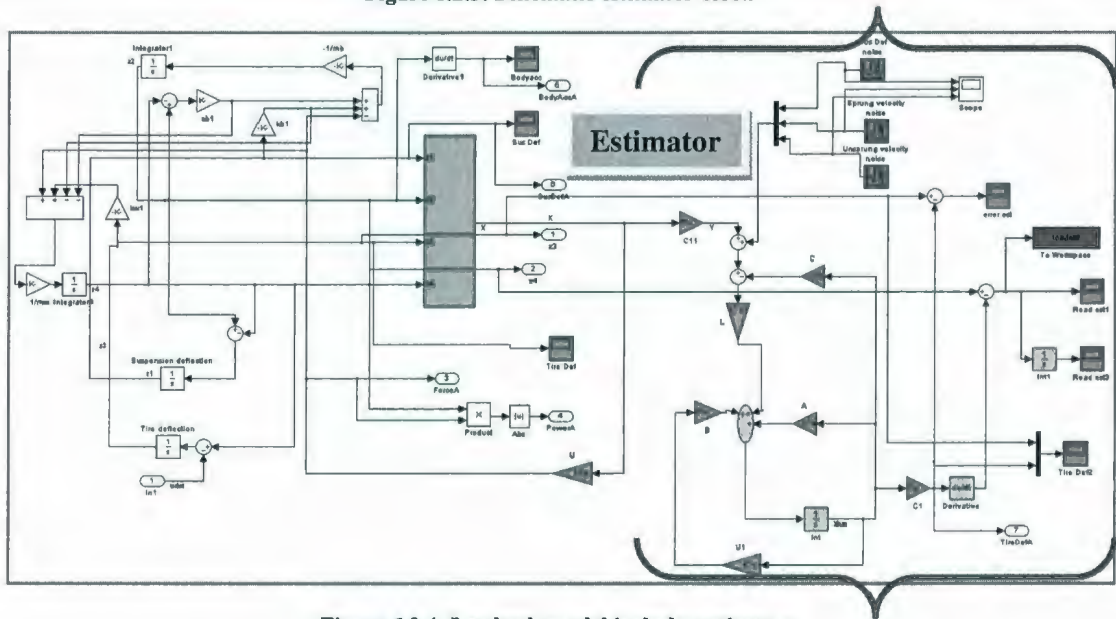


Figure 6.2.4: Lead sub-model includes estimator

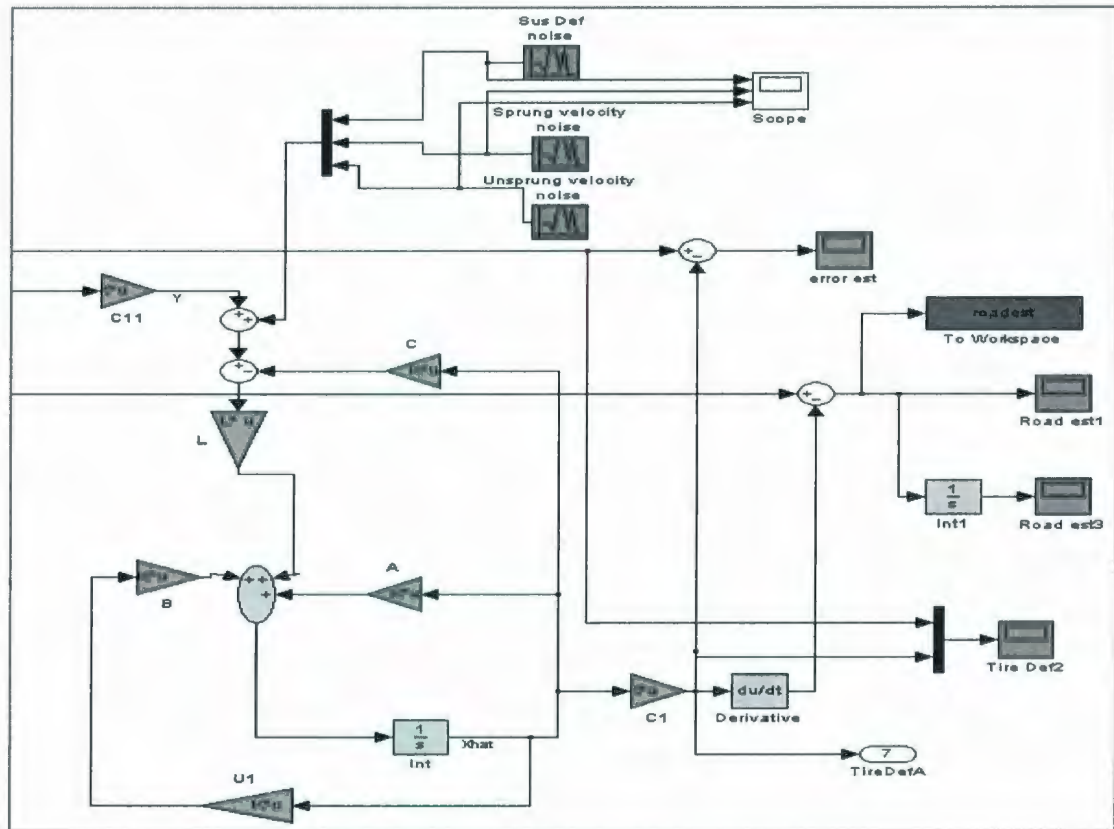


Figure 6.2.5: Estimator model in SIMULINK

As can be seen, a Gaussian white noise block is used to generate measurement noise.

The output of the estimator is estimated tire deflection, and the output of the lead sub-model is the estimated road profile which is transferred, in the form of data arrays, to the preview function in the follower sub-model. Feed forward gain is calculated by interpolating the data from the estimated road profile.

The results of the lead-follower model, in both time domain and frequency domain, are shown in Section 6.3.

6.3 Results

Simulations were carried out for a discrete rough bump road profile: single bump with stochastic road. The suspension variables are compared for the lead (active), and the follower (active preview) in both time and frequency domains. The ability of the lead vehicle to estimate the road profile is assessed.

The system parameters are same as parameters and values used in the Chapter 5. Gaussian white noise is used to generate measurement and input noises [13]. The input (road roughness) and measurement noise parameters and values are given in Table 6.3.1. The roughness coefficient (G_0) and vehicle forward velocity (U_0) are used to calculate input noise deviation (variance) parameter:

$$\sigma^2 = 2\pi G_0 U_0 \quad (6.3.1)$$

Table 6.3.1: Measurement and input noise parameters and values

Parameter	Value
Roughness coefficient (G_0)	5e-6 (m ³ /cycle)
Vehicle speed (U_0)	20 (m/s)
Deviation of noise for suspension deflection (σ^2)	1e-8
Deviation of noise for sprung mass velocity (σ^2)	1e-6
Deviation of noise for unsprung mass velocity (σ^2)	1e-6

The road profile is a single bump with height of 0.2 m with Gaussian white noise (Fig. 6.3.1 and Fig. 6.3.2), which is estimated by the lead vehicle and communicated to the

follower vehicle. Figure 6.3.1 shows that the estimator is very effective at estimating the road profile, with a small amount of error at the end of the bump.

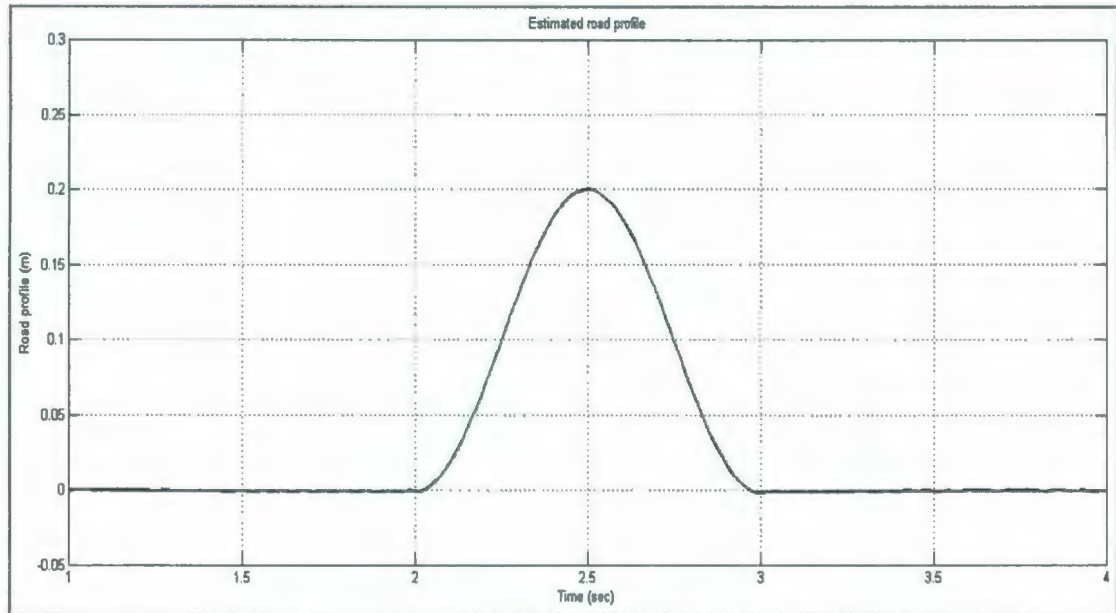


Figure 6.3.1: Estimated road profile

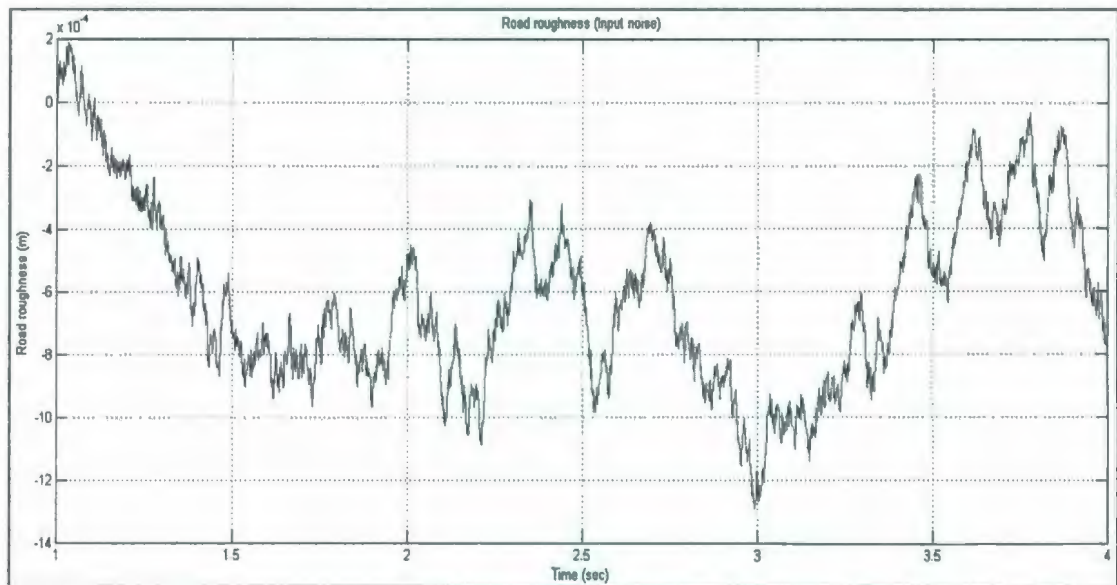


Figure 6.3.2: Road roughness (input Gaussian noise)

As shown in Fig. 6.3.3, the body acceleration is significantly improved by the suspension system with preview information from the lead vehicle's road profile estimator. However, the measurement noises disturb the follower response.

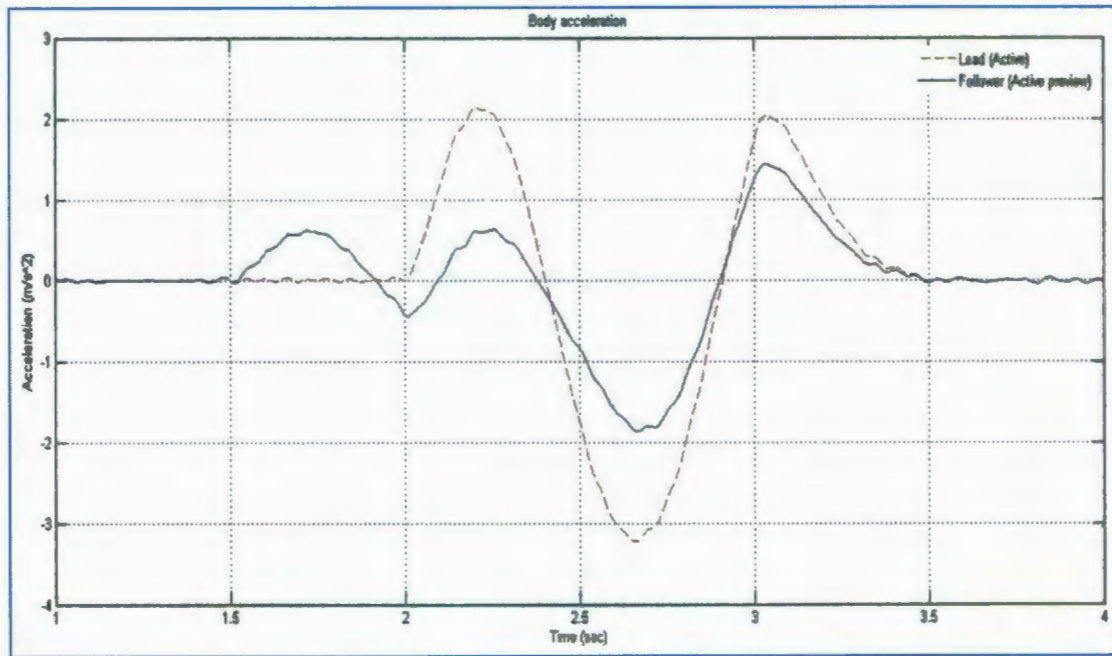


Figure 6.3.3: Body acceleration

The suspension deflection is slightly improved, especially in the second peak value (Fig. 6.3.4). As can be seen in this figure, the suspension deflection is not significantly affected by the measurement noises, in comparison with body acceleration and tire deflection.

In Fig. 6.3.5, the tire deflection is improved at its peak value, but it is strongly affected by measurement noise.

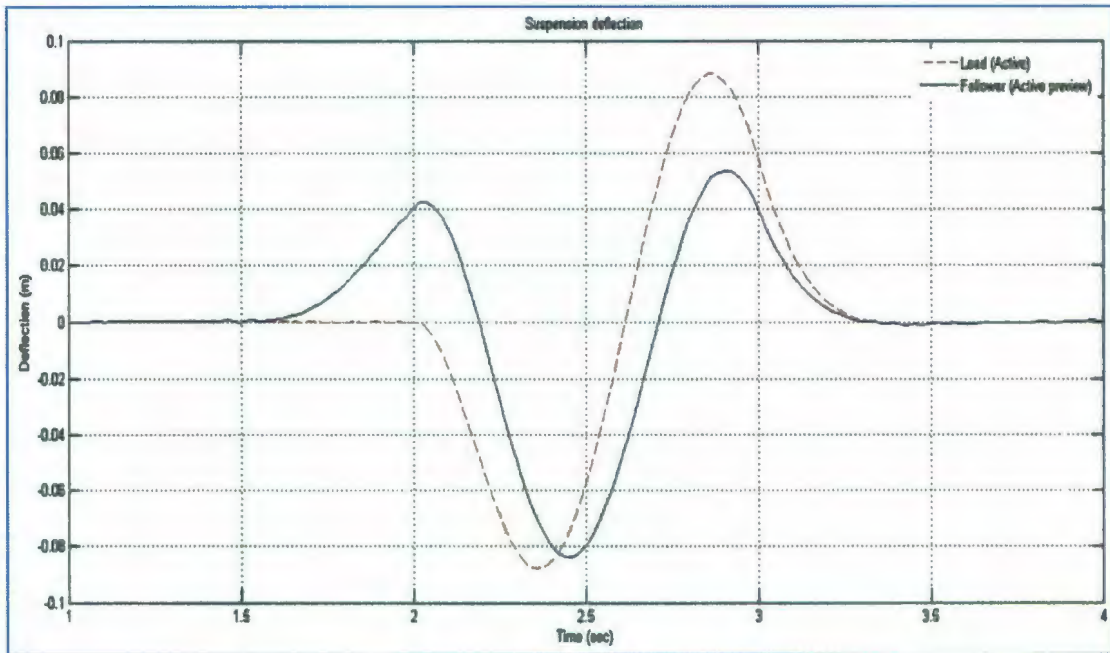


Figure 6.3.4: Suspension deflection

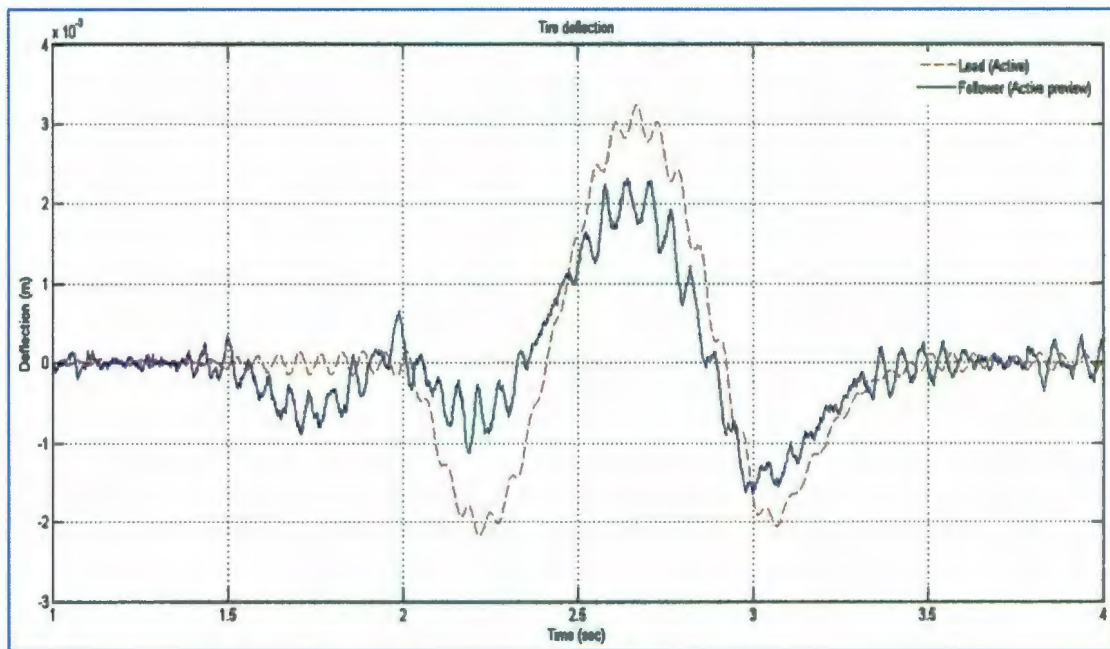


Figure 6.3.5: Tire deflection

The power demand is significantly reduced in the follower vehicle (Fig. 6.3.6), which demonstrates that using some preview time in an active suspension system can significantly reduce power demand [2, 3].

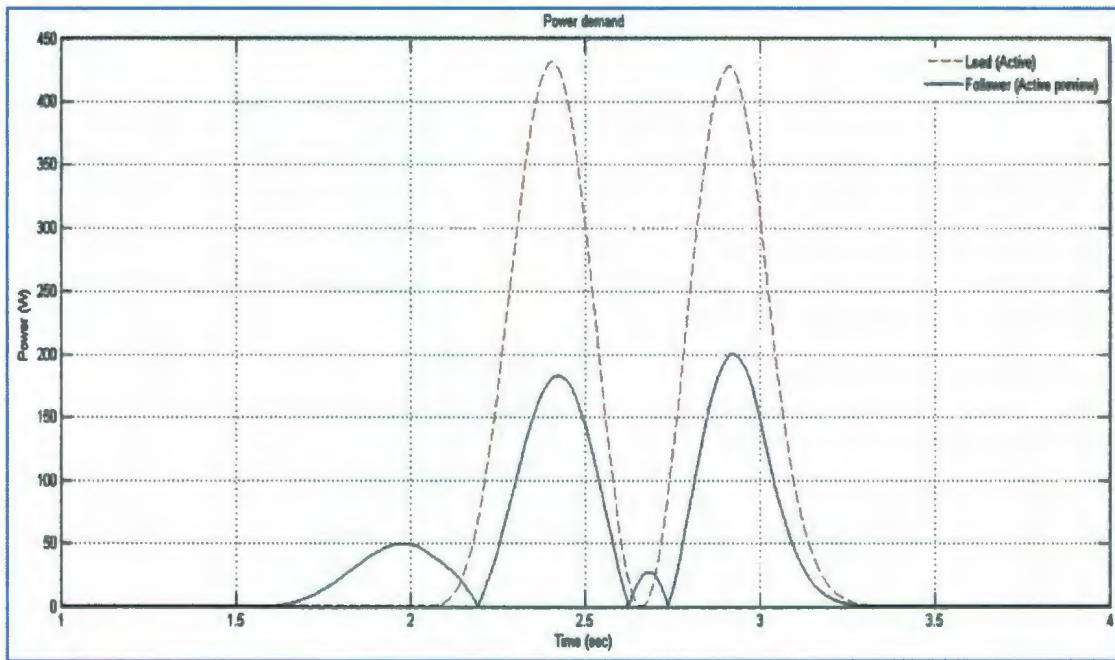


Figure 6.3.6: Power demand

The estimator dynamic error, which indicates the difference between calculated tire deflection and estimated tire deflection in the lead's model, is shown in Fig. 6.3.7. The estimated tire deflection versus calculated tire deflection is shown in Fig. 6.3.8.

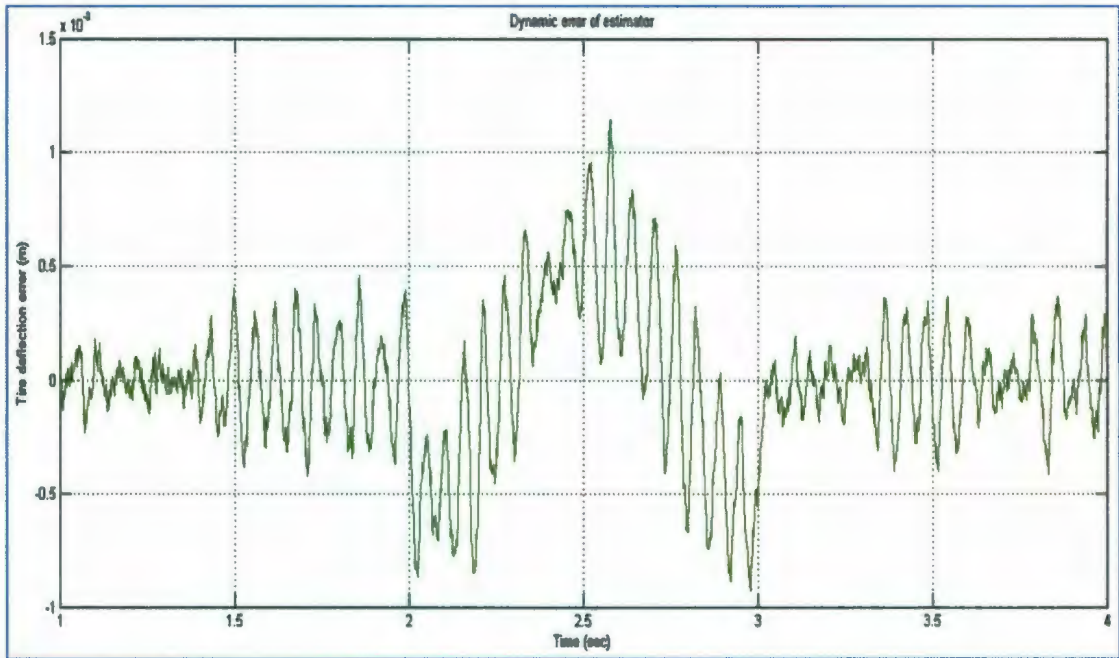


Figure 6.3.7: Estimator dynamic error

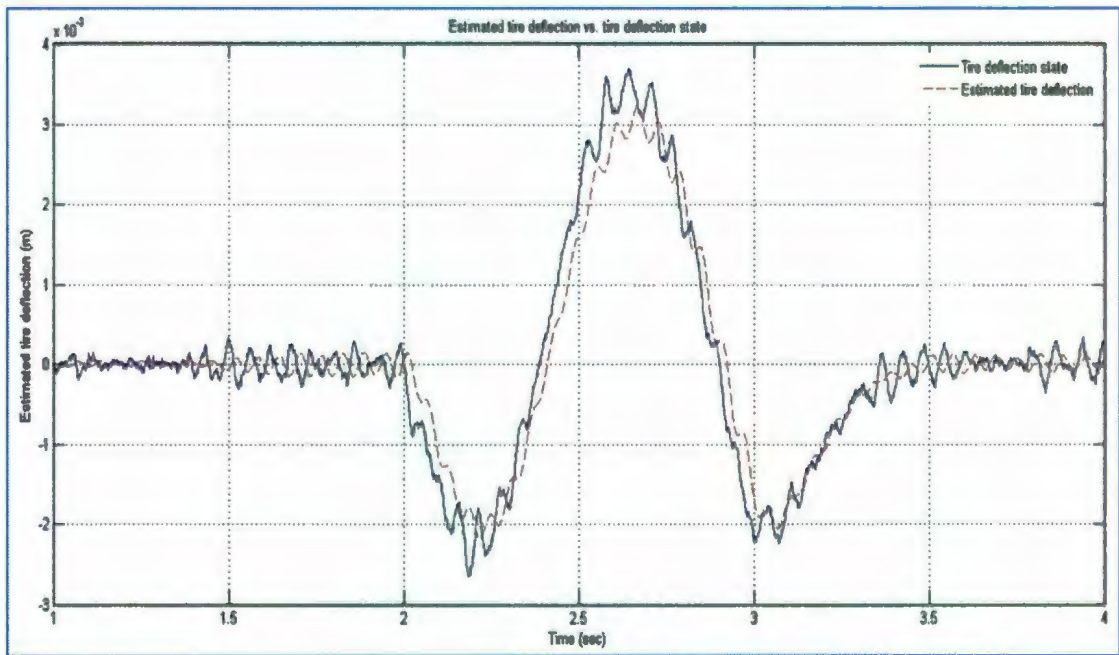


Figure 6.3.8: Estimated tire deflection vs. calculated tire deflection

The Fast Fourier Transform (FFT) of the autocorrelation function is used to illustrate the frequency domain results. As shown in Fig. 6.3.9 and Fig. 6.3.11, the body acceleration and tire deflection are significantly improved in the frequency domain. However, the suspension deflection is only slightly improved (Fig. 6.3.10).

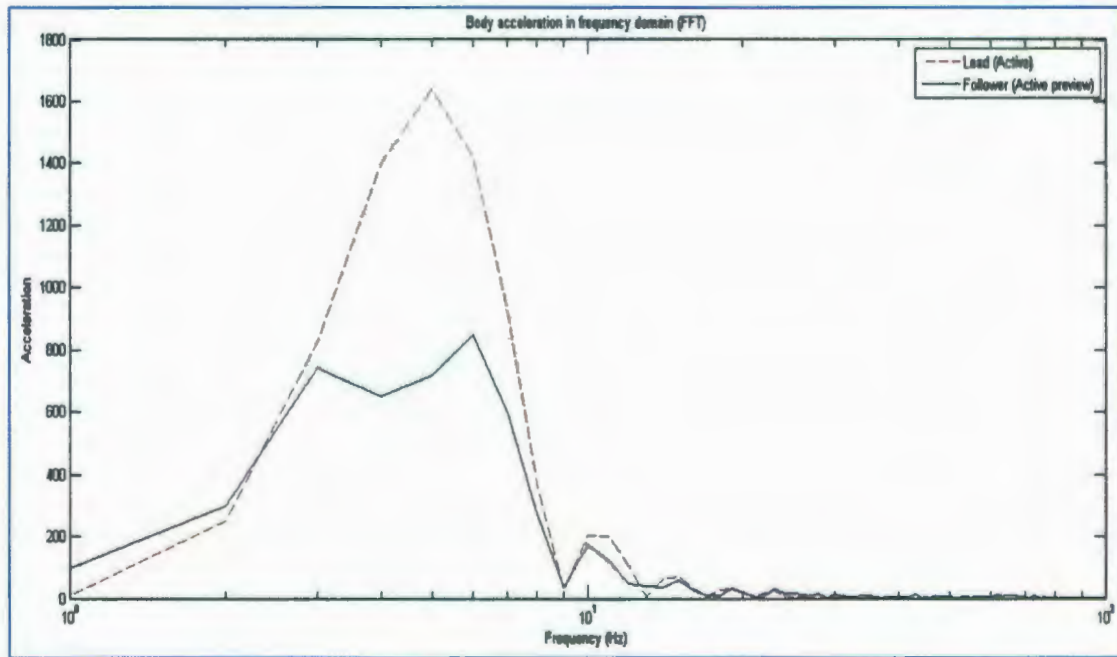


Figure 6.3.9: Body acceleration in frequency domain

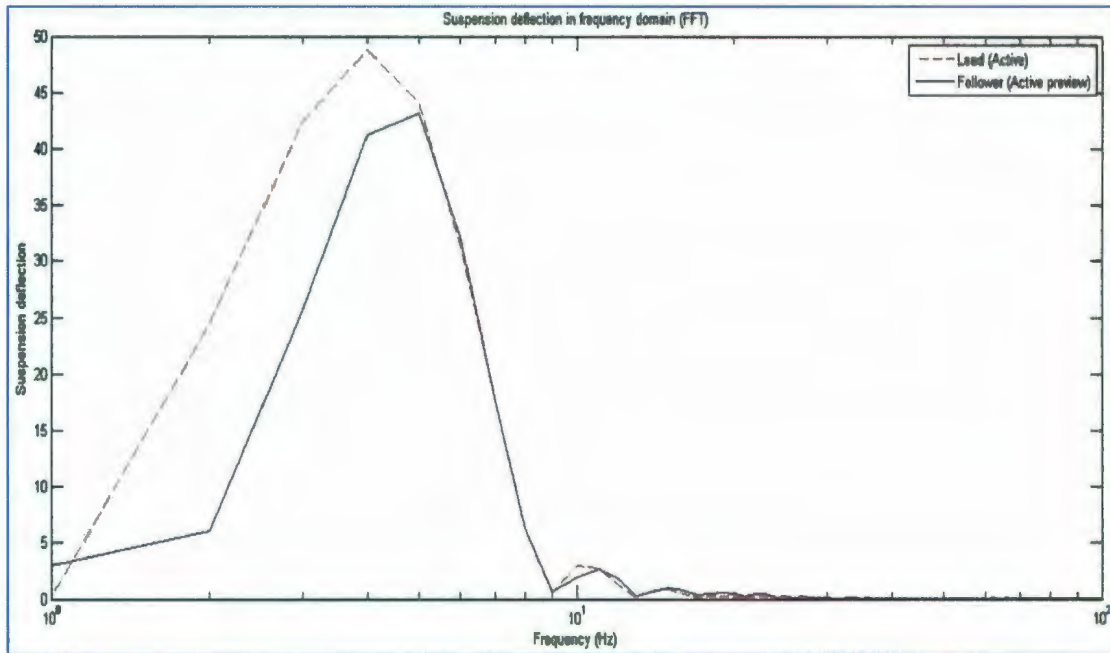


Figure 6.3.10: Suspension deflection in frequency domain

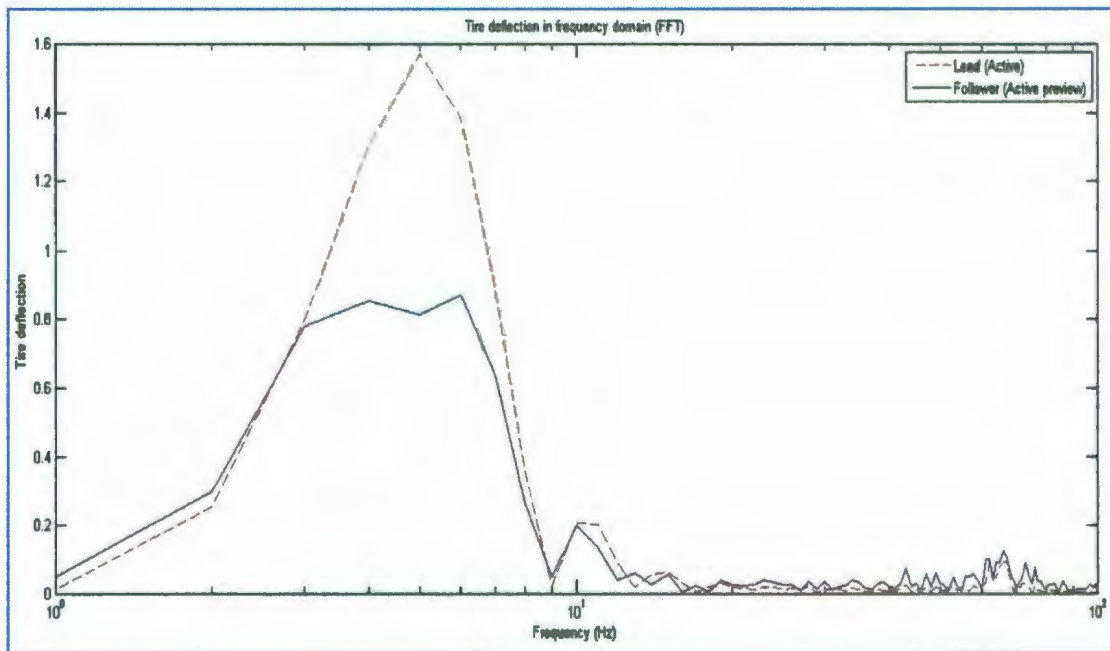


Figure 6.3.11: Tire deflection in frequency domain

6.4 Conclusion

This chapter has studied observer design to estimate the lead vehicles tire deflection and to generate an estimated road profile, which is implemented in the feed forward gain of the follower vehicle.

The results of the lead (active) and follower (active preview) on the noisy discreet bump illustrate that using the estimated road profile, implemented in the follower's feed forward gain, can satisfy the objectives of this method (replacing preview sensors with lead's response to estimate road profile).

Chapter 7

7. Conclusions and future work

7.1 Conclusions

The main goal of this thesis is to investigate active suspension system issues specifically applicable to convoy vehicles, and how to improve vertical dynamics of convoy vehicles by communicating preview information, e.g. road irregularities, from lead vehicle to follower(s). For this purpose, an academic lead-follower convoy model is designed, where the active and active-preview suspension systems are implemented in lead and follower model, respectively.

The main contribution of this project is using the response of the lead vehicle, e.g. tire deflection and unsprung mass velocity, to simulate the road profile for follower(s) [see Chapter 5]. This method suggests the possibility of eliminating the expensive and vulnerable sensors for each vehicle that are required in conventional preview-active suspension systems. However, since measuring the tire deflection is practically impossible, the Kalman observer is used to estimate tire deflection, one of the lead's states, based on the measurable states [see Chapter 6].

The results of lead (active), follower (active-preview) and passive suspension models show that:

The suspension variables related to improving ride comfort, such as body acceleration, are significantly reduced, and the suspension deflection is improved in the follower vehicle model with active-preview suspension system compared with the lead vehicle with active suspension system. The tire deflection and power demand were also reduced. Tire deflection reduction translates to better road holding ability, as available tire lateral force is directly related to tire normal force. Increased road holding potential is important for future work, in which lead vehicle responses in the yaw plane will be used to improve stability control and obstacle avoidance of convoy vehicle. As expected, the suspension variables of the lead vehicle, with active suspension system, are significantly improved compare to the vehicle with passive suspension system.

The optimal preview time, which is calculated, based on minimizing the performance index of the follower (active-preview) model with the proposed convoy parameters, is around 0.5 (sec). Increasing the preview time more than the optimal value does not produce significant improvement. This is consistent with findings in the literature.

Also, in Chapter 4, the longitudinal dynamics of the convoy model are studied, and an Adaptive Cruise Control (ACC) system is implemented which shows longitudinal stability, both individual and string stability, of the proposed convoy model, using the bond graph method.

7.2 Future work

The following areas can be carried on as potential future research:

Semi-active suspension system with preview: the lead vehicle, which would have an active suspension system, would play the role of the preview sensor, and the followers would have a semi-active suspension system with preview. Using a semi-active suspension system is cheaper than fully active suspension system. The performance of a semi-active suspension is not as good as that of a fully active suspension, but applying the short preview time in semi-active suspension systems can significantly enhance a semi-active suspension, and in some cases the fully active suspension performance can be nearly obtained by semi-active with preview [10, 11].

Effect of uncertainty on preview suspension performance: the whole point of the longitudinal dynamics study was to eventually apply the state-based preview control scheme to a convoy of vehicles with longitudinal dynamics and cruise control. It remains to be seen whether or not uncertainties in following distance will degrade preview suspension performance, and how these uncertainties will propagate through the entire convoy if all vehicles have slightly different, and varying, following distances and therefore delay times.

Ergonomics and ride quality: the proposed convoy vehicle system active suspension strategy causes the lead vehicle's driver to experience more vibration than the followers, potentially increasing the lead vehicle driver's risk of fatigue and injury. Studying an

optimal pattern for scheduling the lead vehicles in a convoy would minimize driver fatigue and injury.

Experimental implementation of the proposed lead-follower system: the experimental test of an active suspension system with preview has been carried out by Donahue, 2001, [39]. The application of the proposed lead-follower system, in this research, in a real convoy system, and the implementation of the novel technique to estimate road profile based on the lead vehicle's states can be considered as a potential future work.

Active steering control with preview: the proposed method, using preview information from the lead vehicle to improve response of follower vehicles may be applicable to lateral dynamics of a convoy. The idea is that the lateral states of the lead vehicle such as yaw rate and lateral velocity could be used as preview information for followers (Fig. 7.2.1). Therefore, the followers can generate feed forward gain, e.g. corrective yaw moments, based on the preview information, in addition to the feedback gain to tune an active steering control with preview [17, 31, and 35].

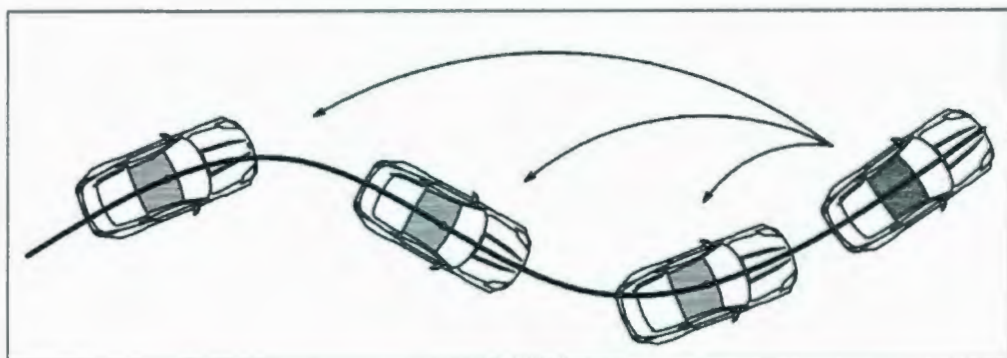


Figure 7.2.1: Schematic lateral motion of convoy vehicles (state communication)

Bibliography

- [1] E.K. Bender. Optimum linear preview control with application to vehicle suspension. American Society of Mechanical Engineers, *Journal of Basic Engineering*, 100, 213-221, (1968).
- [2] A. Hac. Optimal linear preview control of active vehicle suspension. *Vehicle System Dynamics*, 21 (3), 167-195, (1992)
- [3] J. Marzbanrad, G. Ahmadi, Y. Hojjat, H.Zohoor. Optimal active control of vehicle suspension systems including time delay and preview for rough roads. *Journal of vibration and control*, 8, 967-991, (2002)
- [4] D. Hrovat. Survey of advanced suspension development and related optimal control applications. *Automatica*, 33, 1781-1871, (1997)
- [5] A.G. Thompson, C.E.M. Pearce. Performance index for a preview active suspension applied to a quarter-car model. *Journal of Vehicle System Dynamics*, 35 (1), 55-66, (2001)
- [6] A. Vahidi, A. Eskandarian. Influence of preview uncertainties in the preview control of vehicle suspension. *Journal of Multi-body Dynamics*, 216, 295-301, (2002)
- [7] D. Karnopp. Continuum model study of preview effects in actively suspended long trains. *Journal of the Franklin Institute*, 285 (4), 251-260, (1968)

- [8] R.G. Langlois, D.M. Hanna, R.J. Anderson. Implementing preview control on an off-road vehicle with active suspension. *Journal of Vehicle System Dynamic*, 20 (1), 340-353, (1991)
- [9] A.G. Thompson, C.E.M. Pearce. Direct computation of the performance index for an optimally controlled active suspension with preview applied to a half-car model. *Journal of Vehicle System Dynamics*, 35 (2), 121-137, 2001
- [10] A. Hac, I. Youn. Optimal semi-active suspension with preview based on a quarter car model. *Journal of Vibration and Acoustic*, 114 (1), 84-93, (1992)
- [11] A. Soliman, D. Crolla. Preview control for a semi-active suspension system. *Journal of Vehicle Design*, 17 (4), 384-396, (1996)
- [12] J. Marzbanrad, G. Ahmadi, Y. Hojjat, H.Zohoor. Stochastic optimal preview control of a vehicle suspension. *Journal of sound and vibration*, 275 (3), 973-990, (2004)
- [13] F. Yu, D.A. Crolla. State observer design for an adaptive vehicle suspension. *Journal of Vehicle System Dynamics*, 30 (6), 457-471, (1998)
- [14] R.S. Sharp. Optimal preview car steering control. *20th International Congress of Theoretical and Applied Mechanics*. 101-117, (2000)
- [15] R. Rajamani. *Vehicle Dynamics and Control*. Springer, (2006)
- [16] A.R. Orozco. *Evaluation of an active steering system*. M.Sc. thesis, KTH University, Stockholm, Sweden, (2004)

- [17] R.J. Rieveley, B.P. Minaker. Variable torque distribution yaw moment control for hybrid power trains. *Society of Automotive Engineering (2007-01-0278)*, (2007)
- [18] D.C. Karnopp, D. Margolis, R.C. Rosenberg. *Modeling and Simulation of Mechatronic Systems*, John Wiley & Sons Inc, (2006)
- [19] K. Ogata. *Modern control engineering*, Prentice Hall Inc., (2002)
- [20] 20-sim v.4.0, Controllab Products b.v., Enschede, Netherlands (2008)
- [21] D. Margolis, S. Taehyun. Bond graph model incorporating sensors, actuators, and vehicle dynamic for developing controllers for vehicle safety. *Journal of the Franklin Institute*, 338 (1), 21-34, (2001)
- [22] C. Ying, H. Peng. Optimal adaptive cruise control with guaranteed string stability. *Journal of the Vehicle System Dynamic*, 54 (1), 313-330, (1999)
- [23] D. Swaroop, J.K. Hedrick. String stability of interconnected systems. *IEEE Trans. Automat. Contr.*, 41 (3), 349-356, (1996)
- [24] D. Hrovat. Optimal suspension performance for 2-D vehicle models. *Journal of Sound and Vibration*, 146 (1), 93-110, (1991)
- [25] M. Tomizuka. Optimum linear preview control with application to vehicle suspension. *Journal of Dynamic Systems, Measurement and Control*, 98 (3), 309-315, (1976)

- [26] G.S. Newell, N.J. Mansfield. Evaluation of reaction time performance and subjective workload during whole body vibration exposure while seated on upright and twisted posturing with and without armrests. *Journal of Industrial Ergonomics*, 38 (5), 499-508, (2008)
- [27] S.B. McLaughlin. *Measurement of driver performances and intervention responses as influenced by adaptive cruise control deceleration characteristics*. M.Sc. thesis, Faculty of the Virginia Polytechnic Institute and State University, Virginia, US, (1998)
- [28] G. Rideout, J.L. Stein, L.S. Louca. Extension and application of an algorithm for systematic identification of weak coupling and partitions in dynamic system models. *Journal of Simulation Modelling Practice and Theory*, 17 (1), 271-292, (2009)
- [29] H. Kim, Y.S. Yoon. Semi-active suspension with preview using a frequency-shaped performance index. *Journal of Vehicle System Dynamics*, 24 (10), 759-780, (1995)
- [30] J. Ackermann. Active steering for better safety, handling and comfort. *Proceedings of Advances in Vehicle Control and Safety*, (1998)
- [31] U.N. Petersen, A. Rukgauer, W.O. Schiehlen. Lateral control of a convoy vehicle system. *Journal of Vehicle System Dynamics*, 25, 519-532, (1996)
- [32] W. Schiehlen. Motion control of vehicles in convoy. *International Conference on Control of Oscillations and Chaos Proceedings*, (2000)
- [33] MATLAB 7.4.0.287(R2007a), Mathworks, US (2007)

- [34] R. Lomax. *An introduction to statistical concepts*, Lawrence Erlbaum Associates Publishers, (2002)
- [35] A. Fritz. Lateral and longitudinal control of a vehicle convoy. *Journal of Vehicle System Dynamics*, 35, 149-164, (2000)
- [36] H. Adibi asl, D. G. Rideout. Bond graph modeling and simulation of a full car model with active suspension. *20th IASTED International Conference on Modeling and Simulation*, Banff, AB, July 2009.
- [37] D. G. Rideout. *Personal communication with Dr. J. N. Overholt*. U.S. Army Tank-Armament and Automotive Command, 2008.
- [38] C. Kim, P. I. Ro. An accurate full car model using model reducing techniques. *Journal of Mechanical Design*, 124, 697-705, (2002)
- [39] M. Donahue. *Implementation of an active suspension, preview controller for improved ride comfort*. M.Sc. Thesis, University of California at Berkeley, April 2001

Appendix

Appendix A: String stability

Norms of signals are defined as:

$$\|x\|_p = \left[\int_0^{\infty} |x(t)|^p dt \right]^{1/p}$$

The ∞ norm of a signal is the least upper bound of its absolute value (Doyle, et al., 1992): $\|x\|_{\infty} = \sup |x(t)|$

Applying the signal norms to prove string stability is briefly expressed as:

The system is said to be string stable if, given any $\varepsilon > 0$, there is a $\delta > 0$ such that:

$$\sup \|x_i(0)\| \leq \delta \Rightarrow \sup \|x_i(t)\| \leq \varepsilon, \forall t > 0$$

And asymptotically stable if it is string stable and also $\exists \Delta > 0$ such that

$$\sup \|x_i(0)\| \leq \Delta \Rightarrow \sup \|x_i(t)\| \rightarrow 0, t \rightarrow \infty$$

Similarly, for any $p \geq 1$, it is said to be l_p string stable if, given any $\varepsilon > 0$, there is a $\delta > 0$ such that

$$\left[\sum_i \|x_i(0)\|^p \right]^{1/p} \leq \delta \Rightarrow \left[\sum_i \|x_i(t)\|^p \right]^{1/p} \leq \varepsilon, \forall t > 0$$

Also, frequency domain viewpoint can be employed to evaluate disturbance propagation along the string (convoy).

$$x_i(t) = \int_0^t h(t-\tau)x_{i-1}(\tau)d\tau$$

$$H(s) = \frac{X_i(s)}{X_{i-1}(s)}$$

$$\|H(s)\|_\infty \leq 1 \Rightarrow \|y\|_2 \leq \|x\|_2$$

It means that spacing error of a target vehicle must be less than the spacing error of the preceding vehicle to guarantee that disturbance along the string (convoy) is not amplified.

And in addition to the above condition, if $h(t) > 0$, then $\|x_i\|_\infty \leq \|x_{i-1}\|_\infty$ which satisfies the string stability of a system [15, 23].

In summary, the system (convoy vehicles) is string stable if the following two conditions (A and B) are satisfied (Swaroop 1995):

$$H(s) = \frac{X_i(s)}{X_{i-1}(s)} \rightarrow \text{Spacing error transfer function}$$

A. $\|H(s)\|_\infty \leq 1 \rightarrow$ The ∞ norm of a transfer function

B. $h(t) > 0, (\forall t \geq 0) \rightarrow$ The corresponding impulse response of $H(s)$

Appendix B: Linear Quadratic Regulator (LQR)

$$\begin{cases} \dot{x} = A_{nn}x + B_{nr}u + D_{nr}W \\ y = C_{mn}x \end{cases} \rightarrow \text{System state space equation}$$

$$x = \begin{pmatrix} x_1 \\ x_2 \\ x_3 \\ x_4 \end{pmatrix} = \begin{pmatrix} x_s - x_u \\ \dot{x}_s \\ x_u - x_r \\ \dot{x}_u \end{pmatrix} \rightarrow \begin{pmatrix} \text{suspension deflection} \\ \text{sprung mass velocity} \\ \text{tire deflection} \\ \text{unsprung mass velocity} \end{pmatrix}$$

$$J = \frac{1}{2} \int_0^{\infty} (\ddot{x}_s + r_1 \dot{x}_1^2 + r_2 \dot{x}_3^2 + r_3 u^2) dt \rightarrow \text{Cost function (performance index)}$$

$$\begin{aligned} \ddot{x}_s + r_1 \dot{x}_1^2 + r_2 \dot{x}_3^2 + r_3 u^2 &= \left(-C_b/M_b (x_2 - x_4) - K_b/M_b (x_1) + u/M_b \right)^2 + r_1 \dot{x}_1^2 + r_2 \dot{x}_3^2 + r_3 u^2 \\ &= \left(C_b/M_b \right)^2 (x_2^2 + x_4^2) + \left(K_b/M_b \right)^2 x_1^2 + r_1 \dot{x}_1^2 + r_2 \dot{x}_3^2 + \left(C_b/M_b \right)^2 (-2x_2 x_4) \\ &\quad + 2C_b K_b / M_b^2 (x_1 x_2 - x_1 x_4) + u^2 / M_b^2 + r_3 u^2 - 2K_b / M_b^2 u x_1 - 2C_b / M_b^2 u (x_2 - x_4) \end{aligned}$$

$$J = \frac{1}{2} \int_0^{\infty} (x^T Q_1 x + x^T N u + u^T R u) dt \rightarrow \text{Simplified Cost function (performance index)}$$

$$A = \begin{bmatrix} 0 & 1 & 0 & -1 \\ -K_b/M_b & -C_b/M_b & 0 & C_b/M_b \\ 0 & 0 & 0 & 1 \\ K_b/M_w & C_b/M_w & -K_t/M_w & -C_b/M_w \end{bmatrix}, \quad B = \begin{bmatrix} 0 \\ 1/M_b \\ 0 \\ -1/M_w \end{bmatrix}, \quad D = \begin{bmatrix} 0 \\ 0 \\ -1 \\ 0 \end{bmatrix}$$

$$Q_1 = 1/M_b^2 \begin{bmatrix} K_b^2 + r_1 M_b^2 & 2C_b K_b & 0 & -2C_b K_b \\ 2C_b K_b & C_b^2 + r_2 M_b^2 & 0 & -2C_b^2 \\ 0 & 0 & 0 & 0 \\ -2C_b K_b & -2C_b^2 & 0 & C_b^2 \end{bmatrix}, \quad N = 1/M_b^2 \begin{bmatrix} -K_b \\ -C_b \\ 0 \\ C_b \end{bmatrix}, \quad R = 1/M_b^2 + r_3$$

The numerical values for the proposed model in Chapter 5, 6 are:

Parameter	Value
Sprung mass (M_b)	100 kg
Unsprung mass (M_w)	10 kg
Suspension damping (C_b)	100 N/(m/s)
Suspension stiffness (K_b)	10000 N/m
Tire stiffness (K_t)	100000 N/m
Weight factors ($r_1 r_2 r_3$)	1e3, 1e4, 0

$$A = \begin{bmatrix} 0 & 1 & 0 & -1 \\ -100 & -1 & 0 & 1 \\ 0 & 0 & 0 & 1 \\ 1000 & 10 & -10000 & -10 \end{bmatrix}, B = \begin{bmatrix} 0 \\ 0.01 \\ 0 \\ -0.1 \end{bmatrix}, D = \begin{bmatrix} 0 \\ 0 \\ -1 \\ 0 \end{bmatrix}, C = \begin{bmatrix} 1 & 0 & 0 & 0 \\ 0 & 1 & 0 & 0 \\ 0 & 0 & 0 & 1 \end{bmatrix}$$

$$Q_1 = \begin{bmatrix} 1.1e4 & 200 & 0 & -200 \\ 200 & 10001 & 0 & -2 \\ 0 & 0 & 0 & 0 \\ -200 & -2 & 0 & 1 \end{bmatrix}, N = \begin{bmatrix} -1 \\ -0.01 \\ 0 \\ 0.01 \end{bmatrix}, R = 1e-4$$

$$A^T P + PA - PBR^{-1}B^T P + Q_1 = 0 \rightarrow \text{Riccati equation}$$

$$P = \begin{bmatrix} 3.07e3 & 31.3 & 3.16e3 & 0 \\ 31.3 & 102.5 & 9.6 & 0.2 \\ 3.16e3 & 9.6 & 3.6e3 & 0 \\ 0 & 0.2 & 0 & 0 \end{bmatrix} \rightarrow \text{Solution of Riccati equation}$$

Used to calculate active force

$$u(t) = -\frac{B^T [Px(t)]}{R} \rightarrow \text{Actuator force}$$

Appendix C: Controllability and observability

$$\begin{cases} \dot{x} = A_{nn}x + B_{nr}u + D_{nr}W \\ y = C_{mn}x \end{cases} \rightarrow \text{System state space equation}$$

As mentioned in Appendix B:

$$n = 4; \quad m = 3; \quad r = 1;$$

The conditions of controllability and observability are:

$$CM = \{CB|CAB|CA^2B|CA^3B| \dots |CA^{n-1}B\} \rightarrow \text{Controllability matrix}$$

$$OM = \{C'|A'C'| (A')^2C'| (A')^3C'| \dots | (A')^{n-1}C'\} \rightarrow \text{Observability matrix}$$

The system is controllable if and only if the rank of controllable matrix (CM) would be of rank m, (m=3).

The system is observable if the rank of observable matrix (OM) would be of rank n, (n=4).

The numerical values of CM and OM are:

$$CM = \begin{bmatrix} 0 & 0 & -1 & -1108 \\ 0 & 0 & -10 & 1229 \\ 0 & 1 & 1098 & -23287 \end{bmatrix}_{3 \times 4} \rightarrow \text{Rank}(CM) = 3$$

$$OM = \begin{bmatrix} 1 & 0 & 0 & 0 & -100 & 1e3 & -1.1e3 & 1.1e3 & -1.1e4 & 1.2e4 & 9.8e4 & -1.1e7 \\ 0 & 1 & 0 & 1 & -1 & 10 & -11 & -89 & 890 & -979 & 2.08e3 & -1.2e5 \\ 0 & 0 & 0 & 0 & 0 & -1e4 & 1e4 & -1e4 & 1e5 & -1.1e5 & -8.9e5 & 1.09e8 \\ 0 & 0 & 1 & -1 & 1 & -10 & 11 & 89 & -1.09e4 & 1.1e4 & -1.2e4 & 2.2e5 \end{bmatrix}_{4 \times 12}$$

$$\rightarrow \text{Rank}(OM) = 4$$



